S-Velocity Structure of the Upper Mantle

Sergei Lebedev *(Dublin Institute for Advanced Studies),* **Rob D. van der Hilst** *(MIT)*

Sv-velocity structure of the upper mantle (crust–660 km) is constrained by the Automated Multimode Inversion of surface and S-wave forms [*Lebedev et al., 2005*], applied to a large global data set retreived from IRIS facilities [*Lebedev and van der Hilst, 2008*]. Structure of the mantle and crust is constrained by waveform information from both the fundamental mode Rayleigh waves (periods from 20 to 400 s) and S and multiple S waves (higher modes). The reference model used in the waveform inversions and the tomographic linear inversion incorporates 3-D crustal structure. The tomographic model includes isotropic variations in S- and P-wave velocities and also S-wave azimuthal anisotropy. The lateral resolution of the imaging is a few hundred kilometres, varying with data sampling.

The technique has been benchmarked with a 'spectral-element' resolution test: inverting published global synthetic data sets computed with the spectral-element method for laterally heterogeneous mantle models, Lebedev and van der Hilst [2008] have been able to reconstruct the synthetic models accurately.

The tomographic model displays low-Sv-velocity anomalies beneath mid-ocean ridges and back-arc basins that extend down to ~100 km depth only. In the seismic lithosphere beneath cratons, strong high velocity anomalies extend to ~200 km. Pronounced low-velocity zones beneath cratonic lithosphere are rare; where present (South America; Tanzania) they are often neighboured by volcanic areas near cratonic boundaries. The images of these low-velocity zones may indicate hot material possibly of mantle-plume origin—trapped or spreading beneath the thick cratonic lithosphere [*Lebedev and van der Hilst, 2008*].

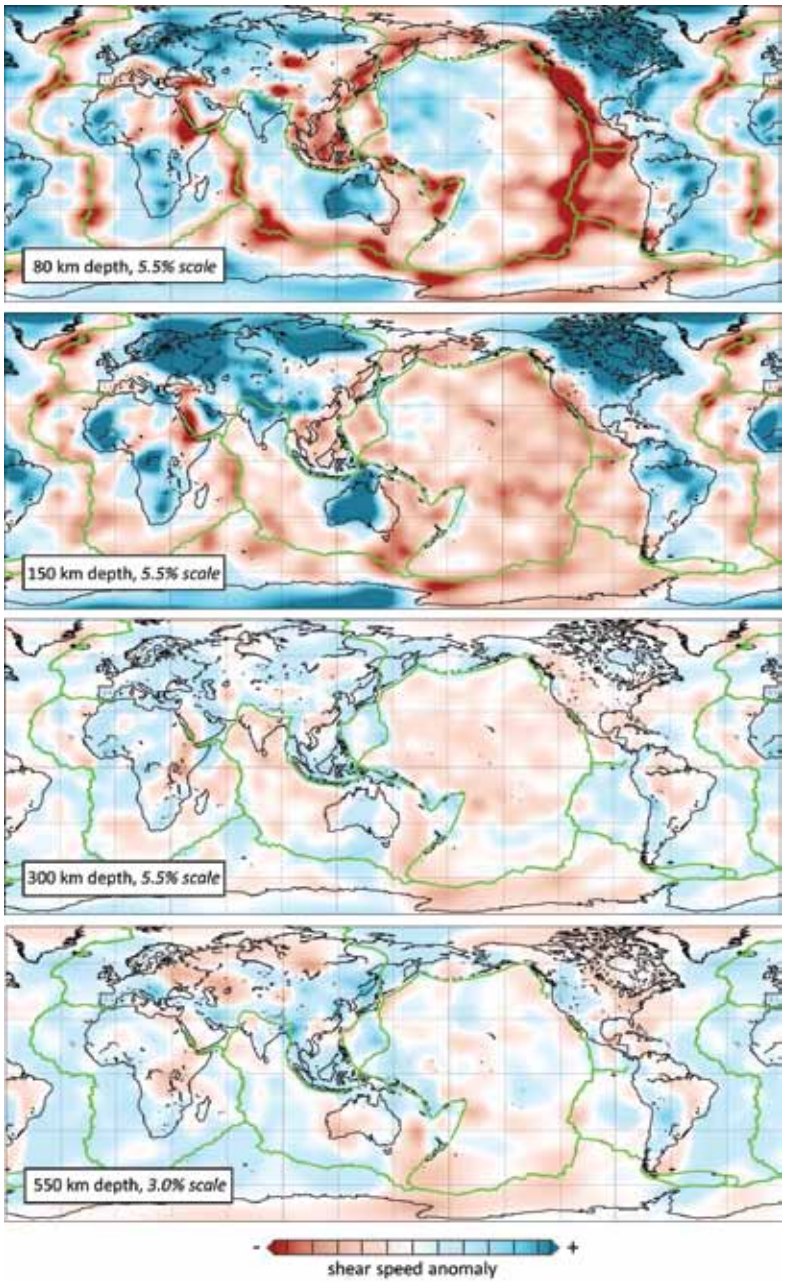

Cross-section depths and color-scale limits are specified within each frame. The reference Sv-wave velocity values are, for increasing depths: 4.38, 4.39, 4.69, 5.27 km/s—all at a reference period of 50 s.

References

Lebedev, S., G. Nolet, T. Meier, R. D. van der Hilst, Automated multimode inversion of surface and S waveforms, *Geophys. J. Int. 162*, 951-964, 2005.

Lebedev, S., R. D. van der Hilst, Global upper-mantle tomography with the automated multimode inversion of surface and S-wave forms, *Geophys. J. Int., 173*, 505-518, 2008.

P and S Body-Wave Tomography of the Western US Upper Mantle

Brandon Schmandt *(University of Oregon),* **Eugene Humphreys** *(University of Oregon)*

We invert teleseismic travel-time residuals from the EarthScope Transportable Array and more than 1700 additional temporary and permanent stations for 3-D velocity perturbations to a depth of 1000 km. The inversion uses recent advances in western U.S. crust models to better isolate the mantle component of travel-time residuals, and frequency-dependent 3-D sensitivity kernels to map travel-time residuals, measured in multiple frequency bands, into velocity structure. In addition to separate Vp and Vs models, we jointly invert the two datasets for Vp/Vs perturbations by imposing a smoothness constraint on the dlnVs/dlnVp field. The joint inversion helps us identify regions where partial melt is probable. The amplitude of Vp, Vs, and Vp/Vs variations is greatest in the upper 200 km of the mantle and the form of velocity anomalies suggests a provincially heterogeneous lithosphere and the occurrence of widespread small-scale convection. Partially molten mantle is inferred beneath Yellowstone and the eastern Snake River Plain (SRP), the Salton Trough, and the Clear Lake volcanic field. The inferred depth extent of partial melt is consistent with a generally hydrated upper mantle and elevated temperatures beneath the eastern SRP and Yellowstone. Despite more than 100 My of continuous subduction, the distribution of sub-lithospheric high-velocity anomalies is dissected (similar to other recent studies). Based on our new tomography models, western U.S. geologic history, and plate-tectonic reconstructions, we infer patchy and incomplete removal of the flat-subducting Laramide slab and slab tearing associated with Eocene accretion in the northwestern U.S.

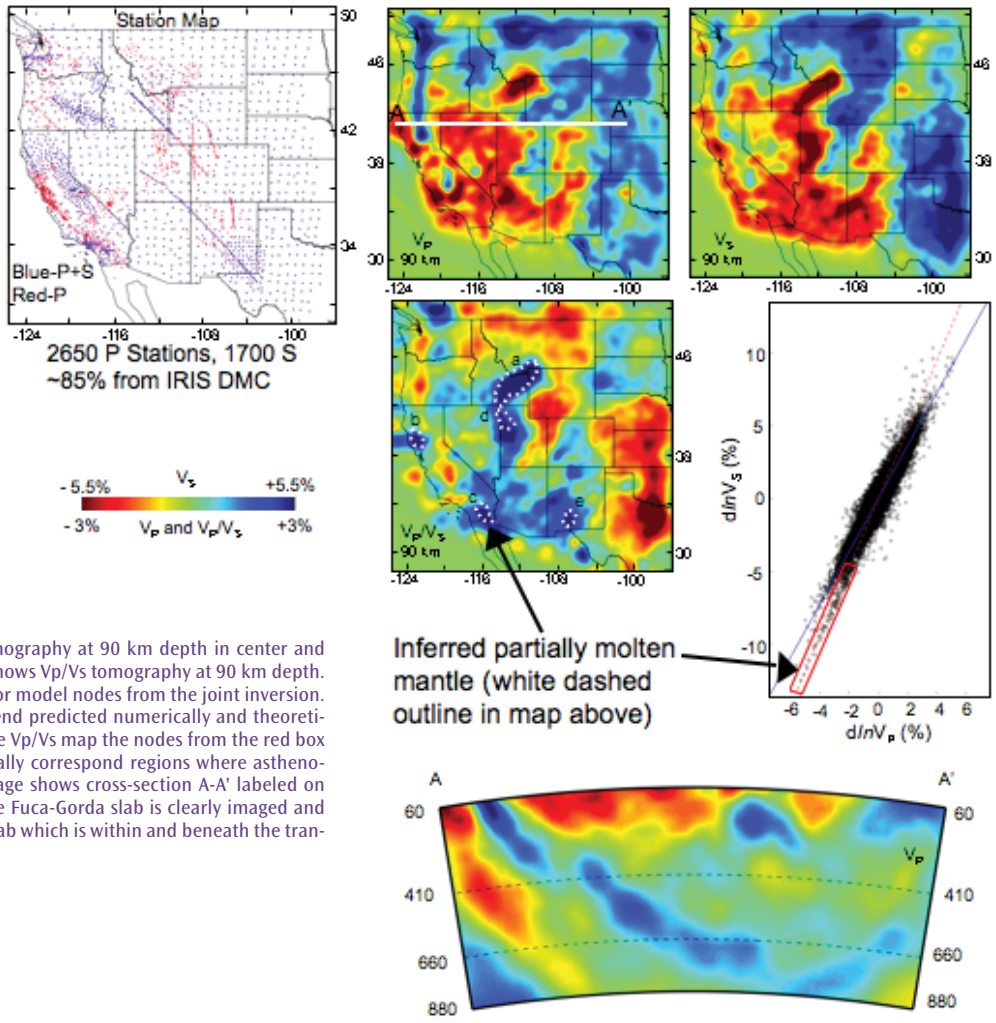

Station map in upper left. P and S tomography at 90 km depth in center and right panels in upper row. Middle left shows Vp/Vs tomography at 90 km depth. Middle right panel shows dlnVs/dlnVp for model nodes from the joint inversion. The nodes in the red box follow the trend predicted numerically and theoretically for partially molten mantle. On the Vp/Vs map the nodes from the red box are outlined (white dashed) and generally correspond regions where asthenospheric ascent is expected. Bottom image shows cross-section A-A' labeled on the Vp map in the top row. The Juan de Fuca-Gorda slab is clearly imaged and disconnected from the older Farallon slab which is within and beneath the transition zone.

Velocity Structure of the Western US from Surface Wave Phase Velocity Measurements

Anna Foster *(LDEO, Columbia University),* **Göran Ekström** *(LDEO, Columbia University),* **Vala Hjörleifsdóttir** *(Instituto Geofísica, UNAM)*

Knowledge of the velocity structure of the crust and upper mantle can improve source studies and aid investigations into mantle dynamics. Using an initial data set of single-station phase measurements of surface waves recorded on the USArray Transportable Array, we investigate the phase-velocity structure of the western United States at discrete periods between 25-100 s using two different methods. First, we estimate the local phase velocity at a station by subdividing the array into a set of mini-arrays, defined to include all stations within 2° radius of the station of interest. This is done for each event. We perform a grid search over back azimuth, and for each trial location, a phase velocity is determined in the least-squares sense that best predicts the observed phase measurements at all stations within the mini-array. The optimal local phase velocity corresponds to the back azimuth yielding the smallest misfit to the observed phase. This back azimuth also provides an estimate of the arrival angle of the energy at the mini-array. Local phase-velocity results from all events for a single station are averaged to produce the map shown in figure 1a. Our second method is based on the difference in phase anomaly between two stations that record the same event and lie roughly along the same great-circle path. The resulting phase anomaly is assigned to the inter-station path. This is done for all events, and data comprised of the median measurement for each path are inverted to obtain a velocity map at a given period. These results can be further improved by correcting for the estimated arrival angle of the wave energy, since off-great-circle arrivals bias the two-station method to higher velocities. We calculate the arrival angle using the previously described method. The arrival angle is used to correct the inter-station distance to which the two-station phase anomaly is assigned prior to inversion, resulting in a small change in the final velocity (up to 2%). This correction has been done for the inversion results shown in figure 1b. Most anomalies observed in both models correspond with well-known geologic features. The strong similarities between these two maps indicate that the methods are robust, and provide encouragement for the ongoing investigation into earth structure.

Acknowledgements: This work is funded by NSF award EAR-0952285 under the EarthScope program.

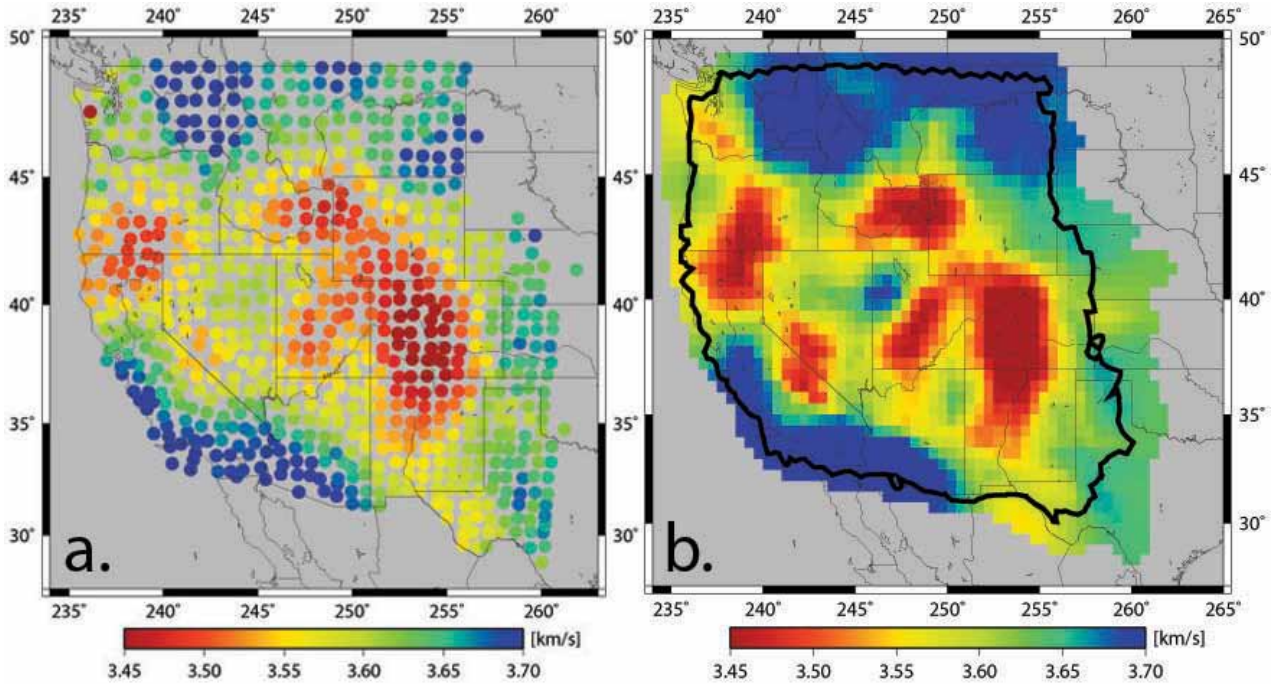

Figure 1: Phase velocity maps for Rayleigh waves at 25 s period. a) Averaged local phase velocity estimates from the mini-array method. b) Results of the inversion of two-station phase anomaly measurements that were corrected for the wave's arrival angle.

Imaging and Interpreting the Pacific Northwest

Eugene Humphreys *(University of Oregon),* **Brandon Schmandt** *(University of Oregon)*

Improved tomographic resolution of Pacific Northwest (PNW) upper mantle distinguishes two high velocity features in addition to subducted Juan de Fuca (JdF) ocean lithosphere:

50 m.y. old slab (Siletzia "curtain"). The large volume of this nearly vertical high-velocity "curtain" can only be attributed to subducted slab, and it lies where the Farallon ocean lithosphere subducted prior to Siletzia accretion at ~53 Ma (see figure). Flat-slab subduction probably occurred prior to accretion (55 Ma), during the amagmatic and compressive Laramide orogeny. We infer that the imaged curtain is Farallon slab that rolled back following accretion, leading to early ignimbrite flareup magmatism (the Challis trend) and core-complex extension that were active at 50 Ma.

Post-flood basalt drip (Wallowa "drip"). A spherical-shaped high-velocity body about 100 km across and centered at 250 km depth is imaged directly beneath the source area for the Columbia River flood basalts (CRB) and the resulting topographic bull's eye (see topography map). This feature could be downwelling North American lithosphere or basalt-depleted asthenosphere. Note that the CRB event occurred adjacent to the Siletzia curtain.

References

Schmandt, B. and Humphreys, E. 2010. Complex subduction and small-scale convection revealed by body-wave tomography of the western U.S. upper mantle. *Earth Planet. Sci. Lett.*, accepted.

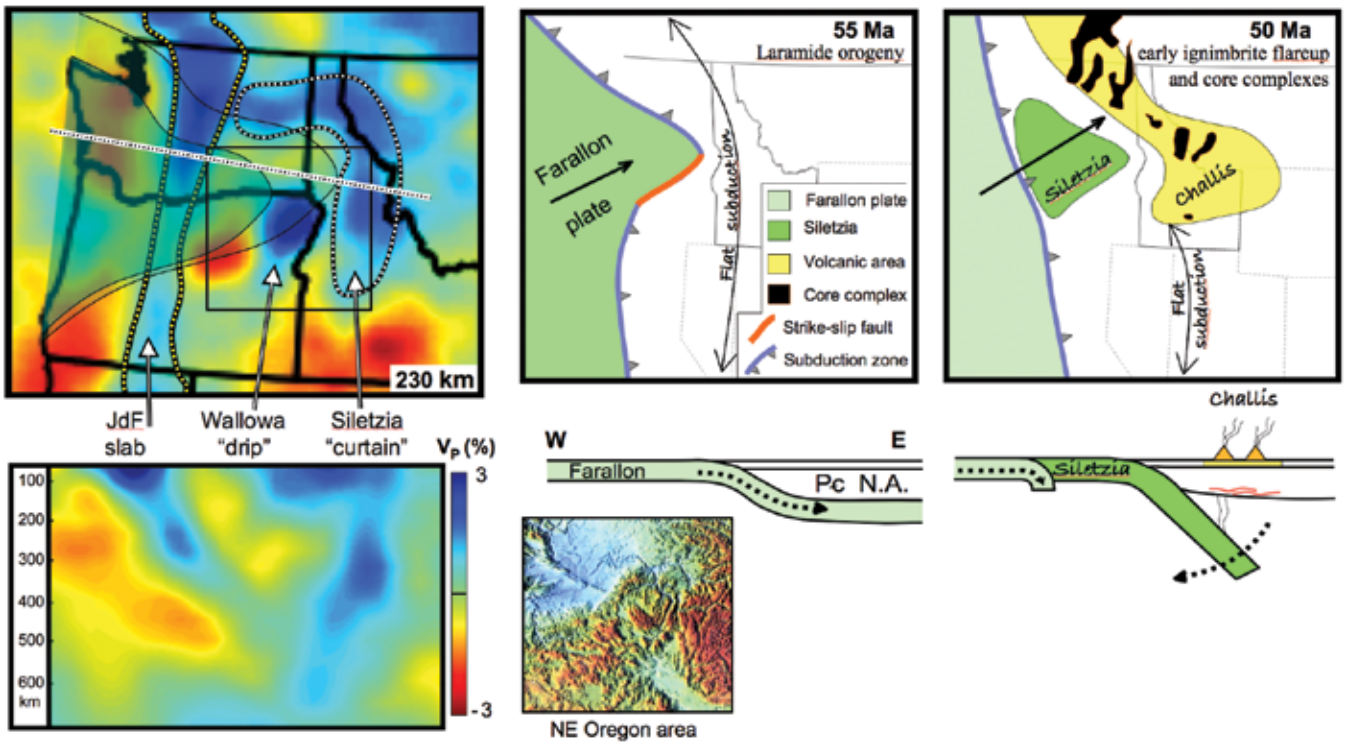

Upper and lower left panels show P tomography in map and cross-section, respectively. Center and right columns shows tectonic cartoons in map (upper) and cross-section (lower) of the PNW just before and just after Siletzia accretion. Dark gray = Siletzia. Light gray = Siletzia forearc. Bottom center panel shows a topographic map of CRB source area, with the high-standing Wallowa Mountains in the center of a topographic bull's eye.

Segmented African Lithosphere beneath Anatolia Imaged by Teleseismic P-wave Tomography

C. Berk Biryol *(University of Arizona),* **Susan L. Beck** *(University of Arizona),* **George Zandt** *(University of Arizona),* **A. Arda Ozacar** *(Middle East Technical University)*

Anatolia, a part of the Alpine-Himalayan orogenic belt, is shaped by a variety of complex tectonic processes that define the major tectonic provinces across which different deformation regimes exist. In order to study the deeper lithosphere and mantle structure beneath Anatolia, we used teleseismic P-wave tomography and data from several temporary and permanent seismic networks deployed in the region. A major part of the data comes from the North Anatolian Fault passive seismic experiment (NAF) that consists of 39 broadband seismic stations operated at the north central part of Anatolia between 2005 and 2008. The instruments for this experiment are provided by the IRIS-PASSCAL consortium. We also used data collected from permanent seismic stations of the National Earthquake Monitoring Center (NEMC) and stations from the Eastern Turkey Seismic Experiment (ETSE). Approximately 34,000 P-wave travel time residuals, measured in multiple frequency bands, are inverted using approximate finite-frequency sensitivity kernels. Our tomograms reveal a fast anomaly that corresponds to the subducted portion of the African lithosphere along the Cyprean Arc (Figure 1a). This fast anomaly dips northward beneath central Anatolia with an angle of approximately 45 degrees. However, the anomaly disappears rather sharply to the east beneath the western margin of the EAP and to the west beneath the Isparta Angle (IA). The western segment of the subducted African lithosphere appears as a continuous fast anomaly beneath the Aegean Sea (Figure 1b) separated from the eastern segment by a sub-vertical tear (Figure 1c). The tear between these segments is occupied by slow velocity anomalies that underlie the Kula Volcanic field in western Anatolia (Figure 1c). We conclude that the current segmented configuration of the subducted African lithosphere controls the geological configuration of Anatolia.

References

Acknowledgements: This research was supported by NSF grant EAR0309838.

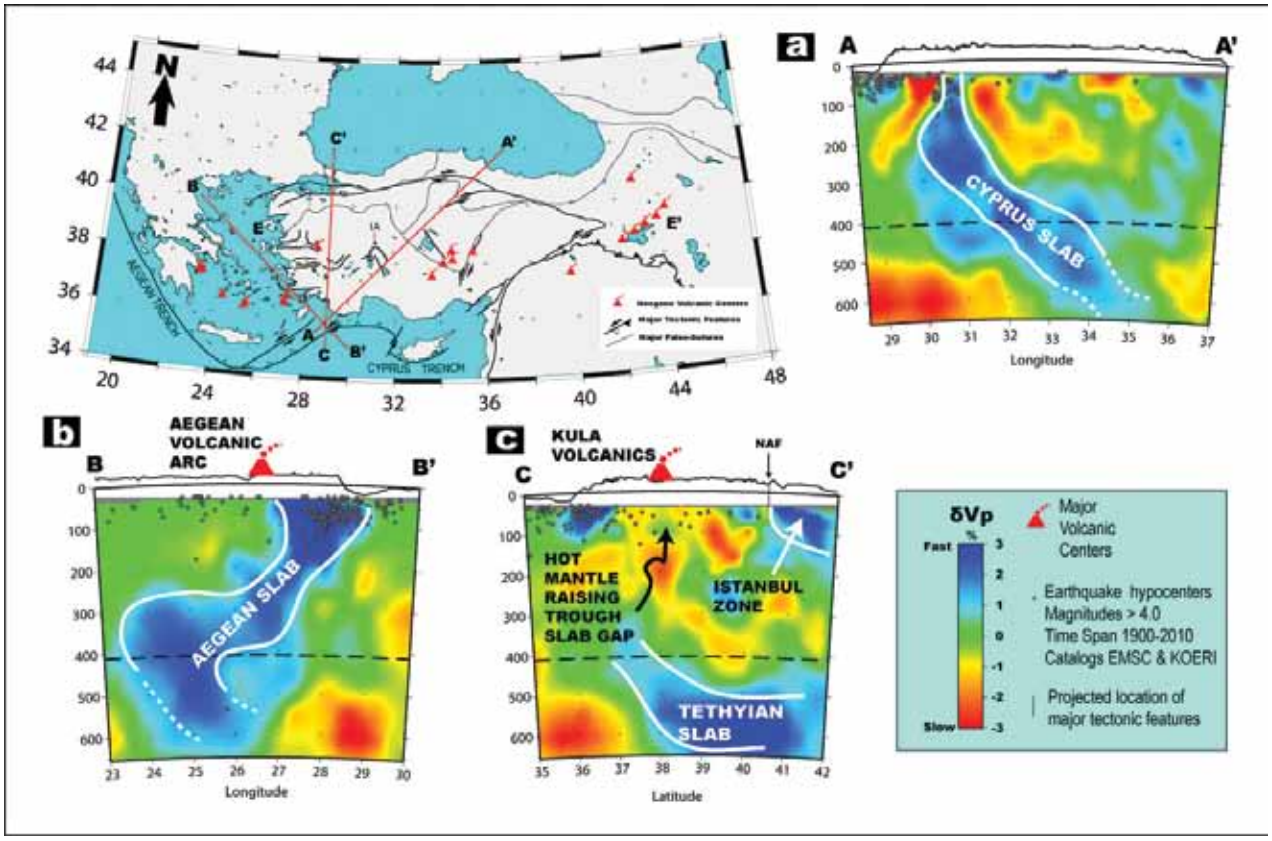

Vertical sections from our tomographic model. IA: Isparta Angle. a. The Cyprus slab and b. the Aegean slab dipping beneath Anatolia. c. The slab tear between the Cyprus and the Aegean slabs, occupied by raising hot mantle. Note that the slow velocity perturbations underlies the Kula volcanics.

High-resolution Images of Mantle-wedge Structure along the Western Hellenic Subduction Zone Using Scattered Teleseismic Waves

F. D. Pearce *(MIT),* **S. Rondenay** *(MIT),* **Maria Sachpazi** *(National Observatory of Athens),* **M. Charalampakis** *(National Observatory of Athens),* **A. Hosa** *(University of Edinburgh),* **J. Suckale (MIT), L. H. Royden** *(MIT)*

The Hellenic subduction zone is located in the east-central Mediterranean region and exhibits large variations in convergence rate along its western edge [McClusky et al., 2000]. Differences in the lithosphere entering the subduction zone are believed to drive the different rates of convergence. While recent work has shown evidence for subducted oceanic crust beneath southern Greece [Suckale et al., 2009], no detailed images of the mantle-wedge structure beneath northern Greece have been available to test this hypothesis. Here, we use high-resolution seismic images across northern and southern Greece to investigate differences in the subducted crust along the strike of the western Hellenic subduction zone. We deployed 40 broadband seismometers from the IRIS Passcal pool across Greece in a northern line (NL) and southern line (SL), each roughly perpendicular to the trench axis as shown in Figure 1a. We recorded over 50 high-quality teleseismic events with good azimuthal coverage from each line and processed them using a 2D migration algorithm based on the generalized radon transform. High-resolution images of perturbations in S-wave velocity reveal NE dipping low-velocity layers beneath both NL and SL as shown in Figure 1b. We interpret the ~10 km thick low-velocity layer beneath SL as subducted oceanic crust and the ~20 km thick low-velocity layer beneath NL as subducted continental crust. The two imaged subducted crusts connect smoothly with images from marine seismic surveys [Finetti, 2005] and show a progressive deepening of the oceanic crust of SL relative to the continental crust of NL (Figure 1c). We conclude that along strike changes in slab buoyancy cause differential rollback between the two segments, which helps drive the large difference in convergence rates along the western Hellenic subduction zone.

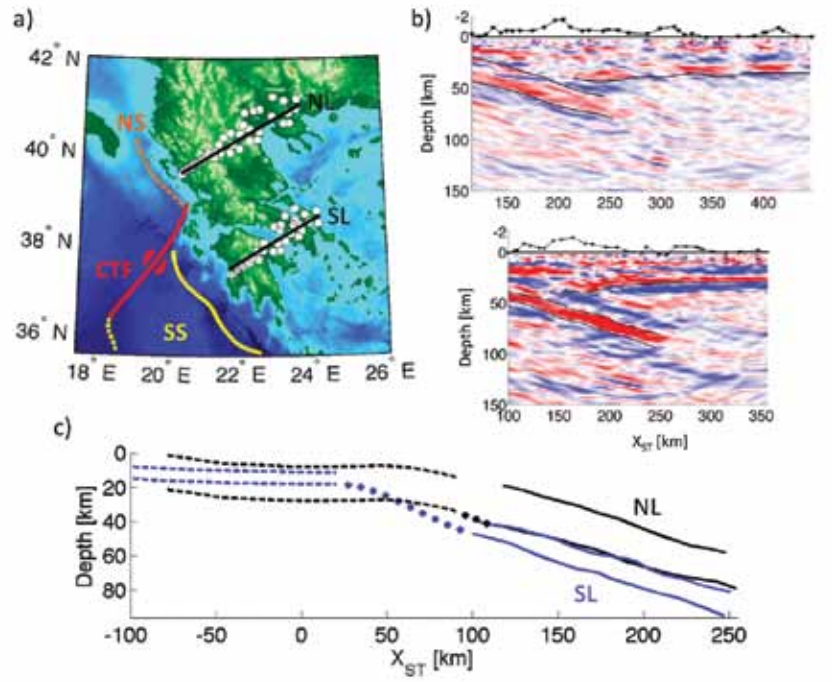

Figure 1: a) Map of study area showing location of southern segment (SS) and northern segment of western Hellenic subduction zone separated by the Cephalonia transform fault (CTF). White circles denote station locations for NL and SL deployments. b) Images of perturbation in S-wave velocity for SL (top) and NL (bottom) at -5% to +%5 (red to blue). Solid lines delineate top and bottom of low-velocity layer, and the Moho of overriding plate. X-axis is horizontal distance perpendicular to strike measured from the intersection of SL with the trench of southern segment (solid yellow line in a)). c) Comparison of subducted crusts imaged from marine seismics (dashed) and this study (solid) for NL (black) and SL (blue), with dots showing smooth interpolation.

References

Finetti, I. R. (2005), Depth contour map of the Moho discontinuity in the central Mediterranean region from new CROP seismic data, in CROP PROJECT: Deep seismic exploration of the central Mediterranean and Italy, edited by I. R. Finetti, pp. 597-606, Elsevier B.V., Amsterdam, The Netherlands.

McClusky, S. et al. (2000), Global Positioning System constraints on plate kinematics and dynamics in the eastern Mediterranean and Caucasus, *J. Geophys. Res., 105*(B3), 5695-5719.

Suckale J., S. Rondenay, M. Sachpazi, M. Charalampakis, A. Hosa, L. H. Royden (2009) High-resolution seismic imaging of the western Hellenic subduction zone using teleseismic scattered waves, *Geophys. J. Int., 178*(2), 775-791.

Acknowledgements: This project was carried out as part of project MEDUSA, funded by the NSF Continental Dynamics Program, grant EAR-0409373.

Imaging the Mantle Wedge in the Central America Subduction Zone: The TUCAN Broadband Seismic Experiment

Geoffrey Abers *(Lamont-Doherty Earth Observatory of Columbia University),* **Karen Fischer** *(Brown University),* **Ellen Syracuse** *(University of Wisconsin),* **Catherine Rychert** *(University of Bristol),* **Laura MacKenzie** *(Schlumberger Data and Consulting Services)*

Central America was selected as a MARGINS Focus Site for the Subduction Factory initiative. In order to understand how the Subduction Factory processes trench inputs into volcanic arc outputs, we make direct observations of mantle structure. The TUCAN (Tomography and other observations Under Costa Rica And Nicaragua) experiment deployed 48 broadband seismographs in the Central America Focus Site in 2004-6. This One-Pager shows results from three kinds of imaging in Nicaragua, where arc output features globally significant geochemical signatures of subduction. The migrated receiver function image (A) shows a strong P-S conversion from what appears to be the top of the subducting plate to 200 km depth, the first time a steep slab has been imaged with these kinds of signals. The velocity contrast at the top of the plate is sharp and below the seismicity shallower than 80 km depth, probably Moho of the subducting crust. Deeper, the mode conversion is broad, consistent with the 15-30 km gradient expected for the thermal boundary layer. Seismic attenuation (B), a proxy for temperature, indicates a typically hot wedge beneath arc and backarc, quantitatively consistent with temperatures and water contents inferred from primitive lavas and melt inclusions [*Plank et al., 2007*]. The updip limit of hot mantle is inferred to be where the slab reaches 80 km depth. These two images show that the subducting crust passes from beneath cold to hot mantle and rapidly metamorphoses to eclogite. The ratio of P to S velocities, Vp/Vs (C), shows a somewhat different pattern, near-normal values for much of the wedge but a narrow, high-Vp/Vs column ascending nearly vertically from the slab to the volcanic arc. Since this pattern differs from that of 1/Qs or 1/Vp alone, this anomaly cannot be purely due to temperature. The presence of partial melt could produce such an effect, and given the relationship between 1/Qs, Vp/Vs and the location of the arc. Thus, we are imaging separately but in one place the wedge geometry, temperature structure and melt distribution across the subduction factory, one of the major goals of MARGINS.

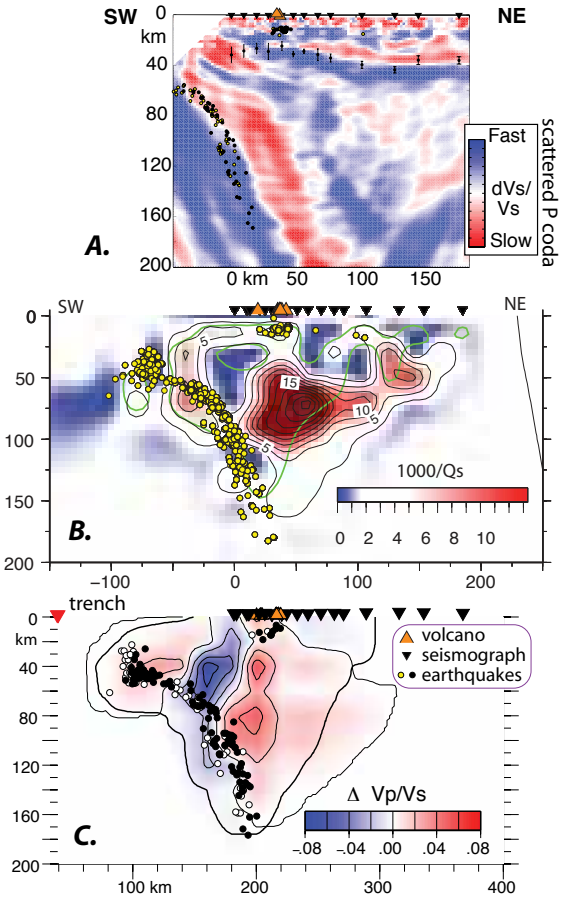

Three seismic images of the Nicaragua Subduction Factory. (A) 2D receiver function migration (MacKenzie et al., 2008, 2010). Image shows S-wave velocity variations needed to generate scattered wavetrain, such as Moho and top of subducting plate. (B) S-wave attenuation as 1000/Qs, from tomographic inversion (Rychert et al., 2008), at 1 Hz. 1/Qs responds to temperature and indicates high-temperature region beneath and behind arc. (C) Vp/Vs anomalies from regional travel-time tomography (Syracuse et al., 2008). In regions of high temperature, high Vp/Vs may indicate presence of melt, perhaps showing a vertical melt column beneath volcanic arc.

References

MacKenzie, L.M., G.A. Abers, S. Rondenay and K.M. Fischer, Imaging a steeply dipping subducting slab in southern Central America, *Earth Planet. Sci. Lett.*, in press, 2010.

MacKenzie, L.S., G.A. Abers, K.M. Fischer, E.M. Syracuse, J.M. Protti, V. Gonzalez, and W. Strauch, Crustal structure along the southern Central American volcanic front, Geochem. *Geophys. Geosyst., 9*, Q08S09, 2008. doi:10.1029/2008GC001991

Rychert, C.A., K.M. Fischer, G.A. Abers, T. Plank, E.M. Syracuse, J.M. Protti, V. Gonzalez, and W. Strauch, Strong along-arc variations in attenuation in the mantle wedge beneath Costa Rica and Nicaragua, *Geochem. Geophys. Geosyst., 9*, Q10S10, 2008. DOI: 10.1029/2008GC002040

Syracuse, E.M., Abers, G.A., K.M. Fischer, McKenzie, L., C. Rychert, J. M. Protti, V. Gonzalez, and W. Strauch, Seismic tomography and earthquake locations in the Nicaraguan and Costa Rican upper mantle, *Geochem. Geophys. Geosyst., 9*, Q07S08, 2008. doi:10.1029/2008GC001963

Acknowledgements: The TUCAN project was carried out in close collaboration with M. Protti and V. Gonzalez of OVSICORI/UNA in Costa Rica, and W. Strauch and colleagues of INETER in Nicaragua. This work funded by the National Science Foundations's MARGINS program, under awards OCE-0203650 (Boston Univ.) and OCE-0203607 (Brown).

Systematic Variation in Anisotropy beneath the Mantle Wedge in the Java-Sumatra Subduction System from Shear-Wave Splitting

J.O.S. Hammond *(University of Bristol, UK),* **J. Wookey** *(University of Bristol, UK),* **S. Kaneshima** *(Kyushu University, Japan),* **H. Inoue** *(Klimatologi dan Geofisika, Indonesia),* **T. Yamashina** *(Klimatologi dan Geofisika, Indonesia),* **P. Harjadi** *(Klimatologi dan Geofisika, Indonesia)*

The tectonic context of south-east Asia is dominated by subduction. One such major convergent boundary is the Java-Sunda trench, where the Australian-Indian plates are being subducted beneath the Eurasian plate. We measure shear-wave splitting in local and teleseismic data from 12 broadband stations across Sumatra and Java to study the anisotropic characteristics of this subduction system. Splitting in S-waves from local earthquakes between 75-300km deep show roughly trench parallel fast directions, and with time-lags 0.1-1.3s (92% less that 0.6s). Splitting from deeper local events and SKS, however, shows larger time-lags (0.8-2.0s) and significant variation in fast direction. To model deformation in the subduction zone we ray-trace through an isotropic subduction zone velocity model, obtaining event to station raypaths in the upper mantle. We then apply appropriately rotated olivine elastic constants to various parts of the subduction zone, and predict the shear-wave splitting accrued along the raypath. Finally, we perform grid searches for orientation of deformation, and attempt to minimise the misfit between predicted and observed shear-wave splitting. Splitting from the shallow local events is best explained by anisotropy confined to a 40km over-riding plate with horizontal, trench parallel deformation. However, in order to explain the larger lag times from SKS and deeper events, we must consider an additional region of seismic anisotropy in or around the slab. The slab geometry in the model is constrained by seismicity and regional tomography models, and many SKS raypaths travel large distances within the slab. Models placing anisotropy in the slab produce smaller misfits than those with anisotropy outside for most stations. There is a strong indication that inferred flow directions are different for sub-Sumatran stations than for sub-Javanese, with >60 degrees change over ~375km. The former appear aligned with the subduction plate motion, whereas the latter are closer to perpendicular, parallel to the trench direction. There are significant differences between the slab being subducted beneath Sumatra, and that beneath Java: age of seafloor, maximum depth of seismicity, relative strength of the bulk sound and shear-wave velocity anomaly and location of volcanic front all vary along the trench. We speculate, therefore, that the anisotropy may be a fossilised signature rather than due to contemporary dynamics.

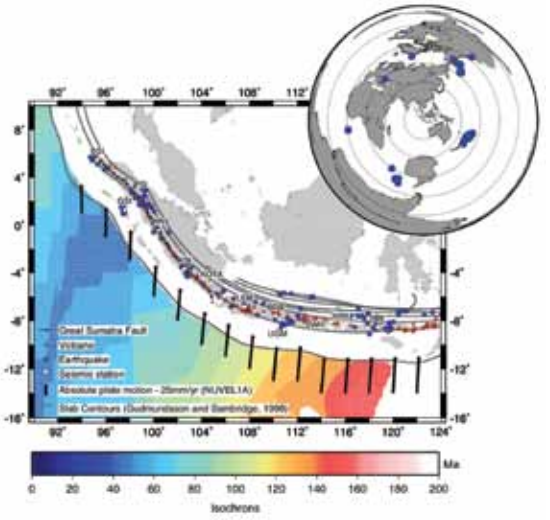

Map showing stations and events used in this study. White inverted triangles mark stations, blue circles show earthquakes (local events on main map, teleseismic events on top right map). Also shown are quaternary volcanos (red triangle), absolute plate motions (Gripp and Gordon (1990), black arrows), slab contours at 100 km depth intervals (Gudmundsson and Sambridge, 1998), the Great Sumatra Fault, and Isochrons (Müller et al., 1997).

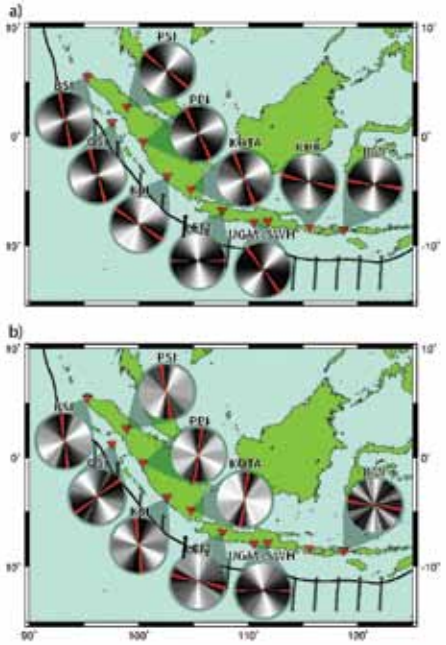

Density rotorgrams for models of subduction zone anisotropy showing the best fitting orientations obtained from forward modelling. (a) Olivine orientations best fitting the splitting results (red bars) obtained from local events <300 km deep; these are predominantly trench parallel. (b) Olivine orientations best fitting splitting results from local events >300 km deep and SKS/SKKS-wave splitting results (red bars). Note the rotation from north-south orientations beneath Sumatra (GSI is an exception), and the east west anisotropy orientations beneath Java. The complicated pattern at BMI reflects the scatter observed in the data. We speculate that this is due to complications arising from the slab bending beneath this station.

References

Hammond, J. O. S., Wookey, J., Kaneshima, S., Inoue, H., Yamashina, T., Harjadi, P. (2010). Systematic variation in anisotropy beneath the mantle wedge in the Java-Sumatra subduction system from shear-wave splitting. *Phys. Earth Planet. Int., 178*, 189-201.

Acknowledgements: Data used in this paper was provided by the Japan Indonesian Seismic Network (JISNET), IRIS, GEOFON and the Ocean Hemisphere Network Project, courtesy of the Earthquake Research Institute, University of Tokyo. This research was funded by a Japan Society for the Promotion of Science (JSPS) postdoctoral fellowship (short term), JSPS/FF1/367

A Slab Remnant beneath the Gulf of California

Hanneke Paulssen *(Utrecht University),* **Xiaomei Zhang** *(Utrecht University),* **Jeannot Trampert** *(Utrecht University),* **Robert Clayton** *(California Institute of Technology)*

Active extension in the Gulf of California is characterized by the transition from continental rifting to seafloor spreading. Puzzling variations in the patterns of both tectonics and magmatism are observed along the length of the gulf and are likely to be related to mantle heterogeneity. Regional-scale mantle structure, however, has been difficult to constrain due to the lack of broadband seismic stations in the region. In this study we utilized data from the deployment of the NARS-Baja array and other networks, and computed a three-dimensional shear-speed model of the upper mantle beneath the region. Applying a combination of cross-correlation analysis and multimode waveform inversion, we measured interstation Rayleigh wave dispersion for 450 pairs of stations in a broad period range of 9–250 s. We computed phase velocity maps and then inverted the phase-velocity data for shear-speed structure. Our results suggest that the location of the transition from seafloor spreading (South) to continental rifting (North) in the Gulf of California, as well as differences in volcanism across Baja California and the gulf, can be explained by heterogeneity in the upper mantle, in particular by the presence of a slab remnant beneath the south-central part and an absence of such a slab remnant beneath the northern part of the gulf.

References

Trampert J., H. Paulssen H, A. van Wettum, J. Ritsema, R. Clayton, R. Castro, C. Rebollar, and A. Perez-Vertti (2003) New array monitors seismic activity near Gulf of California, Mexico, Eos, 84, 4, pp 29,32.

Zhang X., H. Paulssen, S. Lebedev, and T. Meier (2007) Surface wave tomography of the Gulf of California, *Geophys. Res. Lett., 34*, L15305, doi:10.1029/2007GL030631.

Zhang X., H. Paulssen, S. Lebedev, and T. Meier (2009) 3D shear velocity structure beneath the Gulf of California from Rayleigh wave dispersion, *Earth Planet. Sci. Lett., 279*, 255-262.

Acknowledgements: Funding for this project was provided by the U.S. National Science Foundation (Grant number EAR-0111650 of the MARGINS program) and the Dutch National Science Foundation (Grant number NWO-GOA-750.396.01).

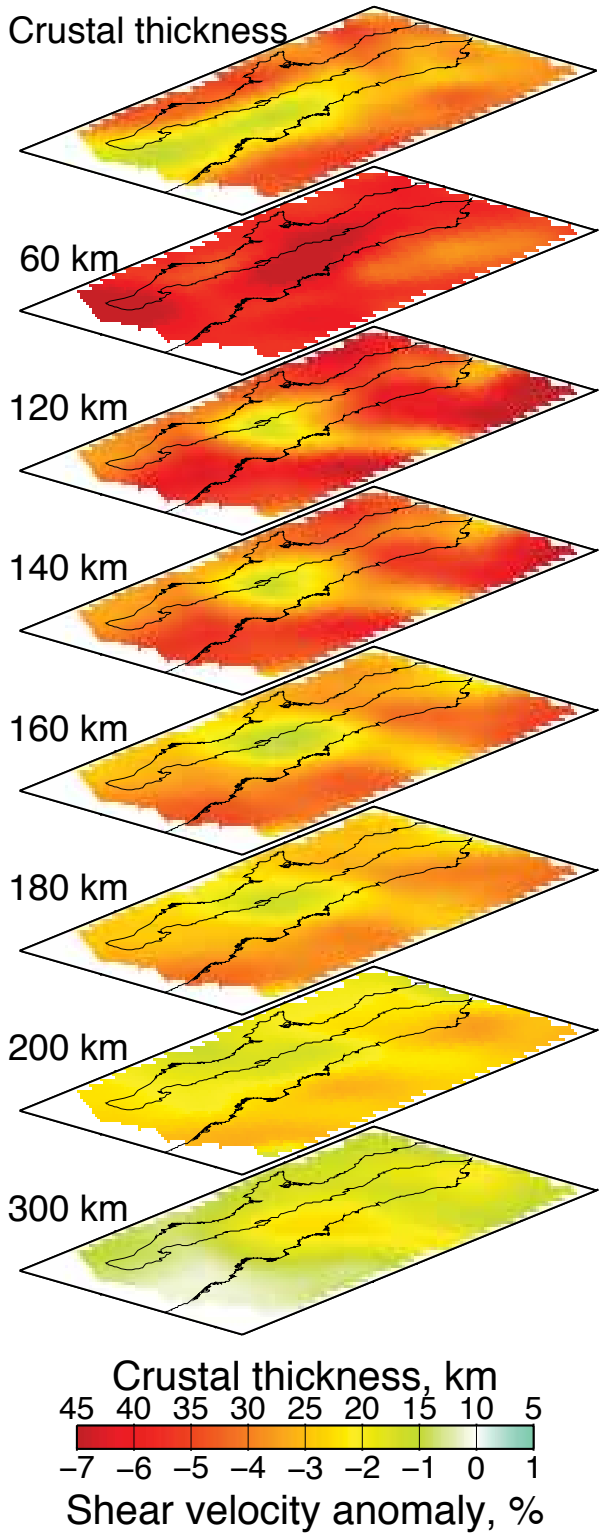

Maps of the crustal thickness (upper panel), and the shear velocity anomalies relative to the global reference model AK135 (Kennett et al., 1995) at depths of 60, 100, 120, 160, 200, and 300 km. The slab remnant is imaged as the relatively high velocity anomaly beneath the south-central part of the Gulf of California at depths between roughly 120 and 160 km.

Three-Dimensional Geometry of the Juan de Fuca/farallon Slab

Gary Pavlis *(Department of Geological Sciences, Indiana University, Bloomington)*

New understanding on the three-dimensional geometry of the western US subduction system is emerging by viewing multiple imaging results in a fully three-dimensional framework. The process is comparable to interpreting 3D seismic reflection data, but is complicated in USArray by the scale, which makes spherical geometry important. The figure shown is a first attempt at a joint interpretation of P tomography models by Burdick et al. [2009], Sigloch et al. [2008], and recently produced scattered wave images of Pavlis [submitted]. The scattered wave images show dipping features above the 410 km discontinuity I have interpreted as defining a shear zone at the boundary layer between the subducting slab and the overriding North American plate. The model shown in this figure is a kinematic model showing flow lines and constant time lines based on the current relative motion of the Juan de Fuca and North American plates. The surface is interpreted from data, but the time lines assume no longitudinal strain in the descending slab. The visualization shows the predicted edge of the slab window from the San Andreas based on the no longitudinal strain approximation and using the current trace of the San Andreas as an anchor point. The new scattered wave images and the reasonable geometry of this slab model provide strong support for the model of the Farallon slab described by Sigloch et al. [2008].

References

Burdick, S., C. Li, V. Martynov, T. Cox, J. Eakins, T. Mulder, L. Astiz, F. L. Vernon, G. L. Pavlis, and R. D. van der Hilst, 2009, Model update December 2008; upper mantle heterogeneity beneath North America from P-wave travel time tomography with global and USArray transportable array data, *Seismol. Res. Lett., 80*(4), 384-392, doi: 10.1785/gssrl.80.4.638.

Pavlis, G. L., submitted, Three-dimensional Wavefield Imaging of Data from the USArray: New Constraints on the Geometry of the Farallon Slab, *Geosphere*, in review.

Sigloch, K., N. McQuarrie, and G. Nolet, 2008, Two-stage subduction history under North America inferred from multiple-frequency tomography, *Nature Geosci., 1*, 458-462, doi:10.1038/ngeo231.

Acknowledgements: This work was supported by the National Science Foundation under CMG-0327827. It also benefited from advanced computing resources provided by the National Science Foundations TeraGrid program at Indiana University.

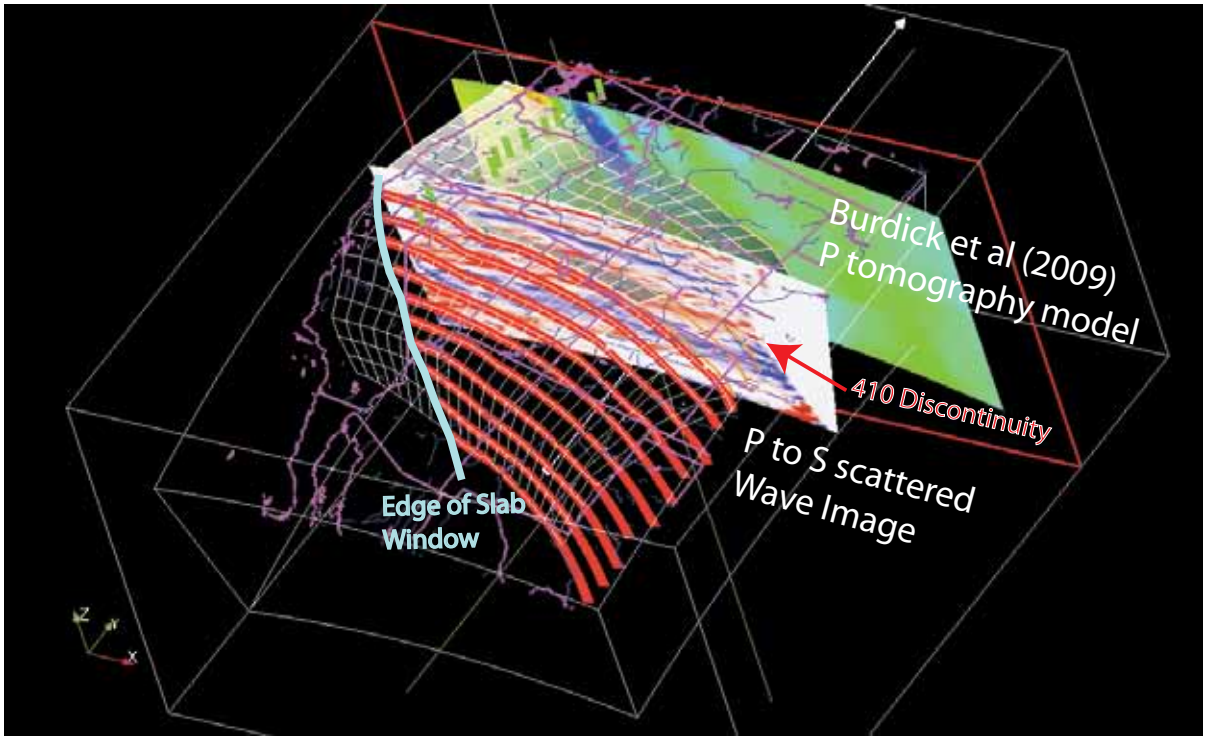

Juan de Fuca/Farallon lab model in 3D visualization framework. This is a still image from a 3D visualization scene used to overlay tomography models and results of a recently developed full 3D, scattered wave imaging method. Coastlines and state boundaries in magenta and rivers shown in blue provide a geographic reference. A section through the Burdick et al. (2009) P model and a section through the scattered wave image are shown to illustrate data that went into the interpretation. The slab model shows flow lines and constant time surface based on the NUVEL1 model of relative plate motion. The time ticks are based on a no strain approximation. The surface is constrained to daylight at the trench and pass through points 100 km below all active volcanoes in the Pacific Northwest. A estimate of the western edge of the slab window based on the no strain approximation is shown as the blue line passing through California and Arizona.

Imaging the Southern Alaska Subduction Zone

Josh A. Calkins *(Lamont-Doherty Earth Observatory),* **Geoffrey A. Abers** *(Lamont-Doherty Earth Observatory),* **Douglas Christensen** *(University of Alaska Fairbanks),* **Stéphane Rondenay** *(Massachusetts Institute of Technology),* **Jeffrey T. Freymueller** *(University of Alaska Fairbanks)*

The southern Alaska subduction zone, where the Pacific plate and the thick Yakutat block subduct beneath the accreted terranes that make up the margin of the North American plate, produced one of the largest ever instrumentally recorded earthquakes: the Mw 9.2 Good Friday earthquake of 1964. Between 1999 and 2009, two PASSCAL arrays were deployed between the coast and 400 km inland, with the aim of imaging the source region of the 1964 earthquake. Using data from the southern array (the "Multidisciplinary Observations of Onshore Subduction" or MOOS array), we produced 2-D scattered wavefield migration images of the upper 80 km of the subduction zone (top center panel in the figure). The cross sections show results of inverting forward and back-scattered S waves for perturbations in Vs, and highlight sharp changes or gradients in seismic velocities.

Our results reveal a shallowly north-dipping low velocity zone that is contiguous on its downdip end with previously obtained images of the subducting plate further north [*Rondenay et al., 2008*], and suggest that both the dip angle and the thickness of the subducting low velocity zone change along strike, across a roughly NNW-SSE striking line drawn through the eastern Kenai Peninsula. Previous geodetic studies [*Suito and Freymueller, 2009*] indicate a distinct change in locking at the subduction interface along the same NNW-SSE boundary. On the west end of the Kenai Peninsula, where seismically imaged downgoing crust appears oceanic, the geodetic signal mainly reflects postseismic deformation from the 1964 earthquake as evinced by southeast trending displacement vectors. While postseismic relaxation also continues on the eastern Kenai Peninsula, NNW-directed elastic deformation due to locking at the plate boundary dominates the geodetic signal, and imaging reveals thickened Yakutat crust is subducting. The collocation of sharp changes in both deep structure and surface deformation suggests that the nature of the plate interface changes drastically across the western edge of the Yakutat block and that variations in downgoing plate structure control the strain field in the overriding plate.

References

Brocher, T. M., G. S. Fuis, M. A. Fisher, G. Plafker, M. J. Moses, J. J. Taber, and N. I. Christensen (1994), Mapping the Megathrust beneath the Northern Gulf of Alaska Using Wide-Angle Seismic Data, *J. Geophys. Res., 99*(B6), 11663-11685.

Rondenay, S., G. A. Abers, and P. E. Van Keken (2008), Seismic imaging of subduction zone metamorphism, *Geology, 36*(4), 275-278.

Suito, H. and J.T. Freymueller (2009). A viscoelastic and afterslip postseismic deformation model for the 1964 Alaska earthquake, *J. Geophys. Res., 114* B11404.

Acknowledgements: This work was supported by NSF grant EAR-0814235.

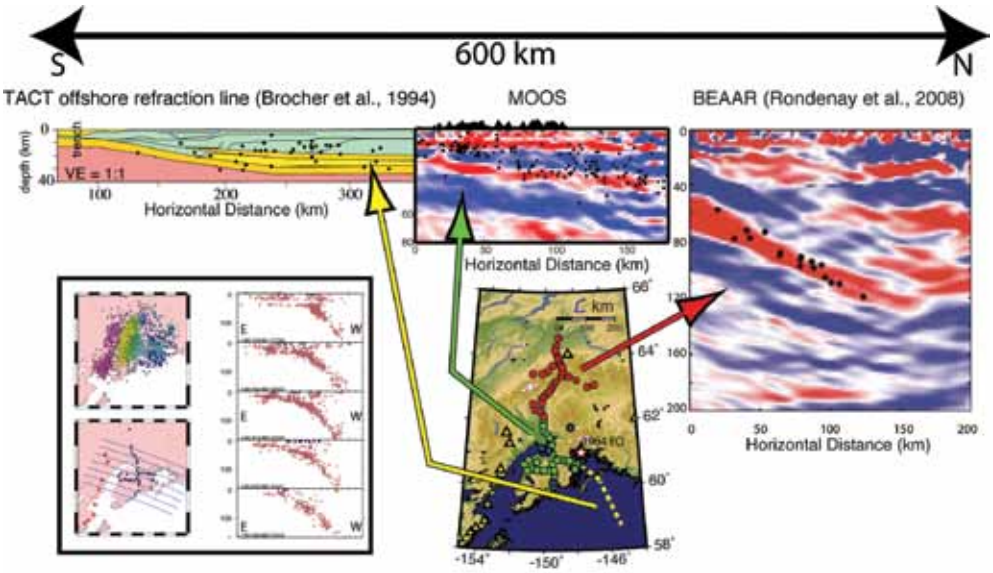

Seismicity and migration imaging results from the BEAAR (Rondenay et al, 2008) and MOOS broadband arrays. Upper (center and right) panels show results of scattered wavefield migration and clearly image the subducting oceanic crust as a prominent N- dipping low velocity (red) structure. Black circles mark the locations of earthquakes located using the two arrays. Joint migration of the two broadband data sets is a work in progress, and when combined with results from the TACT experiment (top left, Brocher et al., 1994)), these data will illuminate the structure along a 600 km cross-strike pro¬file of the southern Alaska subduction zone. The map (bottom center) shows the location of the arrays, and the inset in lower left shows the locations of earthquakes as determined by the MOOS array.

S-Velocity Mantle Structure at the Subducting Chile Ridge

Simon Lloyd *(Northwestern University),* **Suzan van der Lee** *(Northwestern University),* **Raymond M Russo** *(University of Florida),* **Diana Comte** *(University of Chile),* **Victor I Mocanu** *(Bucharest University),* **Alejandro Gallego** *(University of Florida),* **Ruth Elaine Murdie** *(Gold Fields Australia, St Ives Gold Mine),* **John C VanDecar** *(Carnegie Institution of Washington)*

At the triple junction between the Nazca, Antarctica and South American plate an actively spreading ridge is currently being subducted. The ridge continues to spread as it gets subducted beneath South America. However, no new lithosphere is formed in the process. As a result slab windows likeley exist beneath the overiding plate. These gaps allow asthenospheric mantle to flow through the slab, effecting mantle chemistry and thermal regime, seismic velocities and anisotropy as well as surface geology (*e.g.* gaps in arc volcanism).

Slab windows have sucessfully been imaged using P wave tomography [*Russo et al., 2009*]. In this study we analyze Rayleigh waves as they traverse the Chile Ridge Subduction Project (CRSP) array, in order to determine if additional constraints may be obtained from surface wave analysis.

We easily cross-correlated waveforms from an event at different stations to determine the relative arrival times, which allowed us to image the wavefront as it passes through the array. Typical for many events recorded at the CRSP array are wavepaths following the boundary between the Nazca and South American plates. For these events the incoming wavefront is not perpendicular to the great circle paths connecting the source and the receivers.

In order to get a first order estimate of the Rayleigh wave phase velocities we split the array into four regions defined by the 73°W meridian and 46°S parallel. We then invert relative arrival times for the average phase velocity within the defined regions. We repeat the inversion for several events, and combine the results. We conclude that

- Imaging Rayleigh wavefronts as they traverse the array region shows that particularly at shorter periods (*e.g.* 30 s) they are not perpendicular to the great circle path connecting the earthquake source and the seismometers.
- This needs to be taken into consideration when determining the phase velocities.
- A strong velocity contrast between the E (slow) and the W (fast) is derived from the delay times.
- Possibly a similar distinction can be made between the N (fast) and the S (slow).

References:

Russo, R.M., VanDecar, J.C., Comte, D., Mocanu, V.I., Gallego, A. Murdie, R.E., 2010. Subduction of the Chile Ridge: upper mantle structure and flow, *GSA Today*, in press.

Acknowledgements: This work was supported by National Science Foundation grant EAR 0538267.

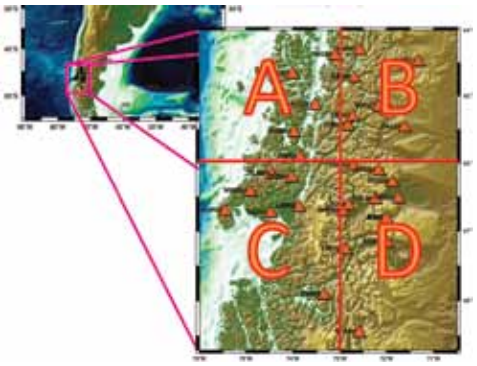

We deployed 39 broadband seismic stations from PASSCAL in southern Chile, aiming to investitgate the possible existance and effects of slab windows.

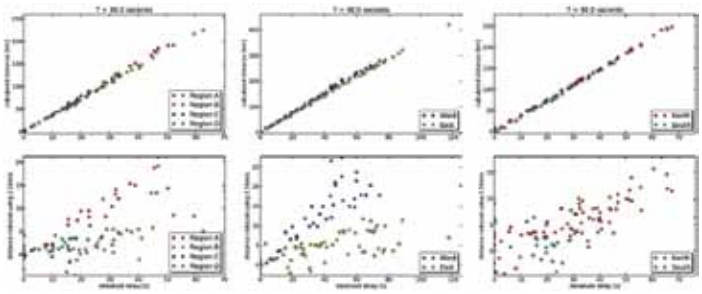

(left) The average Rayleigh wave phase velocity in region A is distinctly higher than in the other regions. (middle) Velocites in the west of the array are clearly higher than in the east. (right) The north-south contrast is not as strong, but the south appears be slightly slower than the north.

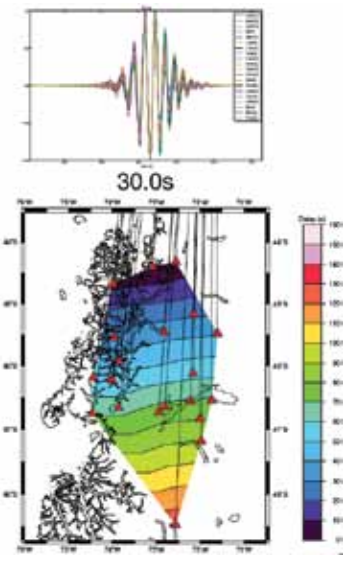

Owing to the small station spacing, the recorded waveforms are very similar at all stations. (below) For wavepaths following the boundary between the Nazca and South American plates, the incoming wavefront is not perpendicular to the great circle paths.

Opposing Slabs under Northern South America

M.J. Bezada *(Rice University, Earth Science Department),* **Alan Levander** *(Rice University, Earth Science Department),* **B. Schmandt** *(University of Oregon, Department of Geological Sciences),* **Fenglin Niu** *(Rice University, Earth Science Department),* **M. Schmitz** *(FUNVISIS, Caracas, Venezuela)*

The eastern boundary of the Caribbean plate is marked by subduction of the Atlantic under the Caribbean plate forming the Lesser Antilles volcanic arc. The southeastern plate boundary is a strike-slip margin while different configurations of subduction of the southwestern Caribbean under South America have been proposed. Using data from the BOLIVAR/GEODINOS experiment [*Levander*, 2006] we investigated the slab geometry in the upper mantle using finite-frequency, teleseismic P-wave tomography. Waveforms from P and PKIKP phases from 285 (Mb > 5.0) events occurring at epicentral distances from 30o to 90o and greater than 150o were bandpass filtered and cross-correlated to obtain up to three sets of delay times for each event. The delay times were inverted using first Fresnel zone approximate finite-frequency kernels. Our results show the subducting Atlantic slab, as well as a second slab in the west of the study area that we interpret as a subducting fragment of the Caribbean plate. Both slabs have steep dips where imaged and can be traced to depths greater than 600 km (Bottom figure). These results are consistent with transition zone boundary topography as determined by receiver function analysis (Juang et al, 2009. Top and middle figures). The Atlantic slab extends continentward south of the South America-Caribbean plate bounding strike-slip margin. We interpret part of this extension south of the faults as continental margin lithospheric mantle that is detaching from beneath South America and subducting along with the oceanic Atlantic slab. The steep subduction of the Caribbean occurs ~600 km landward from the trench, implying an initial stage of shallow subduction as far to the east as the Merida Andes-Maracaibo region, as has been inferred from intermediate depth seismicity. (Submitted to J. Geophys. Res.)

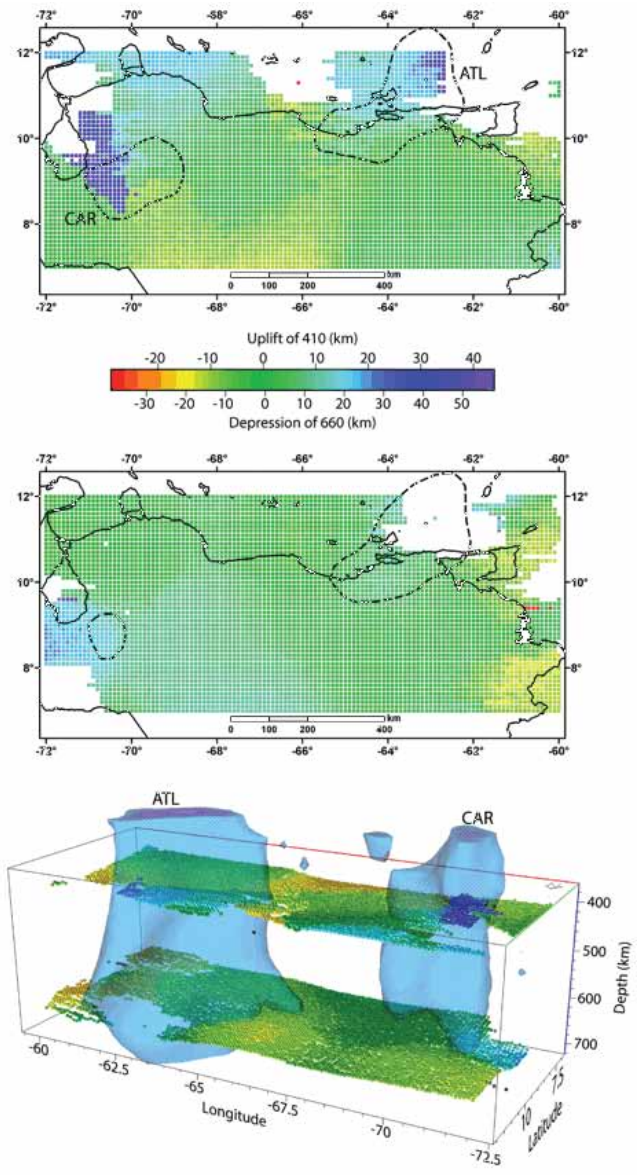

Subducting plate structure under northern South America and the southern Caribbean. ATL is the Atlantic (oceanic South American) plate, CAR is the Caribbean plate. Top: Depth of the 410 discontinuity showing elevated boundary where the slabs intersect the 410. Middle: Depth of the 660 discontinuity showing depressed boundary where the slabs intersect the 660. Bottom: 3D structure viewed from the northwest. The isosurface is the +1.5% anomaly. ATL subducts westward beneath CAR and northern South America. CAR subducts eastward beneath northern CA.

References

J.P. Huang, E. Vanacore, F. Niu, and A. Levander, 2009, Mantle transition zone beneath the Caribbean-South American plate boundary and its tectonic implications, *Earth Planet. Sci. Lett., 289*, 105-111

Levander, A., and 10 others, 2006, Evolution of the Southern Caribbean Plate Boundary, EOS, Trans. AGU, 87, Cover story, 97 and 100-101.

Acknowledgements: We would like to thank our colleagues at FUNVISIS, Caracas, Venezuela, the personnel at the PASSCAL Instrument Center and at OBSIP, and Gary Pavlis and Frank Vernon for outstanding data collection. BOLIVAR was funded by NSF Continental Dynamics Program grants EAR0003572 and EAR0607801, as well as by CONICIT and PDVSA. The 3D graphics were generated using EarthVision¨ software from Dynamic Graphics, Inc.

Arc-Parallel Flow beneath the TUCAN Broadband Seismic Experiment in Central America

David L. Abt *(ExxonMobil Exploration Company),* **Karen M. Fischer** *(Brown University),* **Geoffrey A. Abers** *(Lamont-Doherty Earth Observatory, Columbia University)*

Resolving the geometry of flow in subduction zones is essential in understanding mantle wedge thermal structure, slab dehydration, melting and melt transport in the wedge, and subduction zone dynamics. The TUCAN Broadband Seismic Experiment deployed 48 broadband IRIS/PASSCAL seismometers in Nicaragua and Costa Rica from 2004-2006. In three-dimensional models of anisotropy obtained by tomographically inverting shear-wave splitting measurements from local events recorded by the TUCAN array, olivine a-axes are predominantly arc-parallel in the mantle wedge beneath the arc and back-arc at depths of 50 to 150 km (except in northern Nicaragua). The arc-parallel a-axes extend into mantle wedge well beyond the cold, shallow wedge corner where B-type olivine fabric may occur. The observed anisotropy cannot be explained by simple two-dimensional arc-normal corner flow, and instead suggests significant arc-parallel flow. This hypothesis is confirmed by the trend of a distinct Pb and Nd isotopic signature in arc lavas associated with subducting seamounts offshore of Costa Rica. The anomalous signature systematically decreases for nearly 400 km from a maximum in central Costa Rica, directly inboard of the seamounts, down to background levels in northwestern Nicaragua. As the timing of the initial input of the isotopic signature beneath Costa Rica can be constrained and its transport distance is known, northwestward flow rates can be estimated (~63–190 mm/y) and are comparable to the magnitude of subducting Cocos plate motion (~85 mm/y). These results indicate flow in the mantle wedge can be significantly three-dimensional. Shear-wave splitting in SK(K)S phases recorded by the TUCAN array shows arc-parallel fast directions but significantly larger splitting times than seen in local S phases, indicating significant anisotropy consistent with arc-parallel flow below the slab.

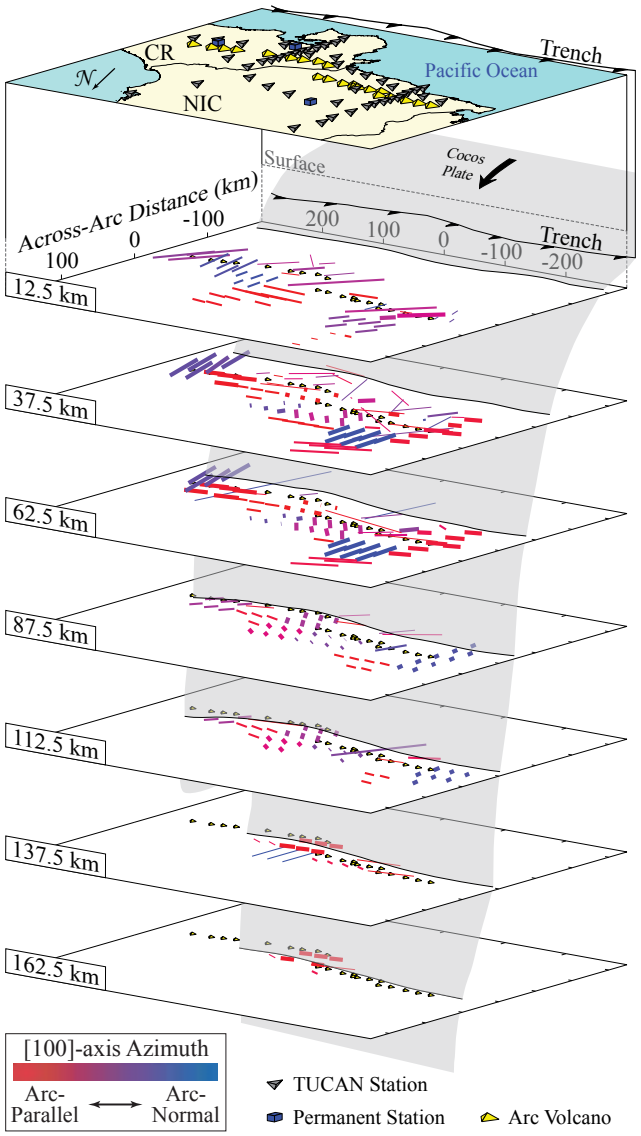

Model of anisotropy in the Nicaragua-Costa Rica subduction zone. Vectors represent well-resolved olivine a-axes in an olivine-orthopyroxene model. Vector orientation and color indicate horizontal azimuth, length corresponds to the strength of anisotropy relative to single-crystal values, and thickness corresponds to model parameter resolution. The TUCAN seismic array and volcanic arc are shown at the surface, and the volcanic arc position is plotted on each slice through the model. The slab–wedge interface is shown by grey shading. The mantle wedge is located in front of the slab in the layers spanning 50–175 km depth. Roughly arc-parallel a-axes dominate well-resolved wedge regions beneath the arc and the rear- and back-arc at depths of 50–150 km.

References

Abt, D. L., K. M. Fischer, G. A. Abers, J. M. Protti, V. González, and W. Strauch (2010), Constraints on upper mantle anisotropy surrounding the Cocos Slab from SK(K)S splitting, *J. Geophys. Res., 115*, B06316.

Abt, D. L., K. M. Fischer, G. A. Abers, W. Strauch, J. M. Protti, and V. González (2009), Shear wave anisotropy beneath Nicaragua and Costa Rica: Implications for flow in the mantle wedge, *Geochem. Geophys. Geosyst., 10*, Q05S15.

Hoernle K., D.L. Abt, K.M. Fischer, H. Nichols, F. Hauff, G. Abers, P. van den Bogaard, G. Alvarado, M. Protti, W. Strauch (2008), Geochemical and geophysical evidence for arc-parallel flow in the mantle wedge beneath Costa Rica and Nicaragua, *Nature, 451*, 1094-1098.

Acknowledgements: This research was supported by the NSF MARGINS program under awards OCE-0203650 (Boston University), and OCE-0203607 and EAR-0742282 (Brown University).

Effect of Prior Petrological Constraints on Global Upper Mantle Models of Radial Anisotropy

Caroline Beghein (University of California at Los Angeles)

Despite efforts from multiple research groups, large discrepancies remain among global models of seismic anisotropy. Besides the inherent non-uniqueness of inverse tomographic problems, one source of uncertainties can originate from the prior information introduced in the inversion. In the case of inversion of global surface wave phase velocity maps to obtain models of radial anisotropy, prior relationships are often imposed between the different elastic parameters. Inversions are then performed for the best-resolved parameters only, i.e. shear-wave velocity and anisotropy.

We tested the robustness of uppermost mantle radial anisotropy models with respect to these prior constraints [*Beghein, 2010*]. We applied a forward modeling technique [*Sambridge, 1999*] to fundamental mode Rayleigh and Love wave global phase velocity maps up to spherical harmonic degree 8. This forward modeling approach enabled us to obtain reliable model uncertainties, and to determine which model features are constrained by the data and which are dominated by the prior.

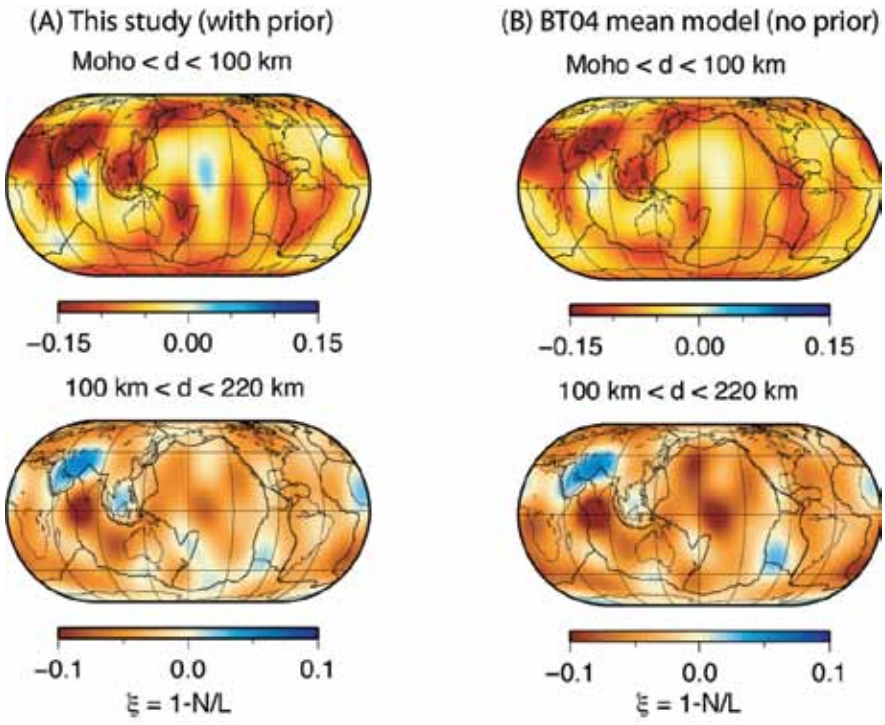

3-D models of S-wave radial anisotropy (ξ) in the uppermost mantle obtained with (A)andwithout(B)prior petrological constraints. In this convention, a negative ξ corresponds to fast horizontally propagating shear-waves. These models correspond to the mean of the model distributions obtained.

We compared the most likely and mean models obtained with and without prior constraints, and found that the most likely models obtained in both cases are highly correlated. This demonstrates that for the best data-fitting solution, the geometry of uppermost mantle radial anisotropy is not strongly affected by prior petrological constraints. We found, however, significant changes in the amplitude of the anomalies, with stronger amplitudes in the best data-fitting model obtained without petrological constraints. This could become an issue when quantitatively interpreting seismic anisotropy models, and thus emphasizes the importance of accurately accounting for parameter uncertainties and trade-offs, and of understanding whether the seismic data or the prior constraints the model.

In addition, we showed that model distributions are not necessarily Gaussian a priori, but that imposing petrological constraints can force the models to follow a Gaussian-like posterior distribution in addition to reducing posterior model uncertainties, in agreement with inverse theory. Finally, we demonstrated that the dependence of seismic wave velocities with the age of the ocean floor is robust and independent of prior constraints. A similar age signal exists for anisotropy, but with larger uncertainties without prior constraints.

References

Beghein, C., Radial Anisotropy and Prior Petrological Constraints: a Comparative Study, *J. Geophys. Res., 115*, 2010.

Sambridge, M., Geophysical inversion with a Neighbourhood Algorithm - I. searching a parameter space, G*eophys. J. Int., 138* (2), 479–494, 1999

Shear Wave Splits, Plate Motions and the Mérida Andes, Western Venezuela

Jeniffer Masy *(Rice University),* **Fenglin Niu** *(Rice University),* **Alan Levander** *(Rice University),* **Michael Schmitz** *(Fundacion Venezolana de Investigaciones Sismologicas-FUNVISIS)*

We measured shear wave splitting from SKS data recorded by the national seismic network of Venezuela and a linear broadband PASSCAL/Rice seismic array across the Merida Andes installed as part of the second phase of the BOLIVAR project. We modified the stacking method of Wolfe and Silver [1998] and applied it to a total of 22 stations. At each station, SKS waveforms from 2 to 36 earthquakes, mostly from the Tonga subduction zone, were stacked to yield a single measurement of the polarization direction and the splitting time. The measured parameters indicate that region can be divided into 3 zones, all congruent with surface motion observed by GPS. The first zone is located north of part of the strike-slip plate boundary prior to 7Ma. Here we observe the largest splitting times (1.6-2.5s), and the fast S-wave directions are orientated roughly in the EW direction, results consistent with previous studies and also with observations made in eastern Venezuela along the active strike slip plate boundary. An interpretation for these observations was proposed by Russo and Silver [1994]. The rollback of the Nazca plate induced a trench-parallel NS flow that passes around the northwest corner of the South America continent and forms an eastward flow beneath the Caribbean plate.

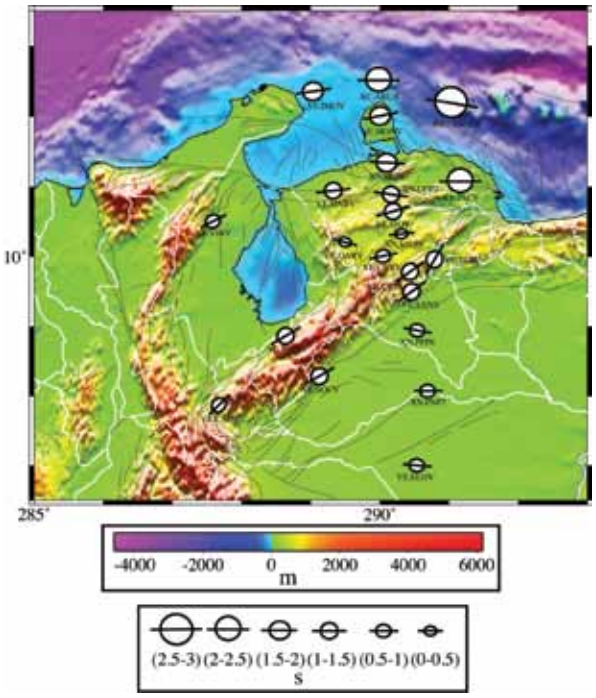

Measured splitting parameters are shown together with the topography of the study region. The orientation of the black solid lines indicates the orientation of the fastest direction. In general the study area can be divided in 3 different zones. The first one is north of the Oca-Ancon dextral strike slip fault, where splitting times are the largest (1.6 - 2.5 s) with an east-west orientation. The second zone is inside Barinas Apure Basin. The smallest split times are present in this region (0.6 - 1 s) also with an east-west orientation. The third zone, southeast of Maracaibo Block, shows a splitting direction N45E, parallel to Bocono Fault and Mérida Andes.

Zone two is located on the SA continent, east of the right lateral Bocono fault, where the measured split times are the smallest (0.6-1.0s) and have EW fastest direction. The observed fast direction and splitting times are consistent with those observed at the Guarico Basin, Maturin Basin and the Guayana shield in the east [Growdon et al., 2009], and are probably related to the westward drift of the South America continent.

Zone three is the Maracaibo block, which is bounded on the southeast by the Bocono fault, and on northwest by the Santa Marta Fault. Split orientations along the Bocono fault are N45°E, suggesting that the observed seismic anisotropy is likely caused by lithospheric deformation parallel to the fault. Split times in this zone range from 1s to 1.5s, requiring a vertically coherent zone of deformation extending to at least 200 km, suggesting a deep origin for the Venezuelan Andes. A recent tomography study [Bezada et al., 2010] suggests that beneath the Merida Andes the top of the flat slab is located at 200 km depth.

References

Russo, R., and P. G. Silver (1994), Trench-Parallel Flow Beneath the Nazca Plate from Seismic Anisotropy, *Science, 263*(5150), 1105-1111.

Growdon, M. A., G. L. Pavlis, F. Niu, F. L. Vernon, and H. Rendon (2009), Constraints on mantle flow at the Caribbean–South American plate boundary inferred from shear wave splitting, *J. Geophys. Res., 114*(B2), 1-7.

Wolfe, C., and P. Silver (1998), Seismic anisotropy of oceanic upper mantle: shear wave splitting methodologies and observations, *J. Geophys. Res.*-Solid Earth, 103(B1), 749-771.

Bezada, M.J., A. Levander, and B. Schmandt, 2010, Subduction in the Southern Caribbean: Images from finite-frequency P-wave tomography, submitted to *J. Geophys. Res.*, May 2010.

Acknowledgements: We would like to acknowledge IRIS-PASSCAL and FUNVISIS for providing the data and the temporal stations used in this study, and also for all the support they gave us during the deployment of the seismic stations. This research was supported by NSF grant EAR-0607801.

Global Azimuthal Seismic Anisotropy and the Unique Plate-Motion Deformation of Australia

Eric Debayle *(Institut de Physique du Globe de Strasbourg, Ecole et Observatoire des Sciences de la Terre, Centre National de la Recherche Scientifique and Universit ´e Louis Pasteur, 61084 Strasbourg, Cedex),* **Brian Kennett** *(Research School of Earth Sciences, The Australian National University, Canberra ACT 0200, Australia),* **Keith Priestley** *(Bullard Laboratories, University of Cambridge, Cambridge)*

Differences in the thickness of the high-velocity lid underlying continents as imaged by seismic tomography, have fuelled a long debate on the origin of the 'roots' of continents. Some of these differences may be reconciled by observations of radial anisotropy between 250 and 300 km depth, with horizontally polarized shear waves travelling faster than vertically polarized ones. This azimuthally averaged anisotropy could arise from present-day deformation at the base of the plate, as has been found for shallower depths beneath ocean basins. Such deformation would also produce significant azimuthal variation, owing to the preferred alignment of highly anisotropic minerals. Here we report global observations of surface-wave azimuthal anisotropy, which indicate that only the continental portion of the Australian plate displays significant azimuthal anisotropy and strong correlation with present-day plate motion in the depth range 175–300 km. Beneath other continents, azimuthal anisotropy is only weakly correlated with plate motion and its depth location is similar to that found beneath oceans. We infer that the fast-moving Australian plate contains the only continental region with a sufficiently large deformation at its base to be transformed into azimuthal anisotropy. Simple shear leading to anisotropy with a plunging axis of symmetry may explain the smaller azimuthal anisotropy beneath other continents.

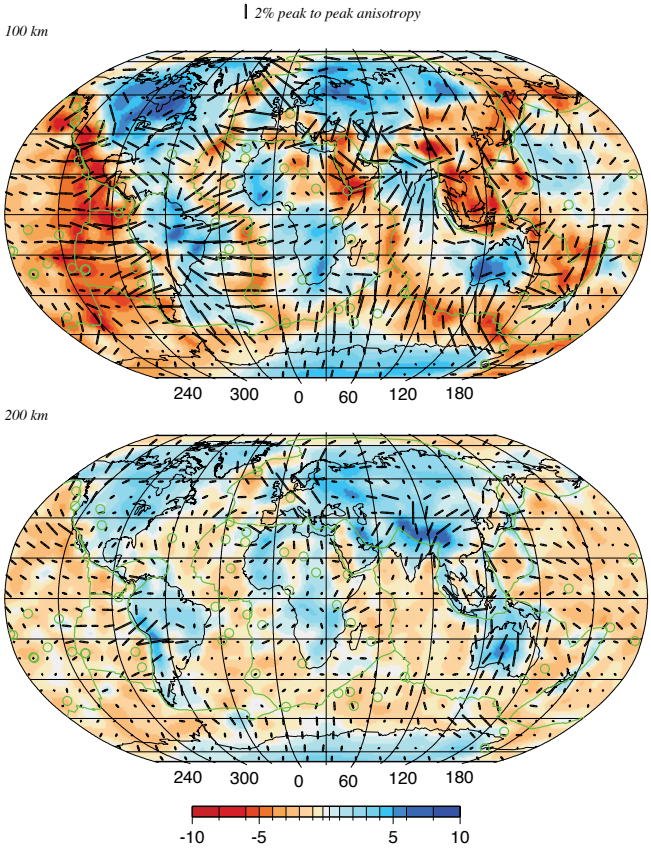

SV-wave heterogeneity and azimuthal anisotropy (black bars oriented along the axis of fast propagation) at 100 and 200 km depth obtained from the inversion of 100,779 Rayleigh waveforms. Hotspot locations are indicated by green circles. The length of theblack bars is proportional to the maximum amplitude of azimuthal anisotropy (bar length for 2% peak to peak anisotropy shown at top). SV-wave perturbations (in per cent relative to PREM) are represented with the colour scale.

References

E. Debayle, B. Kennett and K. Priestley, Global azimuthal seismic anisotropy and the unique plate-motion deformation of Australia, *Nature, 433*, 509-512, doi:10.1038/nature03247, 2005.

Acknowledgements: This work was supported by programme DyETI conducted by the French Institut National des Sciences de l'Univers (INSU). The data used in this work were obtained from the GEOSCOPE, GDSN, IDA, MEDNET and GTSN permanent seismograph networks, and completed with data collected after the PASSCAL broadband experiments, the SKIPPY and subsequent broadband deployments in Australia, and the INSU deployments in the Horn of Africa and the Pacific (PLUME experiment). Supercomputer facilities were provided by the IDRIS and CINES national centres in France. Special thanks to J. M. Brendle at EOST for technical support, S. Fishwick for providing broadband data from the Western Australian craton field deployment, the staff of the Research School of Earth Science who collected the SKIPPY data in the field, and A. Maggi for suggestions that improved the manuscript.

Depth Dependent Azimuthal Anisotropy in the Western US Upper Mantle

Huaiyu Yuan *(Berkeley Seismological Laboratory, University of California-Berkeley),* **Barbara Romanowicz** *(Berkeley Seismological Laboratory, University of California-Berkeley)*

We present the results of a joint inversion [Yuan and Romanowicz, 2010] of long period seismic waveforms and SKS splitting measurements for 3D lateral variations of anisotropy in the upper mantle beneath the western US, incorporating recent datasets generated by the USArray deployment as well as other temporary stations in the region. We find that shallow azimuthal anisotropy (Figure 1) closely reflects plate motion generated shear in the asthenosphere in the shallow upper mantle (70-150 km depth), whereas at depths greater than 150 km, it is dominated by northward and upward flow associated with the extension of the East-Pacific Rise under the continent, constrained to the east by the western edge of the north-American craton, and to the north, by the presence of the East-West trending subduction zone. (Figure 1 here) The strong lateral and vertical variations throughout the western US revealed by our azimuthal anisotropy model reflect complex past and present tectonic processes. In particular, the depth integrated effects of this anisotropy (Figure 2) explain the apparent circular pattern of SKS splitting measurements observed in Nevada without the need to invoke any local anomalous structures (e.g. ascending plumes or sinking lithospheric instabilities [Savage and Sheehan, 2000; West et al., 2009]): the circular pattern results from the depth-integrated effects of the lithosphere-asthenosphere coupling to the NA, Pacific and JdF plates at shallow depths, and in the depth range 200-400 km, northward flow from the EPR channeled along the craton edge and deflected by the JdF slab, and more generally slab related anisotropy. With the accumulating high quality TA data, surface wave azimuthal anisotropy makes it possible to resolve complex depth dependent anisotropic domains in the North American upper mantle. (Figure 2 here)

References

Savage, M. K., and A. F. Sheehan (2000), Seismic anisotropy and mantle flow from the Great Basin to the Great Plains, western United States, *J. Geophys. Res., 105*(6), 13,715-713,734.

West, J. D., M. J. Fouch, J. B. Roth, and L. T. Elkins-Tanton (2009), Vertical mantle flow associated with a lithospheric drip beneath the Great Basin, *Nature Geosci., 2*(6), 439-444.

Yuan, H., and B. Romanowicz (2010), Depth Dependent Azimuthal anisotropy in the western US upper mantle, *Earth Planet. Sci. Lett.*, in revision.

Acknowledgements: We thank the IRIS DMC and the Geological Survey of Canada for providing the waveforms used in this study and K. Liu, M. Fouch, R. Allen, A. Frederiksen and A. Courtier for sharing their SKS splitting measurements with us. This study was supported by NSF grant EAR-0643060. This is BSL contribution #10-05.

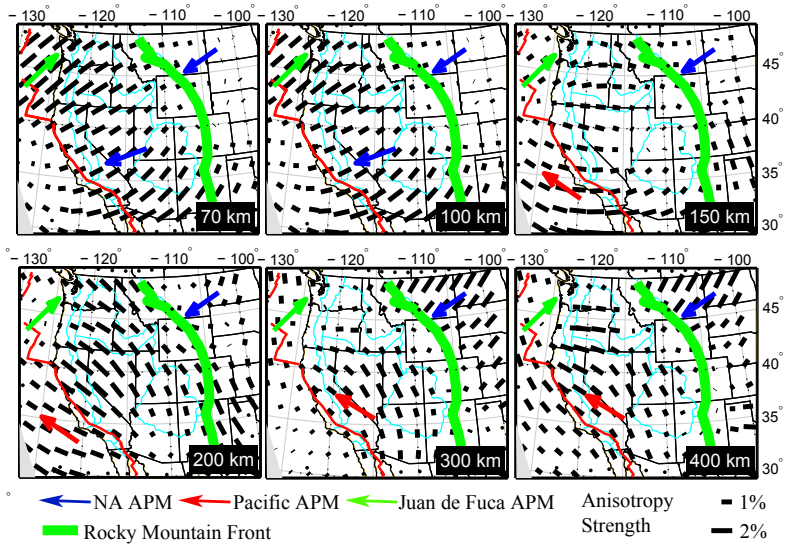

Figure 1. Azimuthal anisotropy variations with depth. Black bars indicate the fast axis direction and the bar length is proportional to the anisotropy strength. Blue, green and red arrows show the absolute plate motion (APM) directions of the North American, JdF, and the Pacific plates respectively, computed at each location using the HS3-NUVEL 1A model.

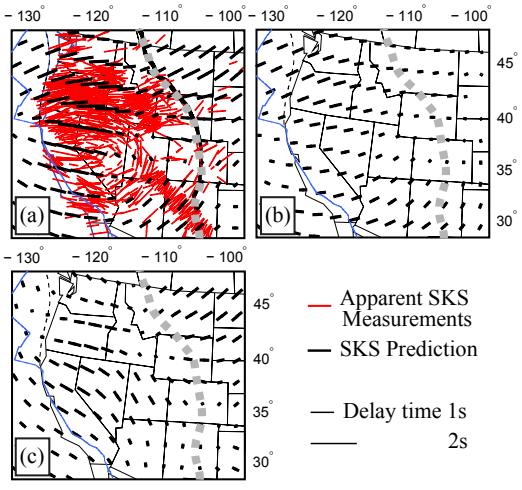

Figure 2. Comparison of observed and predicted station averaged SKS splitting direction and time. Red bars indicate observations and are shown in the left panels only, for clarity. Black bars indicate the model predictions. Predicted splitting is shown for integration of the models over, (a) the full depth range of the azimuthal anisotropy models, (b) the top 150 km of the models, and (c) the portion of the model between 150 and 500 km, respectively.

The Stratification of Seismic Azimuthal Anisotropy in the Western US

Fan-Chi Lin *(University of Colorado at Boulder),* **Michael H. Ritzwoller** *(University of Colorado at Boulder),* **Yingjie Yang** *(University of Colorado at Boulder),* **Morgan P. Moschetti** *(University of Colorado at Boulder),* **Matthew J. Fouch** *(Arizona State University)*

Knowledge of the stratification of seismic anisotropy in the crust and upper mantle would aid understanding of strain partitioning and dynamic coupling in the crust, lithospheric mantle, and athenospheric mantle. It has been difficult, however, to obtain an integrated, self-consistent 3D azimuthally anisotropic model for the crust and upper mantle based on both SKS splitting and surface wave measurements due to the rather different sensitivities of the two wave types. We applied surface wave tomography, including ambient noise tomography (ANT) and eikonal tomography, to data from the Transportable Array (TA) component of EarthScope/USArray to estimate the 3D anisotropic structure of the crust and uppermost mantle. These results were combined with SKS splitting measurements to investigate the deeper anisotropic structures. Figure 1 shows the anisotropic properties of the (a) middle-to-lower crust, (b) uppermost mantle, and (c) asthenosphere in our final model, where the fast propagation direction and anisotropic amplitude are represented by the orientation and length of the yellow/red bars on a 0.6° spatial grid. Isotropic shear wave speeds at depths of 15 and 50 km are color coded in the background of (a)-(b), and the fast direction is shown in the background in (c). The comparison of observations of SKS splitting (blue, red, or black) and predictions (yellow) from the 3D model of anisotropy model shown in (a)-(c) are also shown in (d), where the fast direction and splitting times are summarized by the orientation and length of the bars. The blue, red, and black colors of the observed measurements identify differences with the model predictions of the fast axis directions: Blue: 0°-30°, Red: 30°-60°, Black: 60°-90°. The inferred stratification of anisotropy demonstrates complex and highly variable crust-mantle mechanical coupling. Regional-scale azimuthal anisotropy is dominated by relatively shallow tectonic processes confined to the crust and uppermost mantle, although the patterns of anisotropy in the crust and mantle are uncorrelated. The more homogeneous asthenospheric anisotropy broadly reflects a mantle flow field controlled by a combination of North American plate motion and the subduction of the Juan de Fuca and Farallon slab systems. These results would not have been possible without the TA, and future work will involve applying the method to new TA stations to the east.

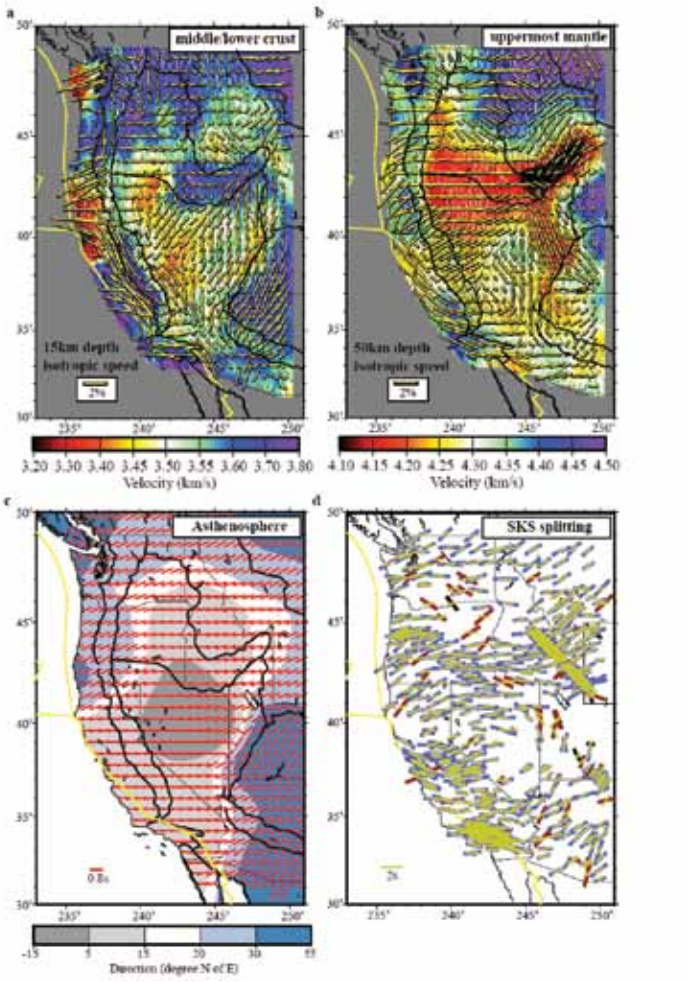

Azimuthal anisotropy in the crust, uppermost mantle, and asthenosphere and the comparison between predicted and observed SKS splitting.

References

Lin, F., Ritzwoller, M. H. & Snieder, R. Eikonal tomography: surface wave tomography by phase front tracking across a regional broad-band seismic array. *Geophys. J. Int. 177*, 1091-1110 (2009).

Lin, F., Ritzwoller, M. H., Yang, Y., Moschetti, M. P., & Fouch, M. J. The stratification of seismic azimuthal anisotropy in the western US. Submitted to *Nature Geosci.*.

Acknowledgements: Data used in this study were made available through EarthScope and the facilities of the IRIS Data Management Center. This work has been supported by NSF grants EAR-0711526 and EAR-0844097.

Rayleigh Wave Phase Velocities, Small-Scale Convection and Azimuthal Anisotropy beneath Southern California

Donald W. Forsyth *(Brown University),* **Yingjie Yang** *(University of Colorado)*

We use Rayleigh waves to invert for shear velocities in the upper mantle beneath southern California [*Yang and Forsyth, 2006*]. A one-dimensional shear velocity model reveals a pronounced low- velocity zone (LVZ) from 90 to 210 km. The pattern of velocity anomalies indicates that there is active small-scale convection in the asthenosphere and that the dominant form of convection is three-dimensional (3-D) lithospheric drips and asthenospheric upwellings, rather than 2-D sheets or slabs. Several of the features that we observe have been previously detected by body wave tomography: these anomalies have been interpreted as delaminated lithosphere and consequent upwelling of the asthenosphere beneath the eastern edge of the southern Sierra Nevada and Walker Lane region; sinking lithosphere beneath the southern Central Valley; upwelling beneath the Salton Trough; and downwelling beneath the Transverse Ranges. Our new observations provide better constraints on the lateral and vertical extent of these anomalies. In addition, we detect two previously undetected features: a high-velocity anomaly beneath the northern Peninsular Range and a low-velocity anomaly beneath the northeastern Mojave block. We also estimate the azimuthal anisotropy from Rayleigh wave data. The strength is 1.7% at periods shorter than 100 s and decreases to below 1% at longer periods. The fast direction is nearly E-W. The anisotropic layer is more than 300 km thick. The E-W fast directions in the lithosphere and sublithosphere mantle may be caused by distinct deformation mechanisms: pure shear in the lithosphere due to N-S tectonic shortening and simple shear in sublithosphere mantle due to mantle flow.

References

Yang, Y. and D.W. Forsyth, Rayleigh wave phase velocities, small-scale convection and azimuthal anisotropy beneath southern California, *J. Geophys. Res., 111*, B07306,2006

Acknowledgements: This work was supported by National Science Foundation grants OCE-9911729 and EAR-0510621.

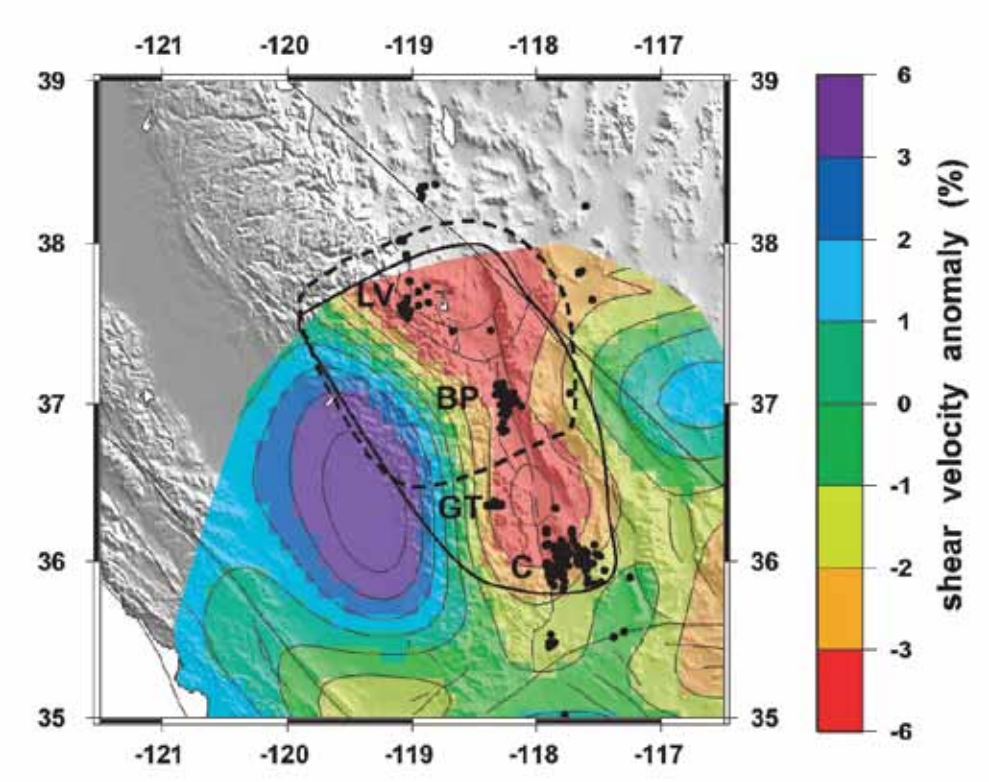

Distribution of volcanism (black dots) in southern Sierra Nevada during the Quaternary (1.5-0 Ma) period. Bold solid line outlines area with which Pliocene (chiefly 4-3 Ma) volcanism was prevalent; note that Quaternary volcanic fields (LV-Long Valley, BP-Big Pine, GT-Golden Trout, C-Coso) are all within area of Pliocene event. Dashed line outlines the area of Pliocene potassic volcanism 4-3 Ma. Colors show shear-wave velocity anomalies at depths of 70-90 km. Note that the Quaternary volcanism coincides with the region of lowest velocities.

Upper Mantle Anisotropy beneath the High Lava Plains, Oregon, USA: Linking Mantle Dynamics to Surface Tectonomagmatism

Maureen Long *(Yale University),* **Lara Wagner** *(University of North Carolina at Chapel Hill),* **Matthew Fouch** *(Arizona State University),* **David James** *(Carnegie Institution of Washington)*

The High Lava Plains (HLP) of southeastern and central Oregon represent a young (< 15 Ma), bimodal volcanic province that exhibits an age progression in silicic volcanism towards the northwest, along with widespread basaltic volcanic activity. A variety of models have been proposed to explain the recent volcanic history of the region, including the Steens and Columbia River flood basalt episodes and the subsequent evolution of the HLP. These models variously invoke the rollback and steepening of the Cascadia slab, interaction between the subduction-induced flow field and the inferred Yellowstone plume, the influence of basal lithospheric "topography," significant lithospheric extension, or a combination of these processes. Measurements of the seismic anisotropy that results from active mantle flow beneath the region can provide a crucial test of such models. To constrain this anisotropy, we measured SKS splitting at approximately 200 broadband seismic stations in eastern Oregon and the surrounding region, including ~100 stations of the temporary High Lava Plains seismic deployment [*Long et al., 2009*]. Stations in the region exhibit strong SKS splitting, with average delay times at single stations ranging from ~ 1.0 sec to ~ 2.7 sec. Nearly all observed fast directions are approximately E-W, which argues for well-organized contemporary mantle flow in an E-W direction beneath the HLP. Mantle flow beneath the HLP appears to be controlled by the rollback of the Juan de Fuca slab; the observed E-W fast directions are not consistent with a model in which mantle flow is driven along the strike of the HLP by Yellowstone plume material. We observe significant lateral variations in average delay times, with a region of particularly large dt that delineate a region in the heart of the HLP province and another region of large delay times just to the north of Newberry Volcano. There is a notable spatial correlation among stations that exhibit large delay times, the location of Holocene volcanic activity, and slow isotropic uppermost mantle wavespeeds from a surface wave velocity model [*Wagner et al., in review*]. Possible explanations for the pronounced lateral variations in splitting delay times include variations in the partial melt fraction or degree of alignment, variations in the strength or fabric type of olivine LPO, or variations in uppermost mantle mineralogy.

References

Long, M. D., H. Gao, A. Klaus, L. S. Wagner, M. J. Fouch, D. E. James, and E. Humphreys (2009), Shear wave splitting and the pattern of mantle flow beneath eastern Oregon, *Earth Planet. Sci. Lett., 288*, 359-369.

Wagner, L., D. Forsyth, M. Fouch, and D. James (2010), Detailed three dimensional shear wave velocity structure of the northwestern United States from surface wave two-plane-wave analyses. *Earth Planet. Sci. Lett.*, in review.

Acknowledgements: The High Lava Plains seismic deployment was funded through NSF awards EAR-0507248 (MF) and EAR-0506914 (DJ).

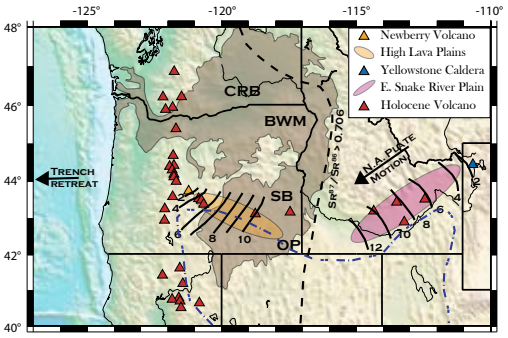

Geologic map of eastern Oregon and the surrounding region. Black contours indicate the age progression (in Ma) of silicic volcanism along both the High Lava Plains (yellow), and the Snake River Plain (pink). The black dashed line shows the location of the Sr87/Sr86=0.706 line, commonly interpreted to mark the boundary between cratonic North America to the east and the accreted arc terranes to the west. The blue dashed line shows the northern limits of Basin and Range extension. The brown highlighted area indicates the region covered by Miocene flood basalts including the Columbia River basalts (CRB) to the north and the Steens basalts (SB) farther to the south. Red triangles indicate locations of Holocene volcanism. The geographical locations of the Owyhee Plateau (OP) and the Blue and Wallowa mountains (BWM) are also shown, along with Newberry Volcano (orange triangle) and Yellowstone Caldera (blue triangle). The arrow at the Cascadia trench indicates its direction of motion.

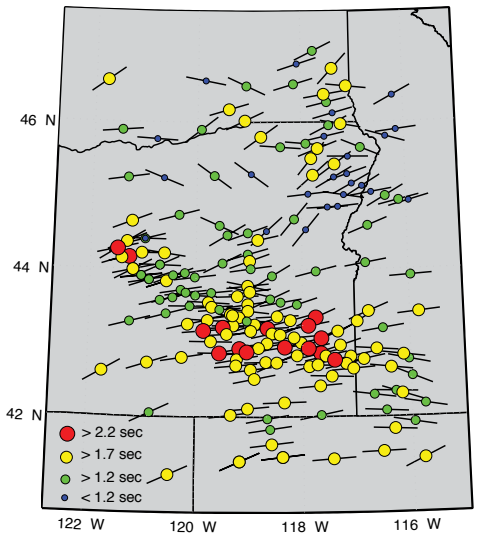

Map of average shear wave splitting parameters in the High Lava Plains and surrounding regions. Estimates were obtained by a simple average of the highest-quality measurements at each station. The symbols are color-coded by the magnitude of the delay time, as indicated by the legend at bottom left.

Mantle Flow in Subduction Systems from the Global Pattern of Shear Wave Splitting above and below Subducting Slabs

Maureen Long *(Yale University),* **Paul Silver** *(Carnegie Institution of Washington)*

The character of the mantle flow field in subduction zone regions remains poorly understood, despite its importance for our understanding of subduction dynamics. Observations of seismic anisotropy, which manifests itself in shear wave splitting, can shed light on the geometry of mantle flow in subduction zones, but placing constraints on anisotropy in various parts of the subduction system (including the overriding plate, the mantle wedge, the subducting slab, and the sub-slab mantle) remains challenging from an observational point of view. In order to identify dynamic processes that make first-order contributions to the pattern of mantle flow in subduction zones, we analyze a global compilation of shear wave splitting measurements for a variety of ray paths, including SK(K)S and teleseismic S phases as well as local S and source-side splitting from slab earthquakes. We have compiled shear wave splitting measurements from subduction zones globally to produce estimates of average shear wave splitting parameters – and their spatial variation – for the mantle wedge and the sub-wedge region for individual subduction segments [*Long and Silver, 2008*]. These estimates are then compared to other parameters that describe subduction. The sub-wedge splitting signal is relatively simple and is dominated by trench-parallel fast directions in most subduction zones worldwide (with a few notable exceptions). Average sub-wedge delay times correlate with the absolute value of trench migration velocities in a Pacific hotspot reference frame, which supports a model in which sub-slab flow is usually trench-parallel and is controlled by trench migration *[Long and Silver, 2009*]. Shear wave splitting patterns in the mantle wedge are substantially more complicated, with large variations in local S delay times and complicated spatial patterns that often feature sharp transitions between trench-parallel and trench-perpendicular fast directions. We find a relationship between average wedge delay times and the ratio of the trench migration velocity and the convergence velocity. This supports a model in which a trench-parallel flow field (induced by trench migration) interacts with a 2-D corner flow field (induced by downdip motion of the slab) in the mantle wedge, with the relative influence of these flows being governed by the relative magnitude of convergence velocity and trench migration velocity in a Pacific hotspot reference frame.

References

Long, M. D., and T. W. Becker (2010), Mantle dynamics and seismic anisotropy, *Earth Planet. Sci. Lett.*, in press.

Long, M. D., and P. G. Silver (2008), The subduction zone flow field from seismic anisotropy: A global view. *Science, 319*, 315-318.

Long, M. D., and P. G. Silver (2009), Mantle flow in subduction systems: The sub-slab flow field and implications for mantle dynamics. *J. Geophys. Res., 114*, B10312.

Acknowledgements: This work was supported by the Carnegie Institution of Washington and by NSF grant EAR-0911286.

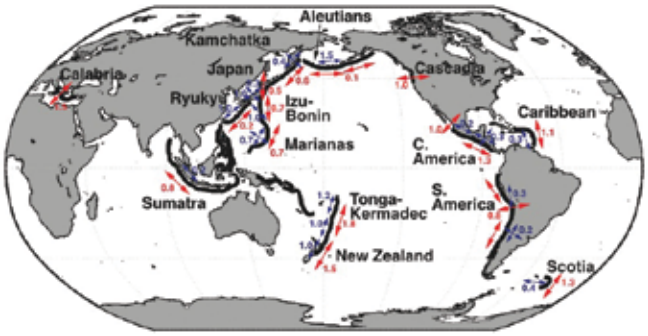

Sketch of constraints on subduction zone anisotropy from shear wave splitting measurements (figure from Long and Becker, 2010, after the compilation of Long and Silver, 2008, 2009). The anisotropic signals of the wedge and sub-slab regions are shown separately. Red arrows indicate average fast directions for the sub-slab splitting signal from SKS, local S, and source-side teleseismic S splitting measurements. The associated average sub-slab delay times are shown in red. Blue arrows indicate average fast directions for wedge anisotropy from local S splitting. In regions where multiple fast directions are shown, splitting patterns exhibit a mix of trench-parallel, trench-perpendicular, and oblique fast directions.

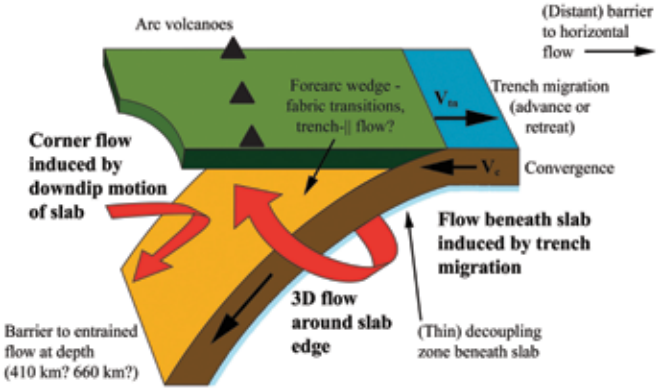

Sketch of the model proposed by Long and Silver (2008) for mantle flow in subduction zones controlled by trench migration.

The Teleseismic Signature of Fossil Subduction: Northwestern Canada

M. G. Bostock *(The University of British Columbia),* **J.-P. Mercier** *(The University of British Columbia),* **P. Audet** *(University of California, Berkeley),* **J.B. Gaherty** *(LDEO, Columbia University),* **E. J. Garnero** *(Arizona State University),* **J. Revenaugh** *(University of Minnesota)*

Between June 2003 and September 2005, 20 broadband, three-component seismometers were deployed along the MacKenzie-Liard Highway in Canada's Northwest Territories as part of the joint IRIS-Lithoprobe Canada Northwest Experiment (CANOE) [*Mercier et al., 2008*]. These stations traverse a paleo-Proterozoic suture and subduction zone that has been previously documented to mantle depths using seismic reflection profiling [Cook et al., 1999]. Teleseismic receiver functions computed from some 250 earthquakes clearly reveal the response of the ancient subduction zone. On the radial component, the suture is evident as a direct conversion from the Moho, the depth of which increases from ~30 km to ~50 km over a horizontal distance of some 70 km before its signature disappears. The structure is still better defined on the transverse component where the Moho appears as the upper boundary of a 10 km thick layer of anisotropy that can be traced from 30 km to at least 90 km depth. The seismic response of this layer is characterized by a frequency dependence that can be modeled by upper and lower boundaries that are discontinuous in material properties and their gradients, respectively. Anisotropy is characterized by a +/-5% variation in shear velocity and hexagonal symmetry with a fast axis that plunges at an oblique angle to the subduction plane. The identification of this structure provides an unambiguous connection between fossil subduction and fine-scale, anisotropic mantle layering. Previous documentation of similar layering below the adjacent Slave province and from a range of Precambrian terranes across the globe provides strong support for the thesis that early cratonic blocks were stabilized through processes of shallow subduction.

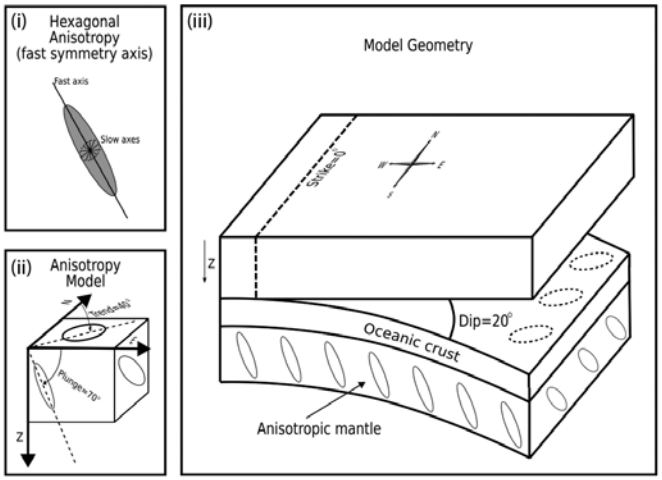

Cartoon showing structural elements of interpretation, including (i) definition of hexagonal anisotropy with fast symmetry axis, (ii) orientation of anisotropy, and (iii) tectonic configuration.

References

Cook, F.A, A.J. van der Velden, K.W. Hall, and B.J. Roberts (1999), Frozen subduction in Canada's Northwest Territories: Lithoprobe deep lithospheric reflection profiling of the western Canada shield, *Tectonics, 18*, 1-24.

Mercier, J.-P., M.G. Bostock, P. Audet, J.B. Gaherty, E.J. Garnero, and J. Revenaugh (2008), The teleseismic signature of fossil subduction: Northwestern Canada, *J. Geophys. Res., 113* B04308.

Acknowledgements: We gratefully acknowledge financial support from the National Science Foundation (grants NSF EAR-0453747 to JG, NSF EAR-0711401 to EG, NSF EAR-0003745-004 to JR) and the Natural Sciences and Engineering Research Council of Canada (NSERC-Lithoprobe supporting geoscience grant CSP0006963 to MB).

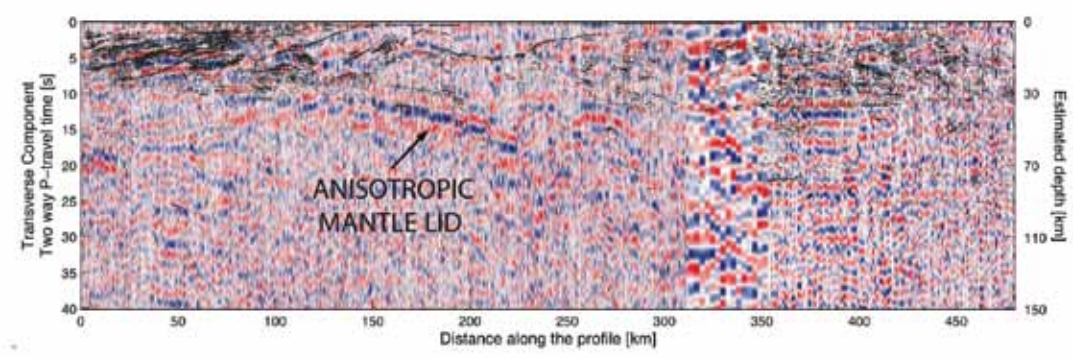

Superposition of line-drawing reflection section of Cook et al (1999) upon transverse component receiver function. Note teleseismic signature of anisotropic mantle lid that parallels reflections from subducted crust.

Seismic Anisotropy beneath Cascadia and the Mendocino Triple Junction: Interaction of the Subducting Slab with Mantle Flow

Caroline Eakin *(Imperial College London),* **Mathias Obrebski** *(UC Berkeley),* **Richard Allen** *(UC Berkeley),* **Devin Boyarko** *(Miami University),* **Michael Brudzinski** *(Miami University),* **Robert Porritt** *(UC Berkeley)*

Mantle flow associated with the Cascadia subduction zone and the Mendocino Triple Junction is poorly characterized due to a lack of shear wave splitting studies compared to other subduction zones. To fill this gap data was obtained from the Mendocino and FACES seismic networks that cover the region with dense station spacing. Over a period of 11-18 months, 50 suitable events were identified from which shear wave splitting parameters were calculated. Here we present stacked splitting results at 63 of the stations. The splitting pattern is uniform trench normal (N67°E) throughout Cascadia with an average delay time of 1.25 seconds. This is consistent with subduction and our preferred interpretation is entrained mantle flow beneath the slab. The observed pattern and interpretation have implications for mantle dynamics that are unique to Cascadia compared to other subduction zones worldwide. The uniform splitting pattern seen throughout Cascadia ends at the triple junction where the fast directions rotate almost 90°. Immediately south of the triple junction the fast direction rotates from NW-SE near the coast to NE-SW in northeastern California. This rotation beneath northern California is consistent with flow around the southern edge of the subducting Gorda slab.

References

Eakin, C.M., M. Obrebski, R.M. Allen, D.C. Boyarko, M.R. Brudzinski, R. Porritt, Seismic Anisotropy beneath Cascadia and the Mendocino Triple Junction: Interaction of the subducting slab with mantle flow, in review.

Acknowledgements: This work was funded by NSF EAR-0745934 and EAR-0643077. The work was facilitated by the IRIS-PASSCAL program through the loan of seismic equipment, USArray for providing data and the IRIS-DMS for delivering it.

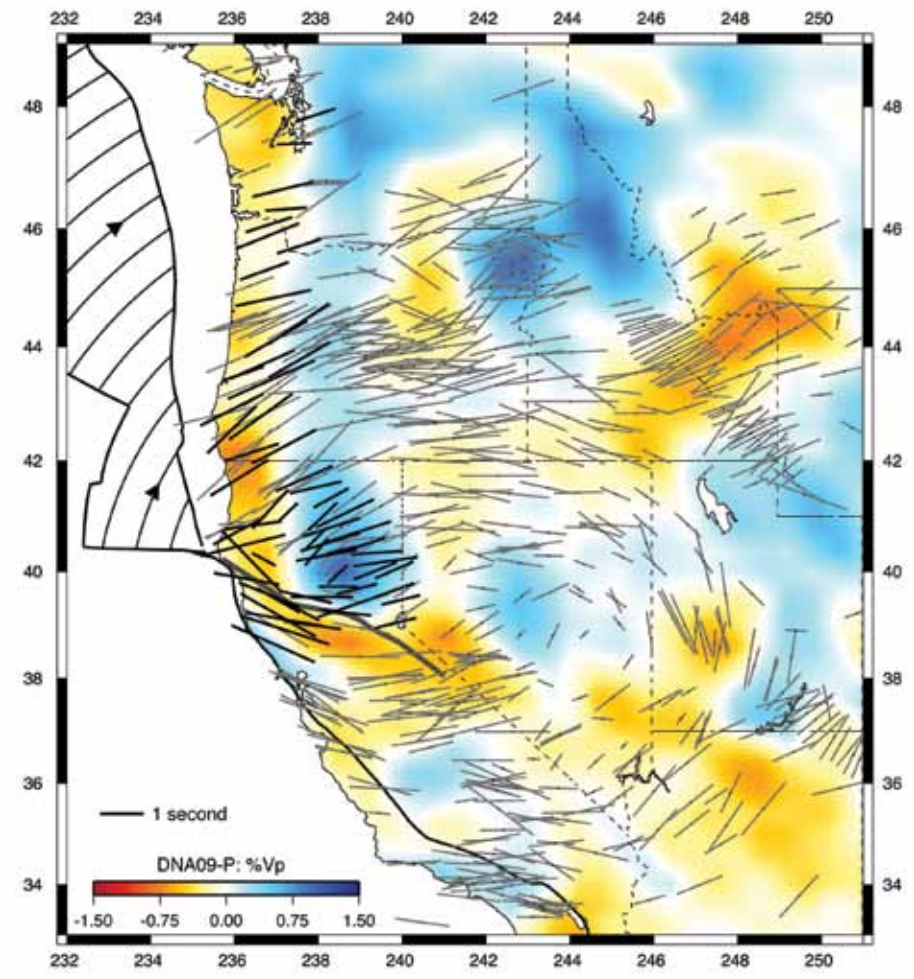

Figure. Regional splitting pattern overlain on the vertically averaged upper mantle velocity anomaly. Our splitting results are shown in black and those of previous studies are in grey (Long et al., 2009; Wang et al., 2008; West et al., 2009; Zandt and Humphreys, 2008 and references therein). The splitting pattern is shown to be uniform trench-normal throughout Cascadia. The velocity anomaly shown is a vertical average of the velocity anomaly from the DNA09 P-wave model over the 100-400km depth range (Obrebski et al., 2010). The slab is imaged as the north-south high velocity feature. The splitting measurements rotate around the southern end of the slab. Curved black lines on the G-JdF plate represent the direction of its absolute plate motion.

Seismic Anisotropy under Central Alaska from SKS Splitting Observations

Douglas Christensen *(Geophysical Institute, University of Alaska Fairbanks),* **Geoffrey Abers** *(Lamont Doherty Earth Observatory of Columbia University)*

Seismic anisotropy under central Alaska is studied using shear wave splitting observations of SKS waves recorded on the Broadband Experiment Across the Alaska Range (BEAAR), 1999-2001. Splitting results can be divided into two distinct regions separated by the 70 km contour of the subducting Pacific plate. Waves that travel through the thicker mantle wedge show fast directions that are parallel to the strike of the slab. These slab-parallel directions appear to indicate along-strike flow in the mantle wedge, and splitting delay times increase with path length in the mantle wedge suggesting anisotropy of 7.9 ± 0.9 percent. The region of along-strike flow corresponds to high seismic attenuation and hence high temperatures. Along-strike flow here may be driven by secular shallowing of the slab driven by subduction of buoyant Yakutat-terrane crust, or by torroidal flow around the east end of the Aleutian slab. Waves traveling southeast of the 70 km contour sample the Pacific plate and the nose of the mantle wedge; they show fast directions that parallel the direction of plate motion. These fast directions are most likely due to flow under the subducting Pacific plate and/or anisotropy within the subducting Pacific lithosphere. The high splitting delay times (0.8-1.7 sec) associated with these convergence-parallel directions cannot be produced in the mantle wedge, which is 10-30 km thick here. Thus, anisotropy shows a sharp 90° change in fabric associated with the onset of high-temperature wedge flow. Results have been published in Christensen and Abers [*2010*].

References

Christensen, D.H., G.A. Abers (2010). Seismic anisotropy under Alaska from SKS splitting observations, *J. Geophys. Res., 115*, B04315, doi:10.1029/2009JB006712.

Acknowledgements: The BEAAR deployment benefited from contributions by many people, including contributions from the Alaska Earthquake Information Center, the IRIS-PASSCAL Instrument Center, and a large number of students who helped with the deployment and its analysis. This work supported by National Science Foundation grant EAR-9725168.

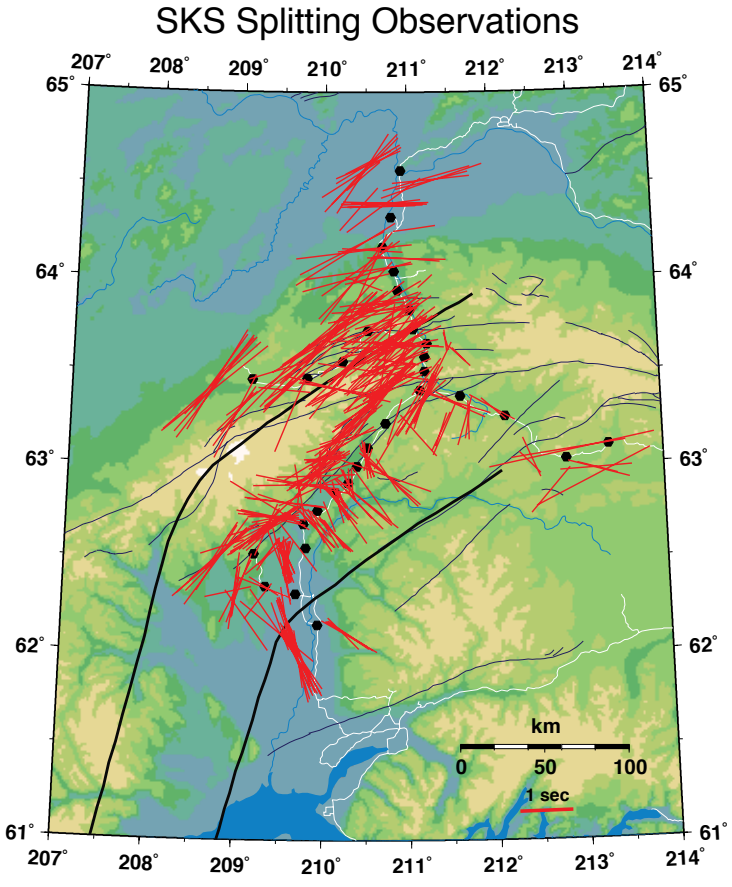

Figure. Compilation of SKS splitting results. Each measurement is plotted as a red line parallel to the fast direction, with length proportional to the delay time. The observations are plotted at the 100 km depth projection of the ray, in order to demonstrate the back- azimuthal pattern. Locations of seismic stations from the BEAAR experiment are shown by the black dots. Thick black lines show contours to slab seismicity (50 and 100 km). Thin dark lines show active faults, and white lines show roads.

Attenuation and Anisotropy in the Northern Apennines, Italy

J. Park *(Yale University),* **D. Piccinini** *(INGV),* **I. Bianchi** *(INGV),* **M. Di Bona** *(INGV),* **F. P. Lucente** *(INGV),* **N. Piana Agostinetti** *(INGV),* **V. Levin** *(Rutgers University)*

The Northern Apennines of Italy is marked by continental convergence and a downgoing slab derived from the Adriatic microplate. Seismicity is sparse, shallow, and lacks historical M>7.5 shallow thrust events. Has subduction ceased? Geodesy indicates near-zero present-day convergence, and fission-track thermochronology suggests that vertical uplift has superseded fold-and-thrust tectonics since 5-10 Ma in a large segment of the orogen. The RETREAT project (REtreating-TRench Extension and Accretion Tectonics) explored this region with broadband seismometers from the IRIS PASSCAL program, the Czech Academy of Sciences and the Istituto Nazionale de Geofisica e Vulcanologia (INGV).

Attenuation estimates from both S and P waves reveal high attenuation on the "back-arc" side of the Apennines orogen (Figure 1), near coastal geothermal areas but extending inland. Pleistocene volcanism is found here, but there is no present-day subduction-arc activity. A crude inversion of t-star (Δt^*) suggests comparable Q values (<100) for both S and P waves in the mantle wedge, suggesting either abundant partial melt or strongly hydrated rocks. Contemporary volcanism is scarce, so we favor hydration derived from the Apennines slab.

Receiver functions (RFs) projected onto a cross-orogen transect highlight how much Apennines subduction differs from typical subduction of oceanic lithosphere. The top of the Apennines slab is a double interface that dips from 40-km depth beneath the orogen crest to 80-km depth near the Tyrrhenian coast of Tuscany (Figure 2). Using constant and harmonic RF stacks with back azimuth, we conclude that a strongly anisotropic layer (~10-km thickness) lies atop the Apennines slab. Evidence for a velocity inversion is lacking, consistent with an eclogitic composition or the "ultra-high-pressure" (UHP) lithologies that are exhumed in the nearby (older) Alpine orogen. Because the top of the slab does not extend upward from 40-km depth, and strong anisotropy occurs deeper than typical for Japan or Cascadia, we hypothesize that Apennines "subduction" has entrained and sheared the lower continental crust of the Adriatic microplate.

If mantle-wedge attenuation suggests water or partial melt, where do these come from? Subducted lower continental crust should contain less water than oceanic crust, but need not be totally dry. Weaker crustal hydration might help explain weaker Tuscan volcanism. Some clues fit together, but our story still has gaps!

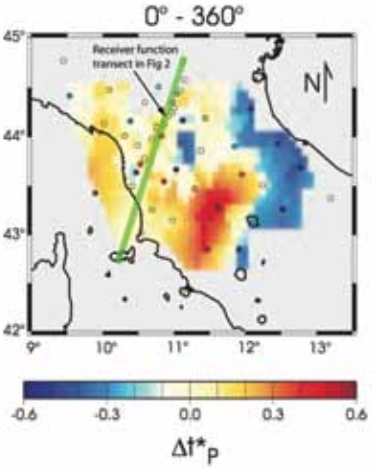

Figure 1. Spatial distribution of Δt^*, an estimate for seismic attenuation based on the high-frequency rolloff of P body-wave spectra recorded in Central Italy by the RETREAT deployment. The map interpolates the average Δt^* estimates at each station. The average Δt^* values at stations are shown as colored circles. The green line locates the receiver-function transect of Figure 2.

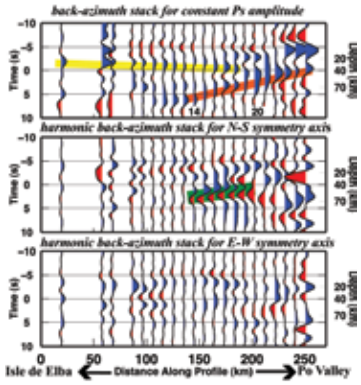

Figure 2. RF data-set along cross-Apennines transect, stacked with constant, $\cos\phi$ (N-S) and $\sin\phi$ (E-W) back-azimuth weighting. Blue and red pulses indicate positive and negative Ps converted-wave amplitudes, respectively. Colored stripes highlight the main features: yellow for the Tyrrhenian Moho, orange for Adriatic Moho and green for the layer atop the Apennines slab. The Y-axis shows RF delay time (depth), in s (km) referenced to a stacking-migration target at 40-km depth, so that pulses at negative delay time correspond to interfaces shallower than 40 km.

References

Piccinini, D., M. Di Bona, F. P. Lucente, V. Levin and J. Park, Seismic Attenuation and mantle wedge temperature in the Northern Apennines subduction zone (Italy) from teleseismic body waves, accepted by *J. Geophys. Res., 2010.*

Bianchi, I., J. Park, N. Piana Agostinetti,V. Levin, Mapping seismic anisotropy using harmonic decomposition of receiver functions: an application to Northern Apennines, Italy, submitted to *J. Geophys. Res., 2010.*

Thomson, S. N., M. T. Brandon, P. W. Reiners, M. Zattin, P. J. Isaacson, and M. L. Balestrieri, Thermochronologic evidence for orogen-parallel variability in wedge kinematics during extending convergent orogenesis of the northern Apennines, italy, *GSA Bulletin, 122* (7/8), 11601179, 2010.

Acknowledgements: JP and VL were supported by NSF grant EAR-0208652. IB is supported by DPC-S1 UR02.02. NPA was supported by project Airplane (funded by the Italian Ministry of Research, Project RBPR05B2ZJ 003). Other researchers supported by INGV

Stress-Induced Upper Crustal Anisotropy in Southern California

Zhaohui Yang *(University of Colorado at Boulder),* **Anne Sheehan** *(University of Colorado at Boulder)*

We use an automated method to analyze shear-wave splitting from local earthquakes recorded by the Southern California Seismic Network (SCSN) between 2000 and 2005. The observed fast directions of upper-crustal anisotropy are mostly consistent with the direction of maximum horizontal compression σHmax, suggesting that anisotropy in the top 20 km of crust under southern California is stress-induced anisotropy. At some stations, fast directions are aligned with the trends of regional faulting and local alignment of anisotropic bedrock. Delay times range widely from 0.02 s to 0.15 s. These upper-crustal anisotropy observations, together with previous studies of SKS shear-wave splitting and receiver functions, show different mechanisms of anisotropy at different depths under southern California. Anisotropy in the upper crust and upper mantle appears to be in response to the current horizontal maximum compression σHmax, whereas lower crustal anisotropy may be caused by the anisotropic schist accreted during the subduction of Farallon plate, which is frozen in the lower crust. We also explore possible temporal variations in upper-crustal anisotropy associated with pre-earthquake stress changes or stress changes excited by surface waves of great earthquakes. However, we do not observe any clear temporal variations in fast directions or time delays.

References

Yang, Z., A. F. Sheehan, and P. Shearer, Stress-Induced Upper Crustal Anisotropy in Southern California, submitted to *J. Geophys. Res.*, 2010.

Gripp, A.E., and R.G. Gordon (1990), Current Plate Velocities Relative to the Hotspots Incorporating the NUVEL-1 Global Plate Motion Model, *Geophysical Research Letters, 17*(8), 1109-1112.

McQuarrie, N., and B.P. Wernicke (2005), An animated tectonic reconstruction of southwestern North America since 36 Ma, *Geosphere, 1*(3), 147-172.

Porter, R., G. Zandt, and N. McQuarrie (2010), Pervasive lower crustal seismic anisotropy in southenr California: Evidence for underplated schists, Submitted.

Acknowledgements: The data used in this study were made available by the Southern California Seismic Network, and we are grateful to E. Hauksson for his assistance in creating a waveform database. We thank J. Polet for providing a digital table of his Southern California SKS measurements, R. Porter for sharing a preprint of his Southern California receiver function work, and M. Savage for her comments. The figures were made using GMT software by P. Wessel and W. Smith. AFS gratefully acknowledges a Green Foundation Fellowship that supported her sabbatical at IGPP/SIO. This work is supported by SCEC project 08129 and NSF EAR grant 0409835, and by U.S. Geological Survey award number G09AP00052.

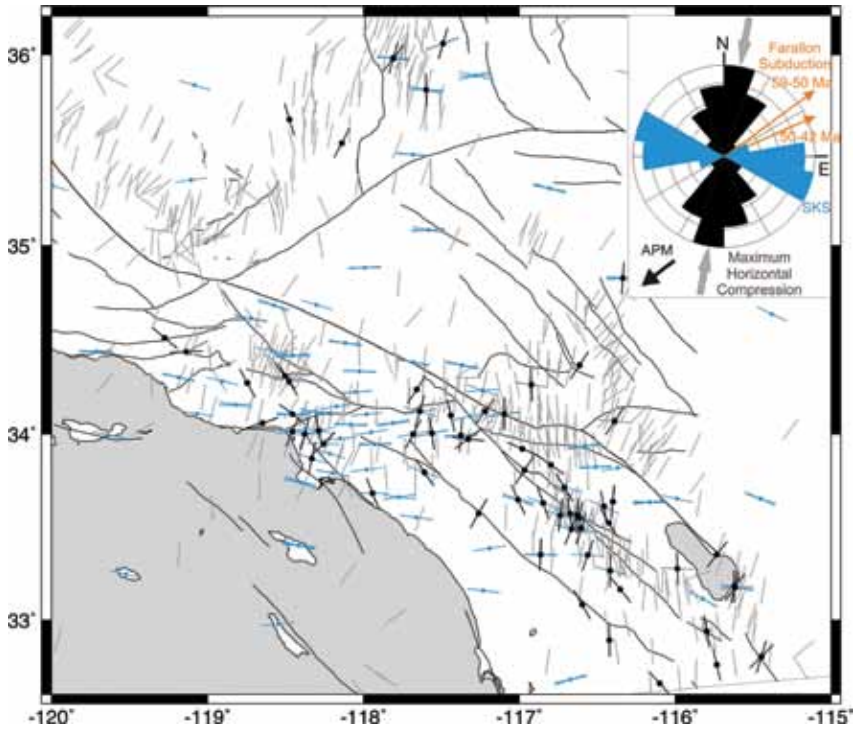

Map showing average fast directions of upper-crustal anisotropy (solid bars), SKS shear-wave splitting anisotropy (blue bars), and stress vectors (gray bars). The inset rose diagram summarizes the trends of anisotropies from three different depths in the area of the map: Top 20 km of crust (black), the fast directions are consistent with the direction of current maximum horizontal compression (gray arrows); and upper mantle, SKS shear-wave splitting show a preferred fast direction orienting E-W (blue bars). The orange arrows are Farallon plate subduction directions during 59-42 Ma [McQuarrie and Wernicke, 2005]. The trends of anisotropy in the lower crust (below 20 km), after rotation back to 36 Ma [Porter et al., 2010], are consistent with the Farallon subduction directions during 59-42 Ma. The black arrow indicates the absolute plate motion (APM) of the North American plate [Gripp and Gordon, 1990].

USArray Observations of Quasi-Love Surface-Wave Scattering: Orienting Anisotropy in the Cascadia Plate Boundary

Duayne M. Rieger *(Yale University),* **Jeffrey Park** *(Yale University)*

Love surface waves scatter to elliptically-polarized Rayleigh waves when they encounter regional concentrations of anisotropy. These scattered waves, called Quasi-Love, or QL waves, are useful for detecting shear near plate boundaries, where the strong lithosphere deforms mantle asthenosphere surrounding the plates as lithosphere sinks at oceanic trenches, spreads at rift zones, or crumples where continents collide. QL waves can be observed on individual seismograms, and complement other analyses of seismic data.

We found QL scattering in and around the Cascadia subduction zone in seismic data from the land-based USArray, a component of Earthscope. The dense sampling and broadband response of the USArray transportable array allows us to detect and correlate the scattering of 100-sec surface waves at closely-spaced locations. We demonstrate that a pattern of Love-to-Rayleigh scattering seen across the western USA (Figure 1) can be related to an anisotropic gradient that scatters energy from a location offshore the Juan de Fuca trench. The azimuthal variation of scattering (Figure 2) indicates an alignment of the anisotropic symmetry axis with present-day plate motion. We reject slab rollback as the causative process and suggest the entrainment of asthenosphere with the overriding Juan de Fuca and Gorda plates.

The strong coherence of scattered waveforms between neighboring stations in USArray suggests that such long-period surface wave motion can detect lateral gradients of anisotropy beneath Cascadia and, potentially, the rest of the western USA. Detailed reconstruction of anisotropy could be tried by grouping great-circle paths that intersect at a distribution of possible scattering points throughout the subduction system in an effort to further constrain its mantle dynamics.

References

Rieger, D. M., and J. Park, USArray observations of quasi-Love surface wave scattering: Orienting anisotropy in the Cascadia plate boundary, *J. Geophys. Res., 115*, B05306, doi:10.1029/2009JB006754, 2010.

Acknowledgements: This work was supported by NSF Grant EAR-0208652.

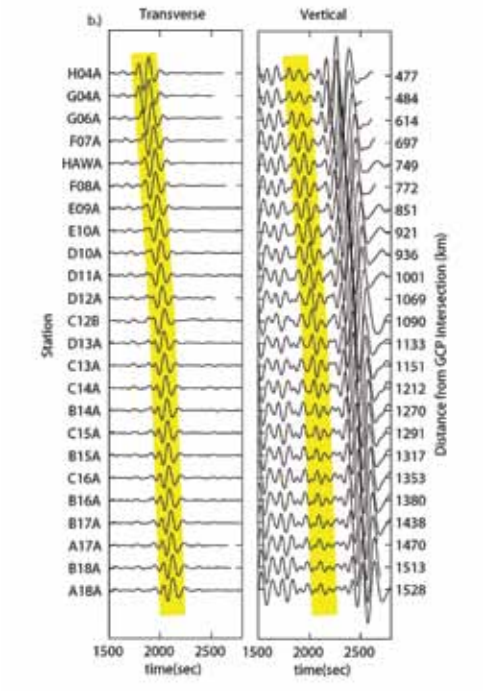

Figure 1. USArray record sweeps along the great-circle path for the Loyalty Islands 4/9/2008 (Ms=7.3) earthquake. The Love wave on the transverse components and the QL wave on the vertical-components are highlighted. The station each record was recorded at is along the left Y-axis and the distance from the great-circle path intersection at 42.5°N 127.5°W is along the right Y-axis. The variation in amplitude of the QL wave with distance appears to be accompanied by the gradual modulation of the waveform. This can be characteristic of an interference pattern that would suggest a more complex anisotropic structure than a single point scatterer with a horizontal axis of symmetry.

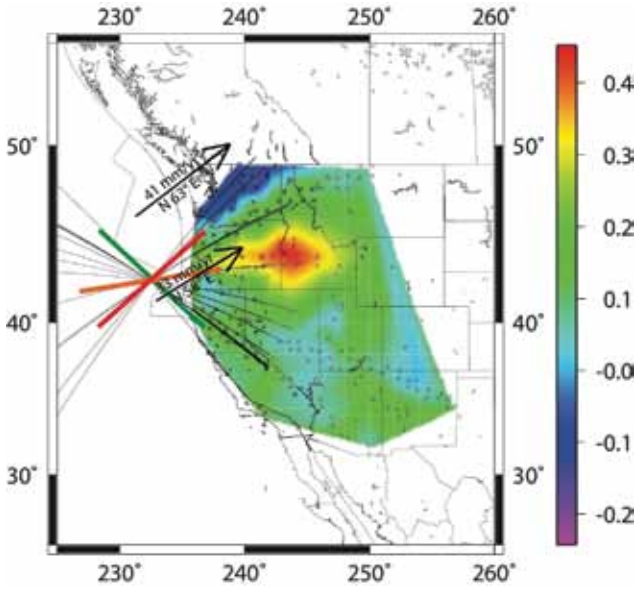

Figure 2. Spatial plot of the QL/Love amplitude ratio at 100s-lowpass, normalized by the Love-wave amplitude along each great-circle path. The black circles are station locations. The red line is the zero-scattering azimuth, parallel to our proposed anisotropic axis of symmetry. This orientation correlates well with the hotspot referenced Juan de Fuca plate motion, illustrated by the black arrows, and regional shear-wave splitting measurements. The orange line represents an oblique orientation to the anisotropic axis of symmetry suggested by the data. The largest QL/Love amplitude ratios are measured close to this orientation which is encouraging. The green line is the azimuth normal to the zero-scattering azimuth.

Tau-p Depropagation of Five Regional Earthquakes Recorded by the Earthscope Usarray to Constrain the 410-km Discontinuity Velocity Gradient

Josh Stachnik *(Univ. Wyoming),* **Ken Dueker** *(Univ. Wyoming)*

Seismic recordings by the EarthScope USArray from three Queen Charlotte region earthquakes and two southern Baja Mexico earthquakes are transformed to the Tau-P domain and the post-critical P-wave branches are picked. Five one dimensional velocity models are formed via depropagation of the picked Tau-P curves. All five models are in good agreement with the ak135 reference model velocity gradients both above and below the 410 km discontinuity and the observed 410 P-wave velocity step is within 10% of ak135. The 410 velocity gradients for three of the models are sharp (<5 km) and for two of the models are gradational (25-30 km). The maximum 410 velocity gradient is found at depths of 392-443 km. From this small sample set, no correlation between the 410 widths and depths is observed. All five models have 2-4% higher velocities in the 50-100 km depth interval above the 660 km discontinuity which may manifest stagnated slabs. The two models with a large 410 gradient can be explained by up to 500 ppm by mass hydration levels.

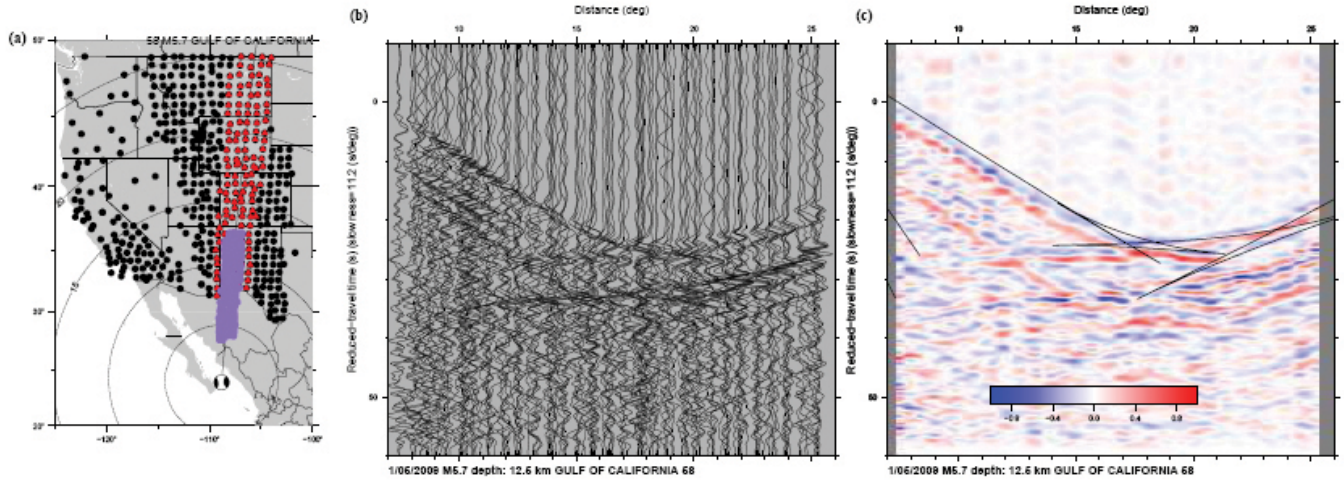

Baja California earthquake P-wave recorded by the Transportable array.

Steep Reflections from the Earth's Core Reveal Small-Scale Heterogeneity in the Upper Mantle

Hrvoje Tkalčić *(The Australian National University),* **Vernon F. Cormier** *(University of Connecticut),* **Brian L. N. Kennett** *(The Australian National University),* **Kuang He** *(University of Connecticut)*

We investigate arrivals of seismic phases reflected from the core-mantle boundary (PcP waves) and those reflected from the inner-core boundary (PKiKP waves) at subcritical angles, with the goal of measuring their amplitude ratios [Tkalčić et al., 2010]. This adds invaluable data points required to study the density jump across the inner-core boundary (ICB). One nuclear explosion and one earthquake, both with favourable focal mechanisms are identified as sources that produce an excellent and abundant record of arrivals of both PcP and PKiKP waves at multiple stations. There is only a limited number of detections of both types of waves on the same seismogram, while more frequently, either one or another of the two phases is detected. Thus, for those cases where at least one phase is above a detectable level, we observe a highly significant negative correlation (anti-correlation) of phase appearances on seismograms, where PcP and PKiKP phase-detections are treated as dichotomous, categorical random variables that can take values detected or undetected. The fact that similar anti-correlation is observed for both explosive and tectonic sources makes less likely the possibility that source effects or a specific near source structure is responsible for this phenomenon. Although laterally varying structure near the core-mantle boundary (CMB) can account for the magnitude of observed fluctuations in the amplitude ratio of PKiKP to PcP, the Fresnel volumes surrounding their ray paths are well separated at the CMB at the frequencies of interest. This separation excludes the possibility that complex structure at or near the CMB is the dominant effect responsible for the observed anti-correlation. We demonstrate that the interaction of the wave-field with near-receiver heterogeneities is an important additional source of amplitude fluctuations across arrays of stations, and the likely cause of the anti-correlation pattern. The combined effects of heterogeneities near the surface and the CMB have a profound impact on the estimates of the PKiKP/PcP amplitude ratios and the subsequent estimates of the density jump at the ICB.

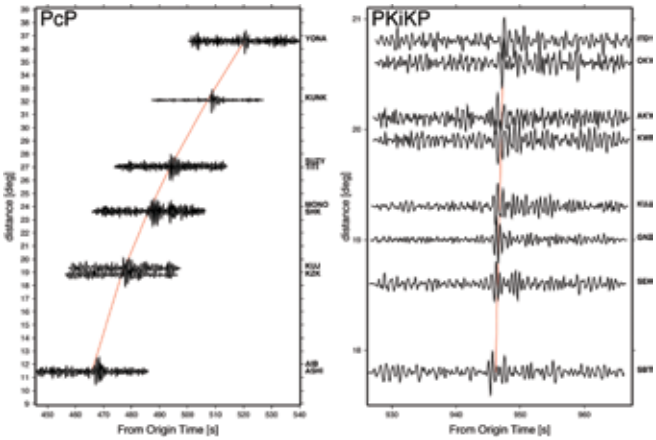

Selected PcP (left) and PKiKP (right) observations for the mb=5.7 earthquake located northwest of Kuril Islands and dated 02/07/2001. The broadband velocigrams are band-pass filtered between 1 and 3 Hz. The theoretical travel time prediction of PcP and PKiKP from the ak135 model is shown by solid line. The scales for PcP and PKiKP records are different to account for the space and changing slowness across the range of selected stations.

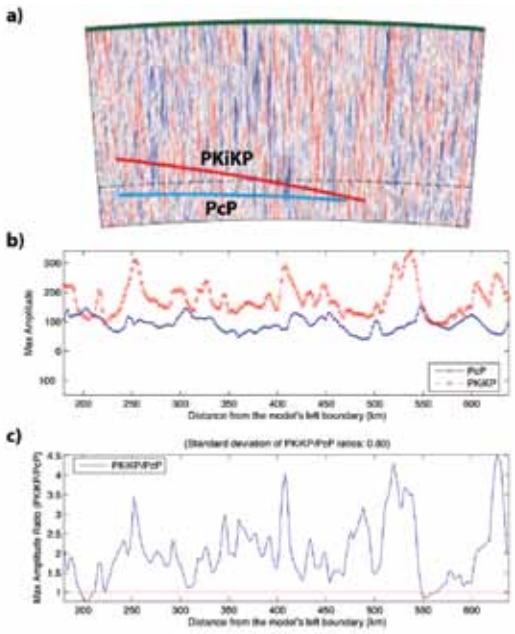

(a) Wavefronts of PcP (blue) and PKiKP (red) in the range 16 to 25 degrees incident on an earth model perturbed by statistically described heterogeneity in the crust and upper mantle beneath a receiver array. A 5 per cent RMS perturbation in P velocity is assumed with an exponential autocorrelation. (b) Predicted amplitude fluctuations of PKiKP and PcP at an array of surface receivers measured from bandpassed seismograms of particle velocity synthesized by a numerical pseudospectral method in anisotropic distribution of scale lengths with a vertical cutoff at 100 km and horizontal cutoff at 2 km. (c) The PKiKP/PcP ratio (includes only the effects of heterogeneity beneath the receiver array).

References

Tkalčić H., V.F. Cormier, B.L.N. Kennett and K. He (2010). Steep reflections from the Earth's core reveal small-scale heterogeneity in the upper mantle, *Phys. Earth Planet. Int., 178*, 80-91, DOI:10.1016/j.pepi.2009.08.004.

Acknowledgements: We would like to thank IRIS DMC for efficiently archiving and distributing continuous waveform data. V.F. Cormier's participation was supported by a grant from the Vice Chancellor of the Australian National University funding travel as a Visiting Fellow, and by the National Science Foundation under grant EAR 07-38492.

Mapping the Upper Mantle with the Spectral Element Method

Ved Lekic *(Berkeley Seismological Laboratory),* **Barbara Romanowicz** *(Berkeley Seismological Laboratory)*

Over the past quarter century, ray- and perturbation-theoretical techniques have enabled tomographers to map the large scale structure of the Earth's mantle. However, the approximations underpinning these techniques prevent them from accurately predicting the effects of sharp or strong heterogeneities [e.g. Wang and Dahlen, 1995], as well as those arising from crustal structures [e.g. Lekic et al., 2010]. As a result, the images obtained are incomplete and contaminated, and amplitudes of observed anomalies are poorly constrained. Yet, it is precisely the amplitude and sharpness of seismic anomalies that are needed to decipher the temperature and composition (T/C) variations that underlie them. Mapping T/C variations in the mantle is crucial for understanding how these control mantle convection, and is one of the grand challenges facing Earth Science.

We have replaced traditional forward modeling approximations by full waveforms computed using the coupled Spectral Element Method [CSEM: Capdeville et al. 2003], and have developed a new model of upper mantle 3D shear velocity and radial anisotropy variations. CSEM is a fully numerical technique that makes possible very accurate simulations of wave propagation through complex 3D Earth structures. Our model – SEMum – confirms the long wavelength structures imaged by previous efforts, but is characterized by stronger amplitudes, which implicate composition in explaining the observed heterogeneities. Furthermore, SEMum reveals structures not clearly imaged by earlier global studies. Perhaps the most intriguing of these is the pattern of low velocities beneath the Pacific Ocean, which might be indicative of ongoing small-scale convection.

Regional comparisons demonstrate that SEMum can match the resolution of smaller-scale studies, and replicate these throughout the globe. This is due to both the improved modeling technique and the wealth of information contained in – and successfully extracted from – high-fidelity recordings of complete seismic waveforms provided by the Global Seismographic Network (GSN), its international partners and regional broadband networks.

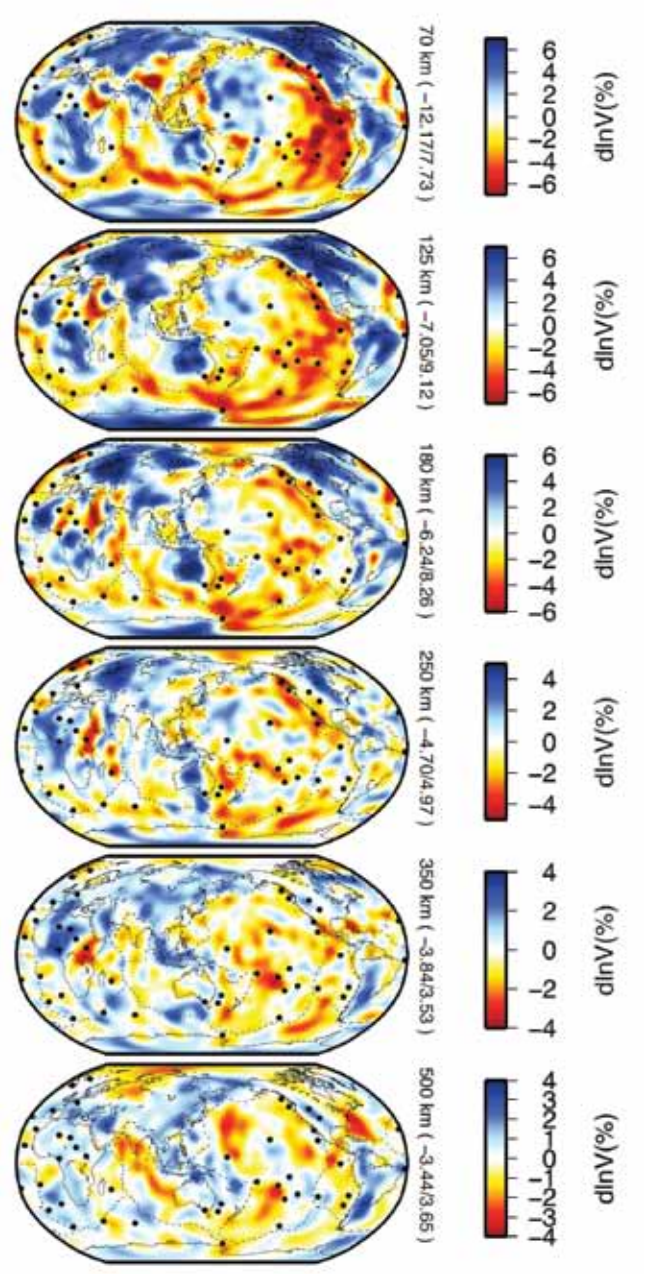

Maps of the Voigt average shear wave-speed variations with respect to the average velocity at each depth. Note that the limits of color scales change with depth and that the colors saturate in certain regions. Black circles indicate locations of hotspots.

References

Capdeville, Y., Chaljub, E., Vilotte, J. P., & Montagner, J. P., 2003. Coupling the spectral element method with a modal solution for elastic wave propagation in global earth models, *Geophys. J. Int., 152*, 34–67.

Lekic, V., Panning, M. & B. Romanowicz, 2010. A simple method for improving crustal corrections in waveform tomography, *Geophys. J. Int.*,

Wang, Z. & Dahlen, F., 1995. Validity of surface-wave ray theory on a laterally heterogeneous earth, *Geophys. J. Int., 123*(3), 757–773.

Acknowledgements: This study was supported by NSF EAR-0738284 to BR and an NSF Graduate Research Fellowship to VL.

Adjoint Tomography for the Middle East

Daniel Peter *(Princeton University),* **Brian Savage** *(University of Rhode Island),* **Arthur Rodgers** *(Lawrence Livermore National Laboratory),* **Jeroen Tromp** *(Princeton University)*

We evaluate 3D models of the Middle East by computing full waveforms for a set of regional earthquakes [Savage et al., 2009]. We measure traveltime shifts between observed broadband data obtained from IRIS and synthetic seismograms for distinct seismic phases within selected time windows using a recently developed, automated measurement algorithm [Maggi et al., 2009]. Based on the measurements for our study region, we selected a best model to feature as the starting seismic model for a fully numerical 3D seismic tomography approach.

In order to improve the initial 3D seismic model, the sensitivity to seismic structure of the traveltime measurements for all available, regional network recordings is computed. As this represents a computationally very intensive task, we take advantage of an adjoint method combined with spectral-element simulations [Tromp et al., 2005]. We calculate such sensitivity kernels for all seismic events and regional records and use them in a conjugate-gradient approach to iteratively update the 3D seismic model. This will lead to various improvements of the initial seismic structure in order to better explain regional seismic waveforms in the Middle East for nuclear monitoring.

References

Maggi, A., C. Tape, M. Chen, D. Chao and J. Tromp, 2009. An Automated time-window selection algorithm for seismic tomography, *Geophys. J. Int., 178*, 257–281.

Savage, B., D. Peter, B. Covellone, A. Rodgers and J. Tromp, 2009. Progress towards next generation, waveform based three-dimensional models and metrics to improve nuclear explosion monitoring in the Middle East, Proceedings of the 31th Monitoring Research Review of Ground-Based Nuclear Explosion Monitoring Technologies, LLNL-PROC-414451, 9 pages.

Tromp, J., C. Tape and Q. Y. Liu, 2005. Seismic tomography, adjoint methods, time reversal and banana-doughnut kernels, *Geophys. J. Int., 160*, 195–216.

Acknowledgements: This research is sponsored by Air Force Research Laboratory and by National Nuclear Security Administration, Contract No. FA8718-08-C-0009.

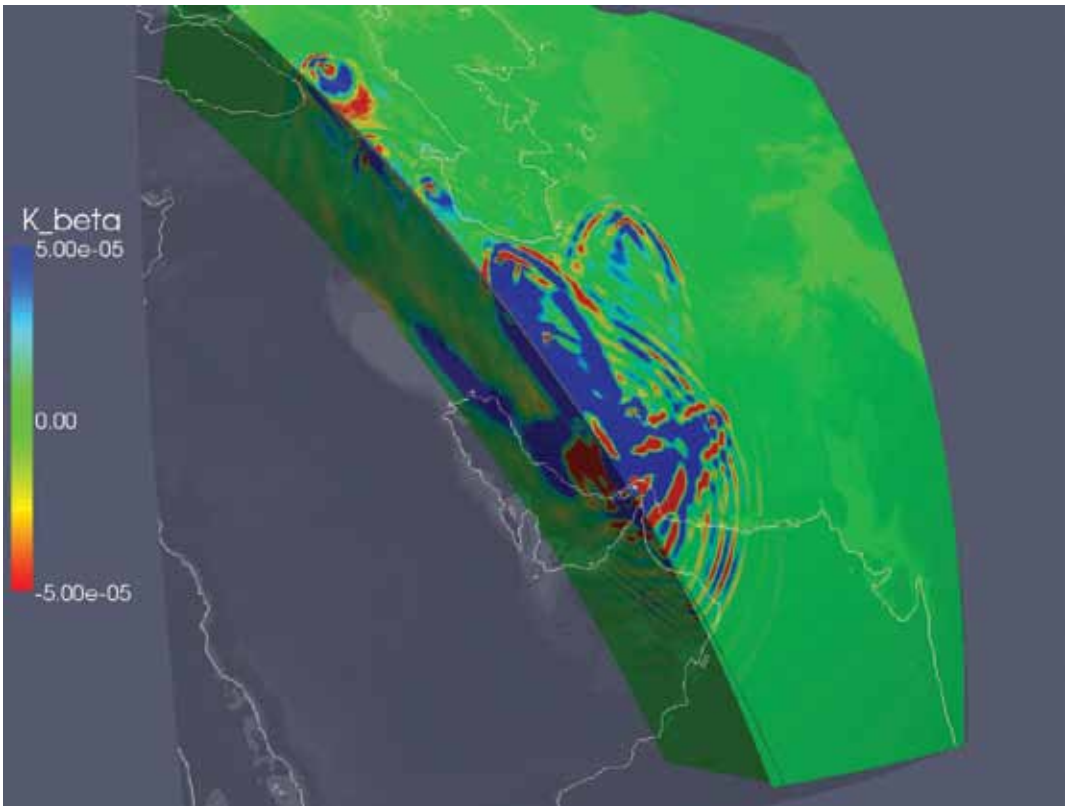

Shear-velocity event kernel for an earthquake in the strait of Hormuz recorded 2005 by several regional stations. Sensitivities are shown on a horizontal cross-section at 5 km depth and a vertical cross-section through the source and a station location down to a depth of 670 km.

Upper Mantle Structure of Southern Africa from Rayleigh Wave Tomography with 2-D Sensitivity Kernels

Aibing Li *(University of Houston)*

A 3-D shear wave model in southern Africa has been developed from fundamental mode Rayleigh wave phase velocities, which are computed at the period range of 20 to 167 s using a two-plane-wave tomography method. 2-D sensitivity kernels are applied in the phase velocity inversion to account for finite-frequency effects, which are significant at periods greater than 100 s. The new model (Figure 1 and 2) confirms the first-order observations found by Li and Burke [2006], a fast mantle lid extending to ~180 km depth and being underlain by a low velocity zone. One new feature in the model is the vertical alignment of a shallow low velocity anomaly with a deep high velocity anomaly at the western Bushveld province. The alignment makes more sense for interpreting the slow as the result of high iron content from the Bushveld intrusion and the fast as a more depleted residual mantle. A low velocity channel at the depths of 220-310 km from the southern end of the Kheiss belt to the northwest of the Kaapvaal craton is also imaged for the first time. It suggests that the hot asthenosphere outside the craton could migrate into the craton area through a weak channel and thermally erode the cratonic lithosphere from below. In addition, low velocity anomalies from 100 to 180 km agree well with the localities of kimberlites erupted at 65-104 Ma in the Kaapvaal craton, providing additional evidence for the depth extent of mantle xenoliths.

References

Li, A., and K. Burke (2006), Upper mantle structure of southern Africa from Rayleigh wave tomography, *J. Geophys. Res., 111*, B10303, doi:10.1029/2006JB004321.

Jelsma, H. A., M. J. De Wit, C. Thiart, P. H. Dirks, G. Viola, I. J. Basson, and E. Anckar (2004), Preferential distribution along transcontinental corridors of kimberlites and related rocks of Southern Africa, *S. Afr. J. Geol., 107,* 301-324.

Yang, Y., and D.W. Forsyth (2006), Regional tomographic inversion of amplitude and phase of Rayleigh waves with 2-D sensitivity kernels, *Geophys. J. Int., 166*, 1148-1160.

Acknowledgements: Data used in this study are from the IRIS DMC. Yingjie Yang kindly provided the inversion codes with 2-D sensitivity kernels. This research is supported by NSF grant EAR-0645503.

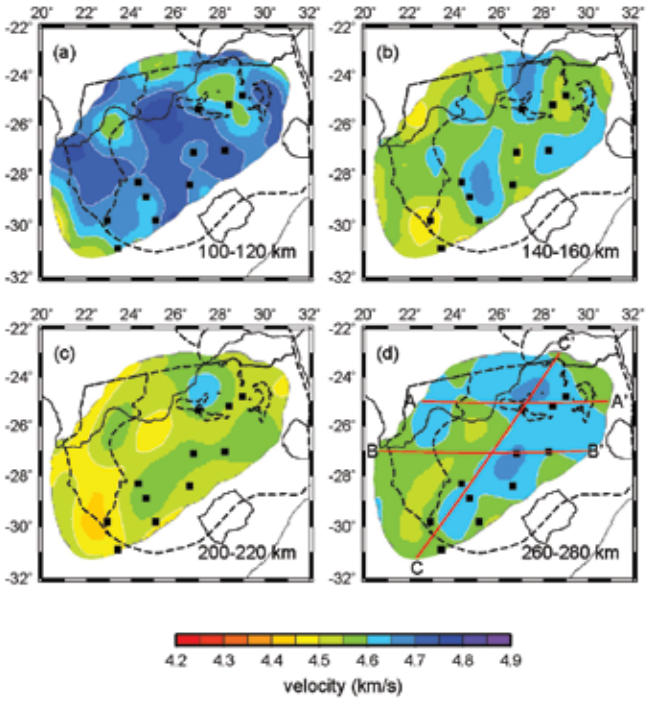

Figure 1. Shear-wave velocity variations at 4 depth ranges. Black squares delineate the sites of kimberlites at 104 to 65 Ma based on Fig. 7c in Jelsma et al. (2004), which show a better correlation with slow regions in shallow upper mantle (a and b). Red lines show the locations of profiles in Figure. 2. Dashed lines are tectonic boundaries.

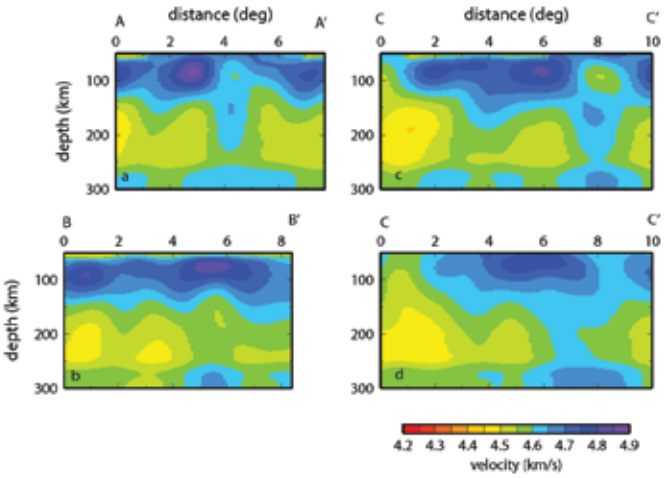

Figure 2. Shear-wave velocity profiles at the depths of 50-300 km. A relative low velocity zone appears on all profiles at roughly 160-260 km depths. (a-c) Velocity profiles of AA', BB' and CC' from this study. (d) Shear-wave velocity profile along CC' from the study of Li & Burke (2006). Note the good alignment of the shallow, slow anomaly and the deep, fast anomaly at the distance of 8 degree in (c), which is not well imaged in (d).

A Low Velocity Zone Atop the Transition Zone in Northwestern Canada

Andrew J. Schaeffer *(The University of British Columbia, now at Dublin Institute for Advanced Studies),* **Michael G. Bostock** *(University of British Columbia)*

Seismic studies over the past decade have identified a S-wave low-velocity zone (LVZ) above the transition zone at various locations around the globe. This layer is hypothesized to be a lens of dense, hydrous silicate melt ponding atop the 410 km discontinuity, beneath the silicate melt-density crossover theorized to exist within the upper mantle [*Bercovici and Karato, 2003*]. We have assembled a P- and S-receiver function (PRF and SRF, respectively) dataset from the CNSN Yellowknife Array (YKA), the CANOE array (obtained from the IRIS DMC), and the POLARIS-Slave array, in order to quantify the physical properties and geographical extent of the layer in Northwestern Canada.

In order to compute the Poisson's ratio, an important discriminant of possible composition and/or fluid content, we generated a suite of 1-D velocity models based on IASP91, but with varying thicknesses and velocity ratios for a hypothetical layer above the 410 km discontinuity. Through utilization of differential times of forward- and back-scattered arrivals from the LVZ bounding interfaces, the Poisson's ratio and thickness is isolated indepedently from the overlying column of material [*Audet et al, 2009*]. From these models, we computed moveout curves over the range of slowness for the main scattering modes (Pds and Ppds) observed in the YKA data. A grid search was performed over the model space of interval thickness and Poisson's ratio to obtain an estimate of the model that best accounts for the moveouts represented in the data. In addition, we performed a linearized inversion of transmission coefficient amplitudes to estimate the shear velocity contrast at the bounding interfaces of the LVZ. Results indicate a LVZ of thickness ~36 km with a Poisson's ratio of 0.42, and shear velocity contrasts of minus and plus 7.5% into and out of the LVZ, respectively. Bootstrap resampling error estimates for thickness and Poisson's ratio are ±3km and ±0.011. In combination, our results require an increase in compressional velocity associated with the shear velocity drop into the LVZ. The Poisson's ratio lies well above the IASP91 average of ~0.29-0.3 for this depth range and favours the presence of high melt or fluid fractions.

Geographic profiles of PRFs and SRFs 1-D migrated to depth from CANOE and POLARIS-Slave arrays reveal 410 km and 660 km discontinuities at nominal depths with little variation in transition zone thickness. PRF results from the Slave craton indicate a potential LVZ beneath many stations at an average nominal depth of ~340 km, highlighted by events from the northwest. The CANOE array SRF profile images an emergent LVZ beginning at ~280 km depth dipping eastwards to 310 km approaching YKA.

Reference

Audet, P., Bostock, M., Christensen, N. I., and Peacock, S. M. (2009). Seismic evidence for over-pressured subducted oceanic crust and megathrust fault sealing. *Nature, 457*, 76-78.

Bercovici, D. and Karato, S. (2003). Whole-mantle convection and the transition-zone water filter. *Nature, 425*(6953), 39-44.

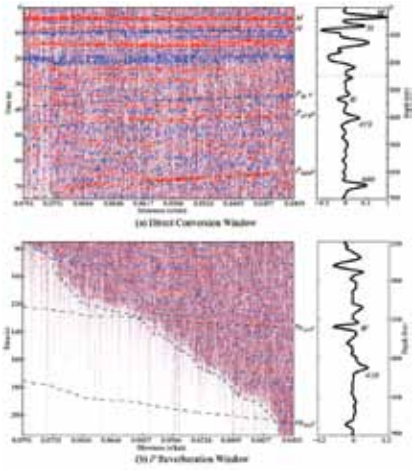

Figure 1: Radial PRFs for the Northwest corridor (274 - 313) YKA dataset. Top panel is windowed for direct conversions converting between the transition zone and the surface, whereas bottom panel is windowed for back-scattered reverberations. The relevant features are indicated in 1D mantle reectivity pro les on the right hand side. The phases utilized include Pds and Ppds.

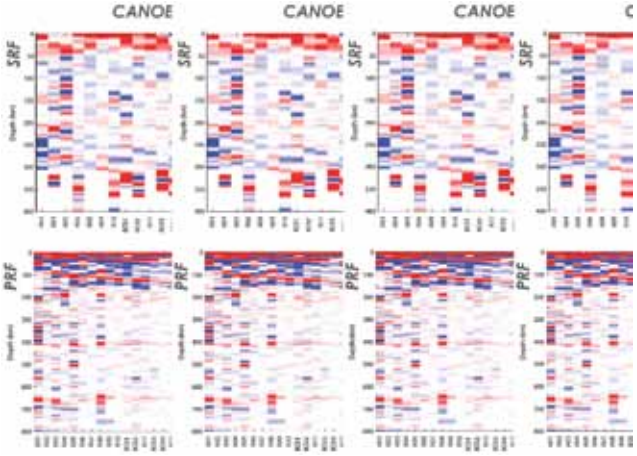

Figure 2: P and SRF pro les for the CANOE and POLARIS-Slave array datasets computing using analogous techniques to that of YKA. Top panels are SRFS and bottom panels are PRFs for CANOE (left) and POLARIS-Slave (right). The LVZ can be seen clearly in the CANOE SRFs at approximately 280 km depth beginning at station A11 and dipping gently eastwards. The Slave PRF image also clearly illustrates a potential LVZ at 330km depth in the Northern stations, and potentially dipping southwards from station MLON.

The Africa-Europe Plate Boundary in Central Italy, Marked by the Seismic Structure of the Crust and Upper Mantle

Vadim Levin *(Rutgers University),* **Jeffrey Park** *(Yale University),* **Nicola Piana Agostinetti** *(INGV, Italy),* **Simone Salimbeni** *(INGV, Italy),* **Jaroslava Plomerova** *(Geophysical Institute, Czech Republic),* **Lucia Margheritti** *(INGV, Italy),* **Silvia Pondrelli** *(INGV, Italy)*

We examined crustal properties in central Italy using receiver-function analysis, and probed mantle texture using observations of splitting in core-refracted shear waves. Our results reveal profound differences between the "Tyrrhenian" and the "Adriatic" sides of the convergence zone that is responsible for the formation of the Apennines.

In the Tyrrhenian domain the crust is apparently thin, and bound by a relatively sharp impedance contrast at a depth of approximately 20-25 km. In the Adriatic domain the definition of the crust–mantle boundary is problematic, suggesting a gradual and/or complicated transition from the crust to the mantle. Receiver function analysis is of less help here, as near-surface structure obscures signals at a number of sites. Where we can resolve it, the crustal thickness is larger (~35 km). We identify the transition between these two crustal thickness regimes, and find it to coincide with the high crest of the Apennines.

The high Apennines also mark the transition in the observations of shear-wave splitting. We see fairly uniform NW-SE fast polarizations beneath Tyrrhenian Sea and Tuscany, while on the Adriatic side we find nearly N-S alignment of fast polarization, as well as evidence for layering of seismic anisotropy.

We posit that the high Apennines mark the easternmost reach of both the "Tyrrhenian" crust and the "Tyrrhenian" upper mantle, and hence define the eastern edge of the Eurasian plate in central Italy.

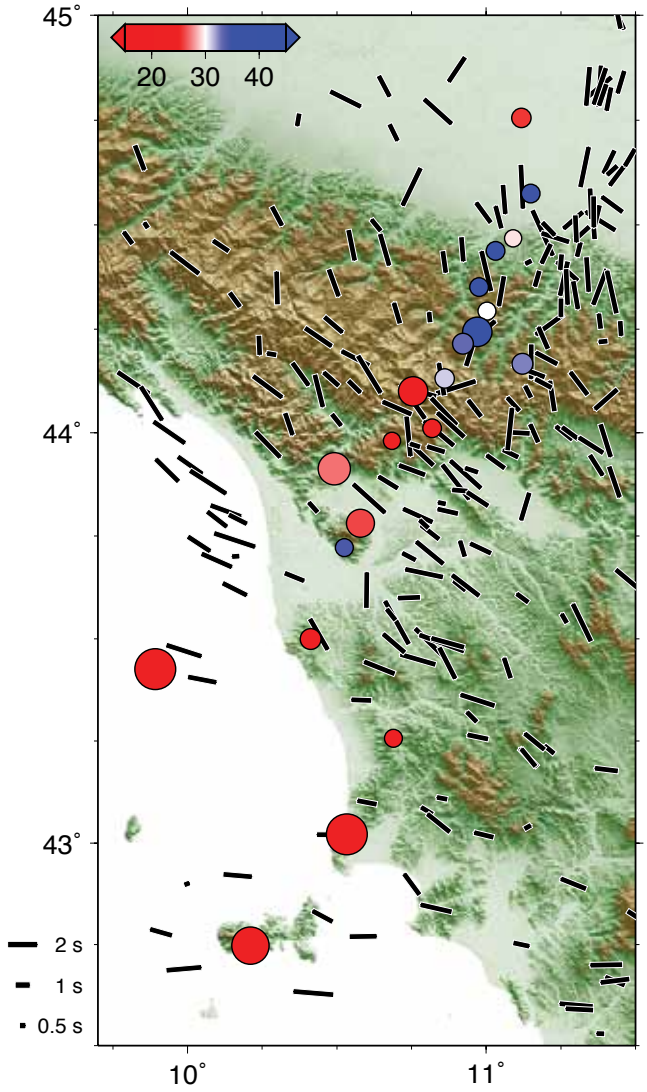

A topographic map illustrates a spatial coincidence of changes in inferred crustal thickness values (circles with depth-scaled color) and observed fast polarization directions of split shear waves (black bars). Circle size is proportional to confidence in the result (largest are most certain). Splitting observations are scaled with delay and aligned with the fast polarization. Both types of observations change dramatically across the highest part of the Apennines.

References

Piana Agostinetti, N., V. Levin and J. Park, Crustal structure above a retreating trench: Receiver function study of the northern Apennines orogen, *Earth Planet. Sci. Lett., 2008.*

Salimbeni, S., S. Pondrelli, L. Margheriti, V. Levin, J. Park, J. Plomerova and V. Babuska, Abrupt change in mantle fabric across northern Apennines detected using seismic anisotropy, *Geophys. Res. Lett., 34*, L07308, 2007

Plomerova, J., L. Margheriti, J. Park, V. Babuska, S. Pondrelli, L. Vecsey, D. Piccinini, V. Levin, P. Baccheschi, and S. Salimbeni, Seismic anisotropy beneath the Northern Apennines (Italy): Mantle flow or lithosphere fabric *Earth Planet. Sci. Lett.., 247*, pp. 157- 170, 2006.

Acknowledgements: Research reported here resulted from the PASSCAL deployment in Italy (http://www.iris.edu/mda/YI?timewindow=2003-2006) that was a part of the RETREAT project funded by the NSF Continental Dynamics program. Field operations and subsequent work on data were supported by Istituto Nazionale di Geofisica e Vulcanologia (INGV) and the Geophysical Institute of Prague.

Imaging Lithospheric Foundering beneath the Central Sierra Nevada with Receiver Functions, Teleseismic Surface Waves, and Earthquake Locations

Andy Frassetto *(University of Copenhagen),* **Hersh Gilbert** *(Purdue University),* **Owen Hurd** *(Stanford University),* **George Zandt** *(University of Arizona),* **Thomas J. Owens** *(University of South Carolina),* **Craig H. Jones** *(University of Colorado)*

The southern Sierra Nevada represents a fundamental example of a Cordilleran batholith which has recently lost its eclogitized, mafic-ultramafic lower crust and lithospheric mantle. From May 2005 through September 2007, the Sierra Nevada EarthScope Project (SNEP) targeted the central and northern Sierra Nevada with an array of broadband seismometers to characterize how lithospheric foundering relates to the Isabella and Redding deep seismic anomalies, the modern relief of the Sierra, and ongoing deformation and volcanism in eastern California. Selected key findings from our current study show evidence for ongoing foundering beneath the west-central Sierra Nevada, just southwest of Yosemite National Park.

Conversions from the Moho in stacked receiver functions change from high amplitude and shallow (30-35 km depth) along the High Sierra and Walker Lane to low amplitude and deep (50-55 km) beneath the west-central foothills (Figure 1). Strong negative conversions beneath the Walker Lane, including Long Valley Caldera, are consistent with low wavespeed layering associated with partial melt. Coincidently, surface wave phase velocities show an extensive region of fast material beneath the central Sierra foothills within the lower crust and upper mantle (Figure 2). This fast anomaly merges with the Isabella Anomaly at deeper levels beneath the south-western Great Valley. Beneath the eastern portion of the Sierra, a broad slow anomaly underlies much of the Walker Lane and regions of recent volcanism, indicating the presence of asthenospheric mantle encroaching beneath the High Sierra. Earthquakes located by SNEP show two distinct trends localized along the west-central foothills and batholith. A scattered zone of seismicity lies above the region encompassing diffuse Moho. A more confined trend of earthquakes occurs near where the conversions from the Moho diminish and deepen. This seismicity includes long-period events which occasionally occur at the Moho, likely signaling magma intrusion into the lower crust.

Incorporating observations from geophysical studies and xenoliths sampling the crust and upper mantle, we interpret the region of diffuse Moho and fast lower crust and upper mantle as the remaining gravitationally unstable, actively foundering root of the central Sierra Nevada batholith. The region of slow upper mantle phase velocities and sharp Moho demarcates the region where the batholithic root has been removed.

References

Zandt, G., Gilbert, H., Owens, T.J., Ducea, M., Saleeby, J., and Jones, C.H., 2004, Active foundering of a continental arc root beneath the southern Sierra Nevada in California, *Nature,* ***431***, 41–46.

Acknowledgements: This work was supported by the National Science Foundation's EarthScope grants EAR-0454554, EAR-0454524, and EAR-0454535 to the Universities of Arizona, Colorado, and South Carolina. This work was also made possible by funding from the National Science Foundation through the Graduate Research Fellowship Program.

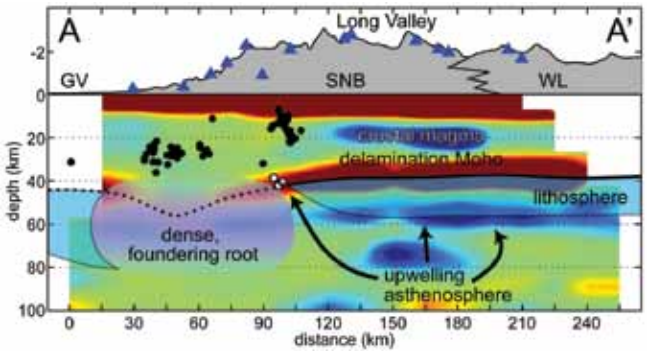

Figure 1: Interpreted common-conversion-point stack of receiver functions from broadband stations (blue) deployed across the central Sierra Nevada. Red represents strong conversions off the up-going P-wave from high-to-low steps in wavespeed; blue represents low-to-high steps. Locations of nearby earthquakes are projected onto the profile. White circles denote long period earthquakes. GV = Great Valley, SNB = Sierra Nevada batholith, WL = Walker Lane. The transect is shown in map view in Figure 2.

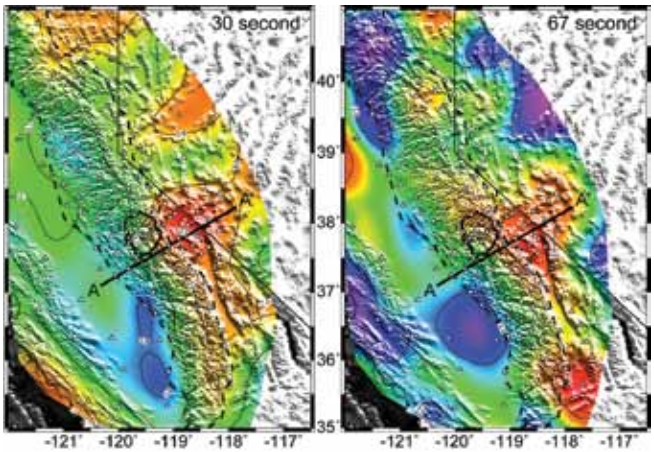

Figure 2: Phase velocities for 30 second (left) and 67 second (right) period teleseismic surface waves. Shading ranges from pink (>4.2 km/s) to red (<3.3 km/s). White triangles denote stations used, including the more densely spaced SNEP array. Locations of receiver function transect (A-A') and Yosemite National Park (north of profile) are shown.

The Isabella Anomaly Imaged by Earthquake and Ambient Noise Rayleigh Wave Dispersion Data: A Composite Anomaly of Sierra Nevada Batholith Root Foundering and Pacific Plate Slab-Flap Translation?

Josh Stachnik *(Univ. Wyoming),* **Ken Dueker** *(Univ. of Wyoming),* **Hersh Gilbert** *(Purdue Univ.),* **George Zandt** *(Univ. of Arizona)*

Sierra Nevada Earthscope Project (SNEP) and Earthscope Transportable Array (TA) Rayleigh wave dispersion data are inverted to construct a shear velocity model of the Sierra Nevada and San Joaquin valley. The Rayleigh wave dispersion dataset was measured using the two-plane wave method with earthquake records and the parametric Bessel-zeros method [*Ekstrom et al.*, 2009] with correlated ambient noise records. Two starting velocity models have been tested: a uniform (4.4 km/s) starting model and a starting model with the Moho mapped by Pn station time terms [*Buehler and Shearer*, in review].

With respect to previous body and surface wave tomograms, the Isabella anomaly is imaged as more geometrically rich. This observation leads us to consider a composite explanation of the anomaly as a Pacific plate slab-flap (Monterey microplate) and the foundering roots of the southern Sierra Nevada batholith. The slab flap is identified as a 4.4-4.6 km/s NW-SE striking 140 km wide planar anomaly imaged at 60-110 km depth beneath the San Joaquin valley. The foundering southern Sierra batholithic root is identified as an N-S trending 4.4-4.5 km/s high velocity region beneath the southern Sierran foothills. This anomaly is bowed down beneath the high standing southern Sierra block to form a wedge filled with 4.2 km/s mantle which is interpreted as in-flowed asthenosphere. The pros and cons of this composite interpretation will be discussed.

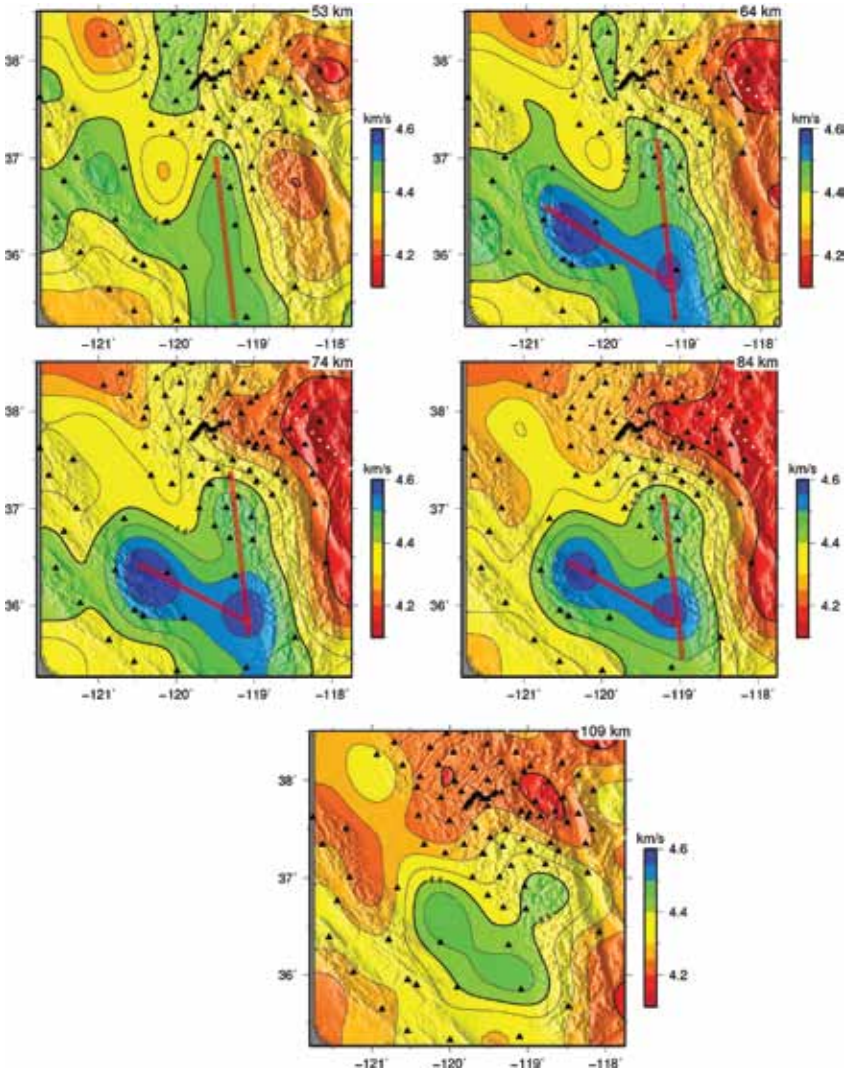

Shear velocity image from inversio of ambient and earthquake Rayleigh wave dispersion measurements using SNEP and Transportable array data.

Comparison of our velocity model with the only other joint ambient/earthquake surface wave model [*Moschetti et al.*, in review] finds that the two models are well correlated. Comparison of our velocity model with teleseismic body wave tomograms reveals substantial differences in the geometry and depth extent of the Isabella anomaly related to differences in the resolution of surface and body waves.

References

Ekström, G., G. A. Abers,and S. C. Webb, Determination of surface-wave phase velocities across USArray from noise and Aki's spectra formulation, *Geophys. Res. Lett., 36*, L18301, 2009.

Detection of a Lithospheric Drip beneath the Great Basin

John D. West *(Arizona State University),* **Matthew J. Fouch** *(Arizona State University),* **Jeffrey B. Roth** *(Arizona State University/ExxonMobile),* **Linda T. Elkins-Tanton** *(Massachusetts Institute of Technology)*

Using a combination of shear-wave splitting and seismic P-wave delay time tomography, we investigated a region of greatly diminished shear-wave splitting times, collocated with a sub-vertical cylinder of increased seismic velocity in the upper mantle beneath the Great Basin in the western United States. The localized reduction of splitting times is consistent with a rotation in flow direction from predominantly horizontal to sub-vertical, and the high velocity cylinder is characteristic of cooler lithospheric mantle. We suggest that the reduced splitting times and higher than average seismic velocities are the result of a cold mantle downwelling (a lithospheric drip). The cylinder of higher seismic velocities is approximately 100 km in diameter, extends near-vertically from ~75 km depth to at least 500 km, and plunges to the northeast. Near 500 km depth, the cylinder merges with a separate zone of high-velocity material, making resolution of a distinct cylinder difficult below this depth.

We generated geodynamic numerical models of Rayleigh-Taylor instabilities originating in the mantle lithosphere, using structural constraints appropriate to conditions in the central Great Basin. These models predict downwelling lithospheric mantle in the form of a strong, focused lithospheric drip developing over time periods of <1 to ~25 Myr, triggered from local density anomalies as small as 1% and initial temperature increases of ~10%.

Lithospheric drips are often inferred based on surface expressions of rapid uplift, subsidence, or voluminous magmatic activity, but have remained challenging to detect directly due to their relatively small size and transient nature. The Great Basin drip was detected by purely geophysical means and does not exhibit significant recognizable surface topography modifications, consistent with our numerical models.

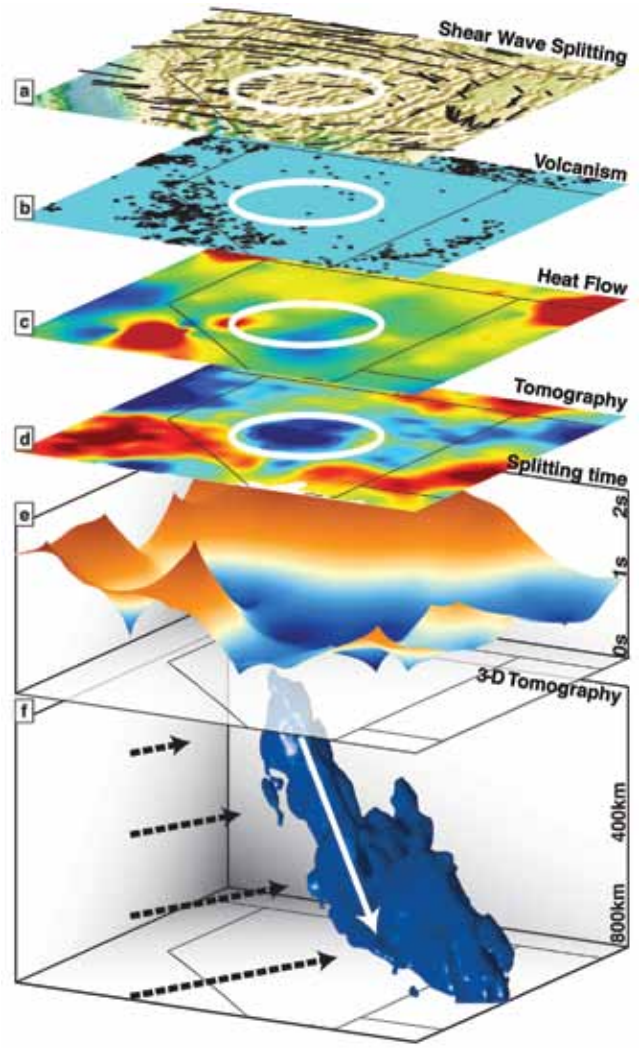

Summary of geological and geophysical constraints for the central Great Basin. a, Shear-wave splitting with the topography background for reference. b, Post-10-Myr volcanism (black circles) shows a regional dearth of volcanic activity. c, Heat flow showing reduced values (~50mWm, blue) in the regional high (>100mWm; yellow and red). d, Seismic tomography horizontal slice at 200 km depth. e, Shear-wave splitting times surface showing the strong drop in the central Great Basin. f, Isosurface at +0:95% velocity perturbation for NWUS08-P2 showing the morphology of the drip, which merges with a larger structure at ~500 km depth. The black arrows denote the inferred mantle flow direction; the white arrow denotes the flow direction of the Great Basin drip.

The interpretation of a lithospheric drip beneath the Great Basin is consistent with geophysical and geological characteristics of the region, including a distinct paucity of post-12 Ma volcanic activity and a heat flow low. Lithospheric material feeding horizontally into the drip would be expected to generate contractional forces if significant mantle/crust coupling exists, and surface contraction centered near the drip has been observed. The northeast plunge of the drip provides a unique indicator of northeast-directed regional mantle flow relative to the North American plate.

References

West, J.D., M.J. Fouch, J.B. Roth, and L.T. Elkins-Tanton, (2009), Vertical mantle flow associated with a lithospheric drip beneath the Great Basin, *Nature Geosci., 2*, 439-444

Holt, W., M.J. Fouch, E. Klein, and J.D. West, (2010), GPS measured contraction in Nevada above the Great Basin mantle drip, in preparation.

Acknowledgements: Thanks to the USArray Transportable Array team for the instrumentation which made this study possible, and to the IRIS Data Management Center for providing access to the data. Partial support for this project came from US National Science Foundation grants EAR-0548288 (MJF EarthScope CAREER grant) and EAR-0507248 (MJF Continental Dynamics High Lava Plains grant).

Tomographic Image of the Crust and Upper Mantle Beneath the Western Tien Shan from the MANAS Broadband Deployment: Possible Evidence for Lithospheric Delamination

Steven Roecker *(Rensselaer Polytech. Inst.),* **Li Zhiwei** *(Rensselaer Polytech. Inst)*

We combined teleseismic P arrival times from the MANAS deployment of broad band sensors with P and S arrival times from local events recorded by the GENGHIS deployment and analogue observations from the Kyrgyz Institute of Seismology to generate a high resolution (~20 km) image of elastic wavespeeds in the crust and upper mantle beneath the western Tien Shan. The total data set consists of 29,006 P and 21,491 S arrivals from 2176 local events recorded at 144 stations along with 5202 P arrivals from 263 teleseismic events recorded at 40 stations. The most significant feature in our image of the mantle beneath the Tien Shan is a pair of large, elongated high wavespeed regions dipping in opposite directions from the near surface to depths of at least 400 km. These regions appear to be continuous and extend upwards to bounding range fronts where the Tarim Basin is being overthrust by the Kokshal range on the south side, and the Kazach shield underthrusts the Kyrgyz range on the north side. While it is tempting to interpret these high wavespeed anomalies as evidence for contemporary subduction of continental lithosphere, such a scenario is difficult to reconcile with both 2the timing of the orogen and the size of the wavespeed anomaly. We suggest instead that they represent downwelling side-limbs of a lithospheric delamination beneath the central part of the Tien Shan, possibly by siphoning of the bordering continental lithosphere as the central part descends.

Acknowledgements: All of the broad band seismic equipment used in the MANAS and GHENGIS projects was provided by the IRIS PASSCAL program. This work was supported by the NSF Continental Dynamics Program (EAR-0309927).

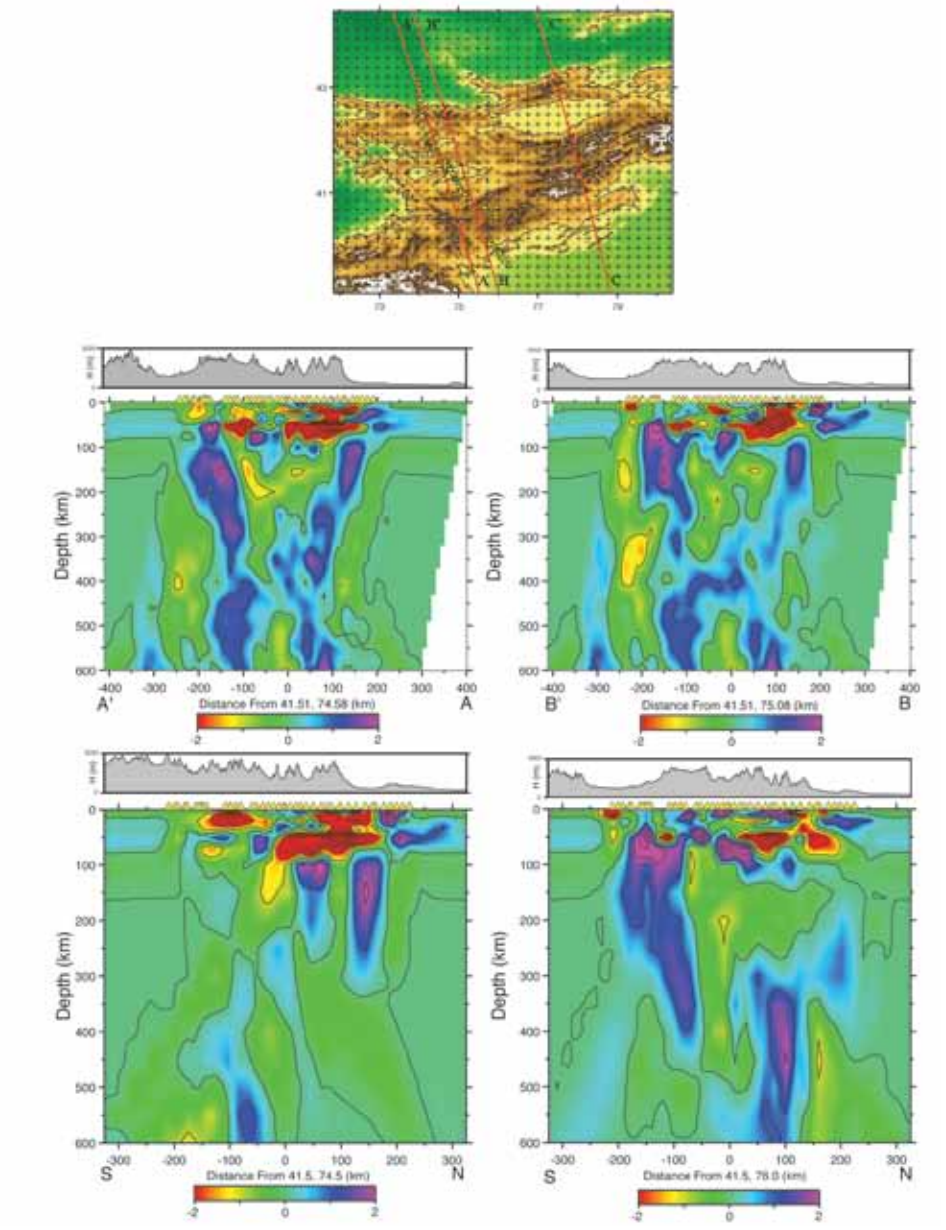

Perturbations to P wavespeed (dVp/Vp) from an average 1D background model determined by inversion of the teleseismic travel time residuals. The locations of the slanted cross sections are shown at the top of the figure: the maximum resolution projection onto a plane extending from AA' to CC' is shown on the upper left. A slightly displaced plane from BB' to CC' is shown on the upper right. The vertical axis in these sections is true depth in km (as opposed to downdip length). The lower two plots are NS sections taken at 74.5o (left) and 76.0 o (right) longitude. The 74.5 o section has better resolution at shallow depths in the north, while the 76.0 o section has better resolution at shallow depth in the south. Perturbations relative to the 1D average background wavespeeds are in percent as indicated in the palettes below each section. Locations of the MANAS stations are shown as yellow triangles at the surface. Topography along each section is shown in the box above each section.

Global Variations of Temperature and Water Content in the Mantle Transition Zone from Higher Mode Surface Waves

Jeannot Trampert *(Utrecht University),* **Ueli Meier** *(IDSIA Lugano),* **Andrew Curtis** *(University of Edinburgh)*

We estimated lateral variations of temperature and water content in Earth's mantle transition zone from models of transition zone thickness and S-wave velocity (Meier et al., 2009). The latter were obtained by a fully nonlinear inversion of surface wave overtone phase velocities using neural networks. Globally we observe a broader than previously reported transition zone and explain this by a broad olivine to wadsleyite transition at around 400 km depth where the minerals co-exist with water induced melt. Within the transition zone we observe relatively cold subduction zones as well as relatively warm regions beneath continents and hot spots. We find that the transition zone is wettest away from subduction zones.

References

Meier U., Trampert J., Curtis A., 2009. Global variations of temperature and water content in the mantle transition zone from higher mode surface waves, *Earth Planet. Sci. Lett., 282*, 91-101.

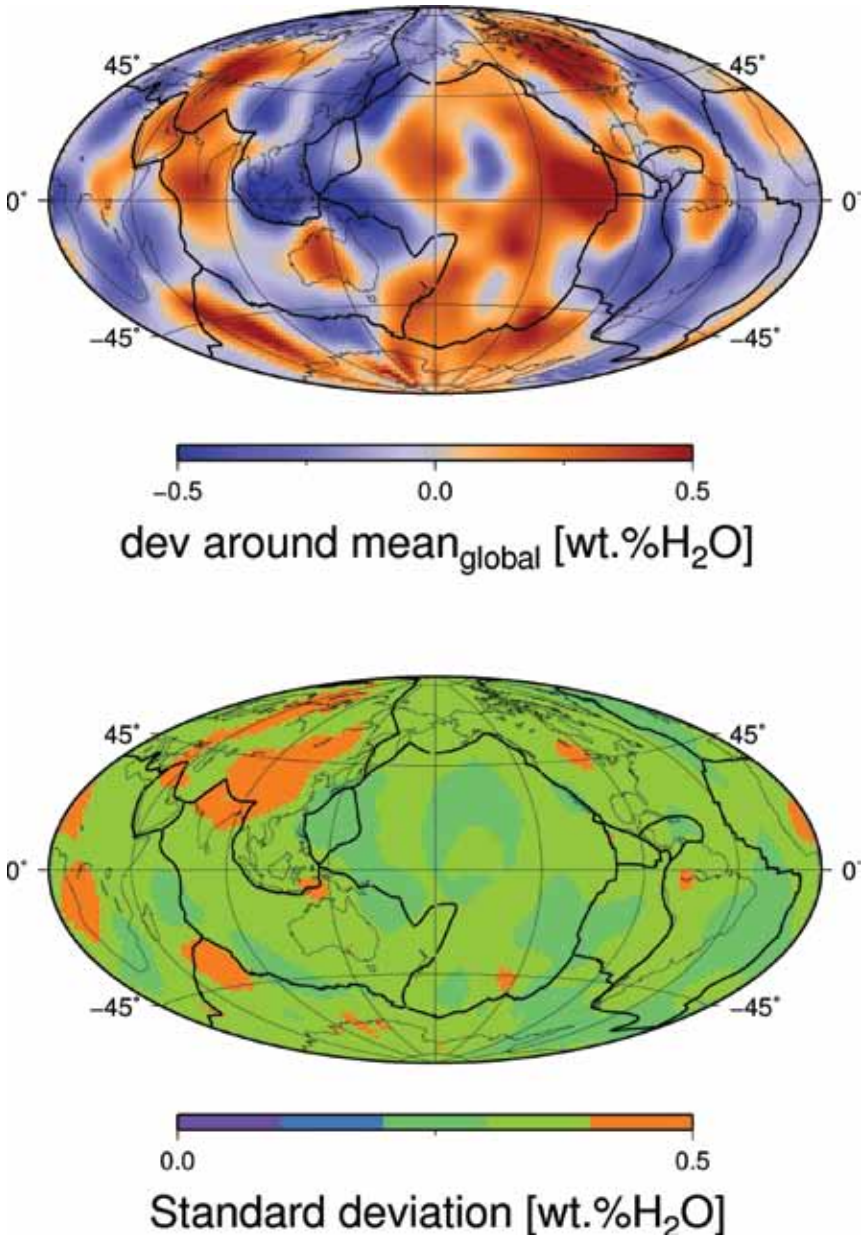

Mean water content variation from the unknown global mean in the mantle transition zone (top) together with the corresponding standard deviations (bottom).

Small-Scale Mantle Heterogeneity and Dynamics beneath the Colorado Rocky Mountains Revealed by CREST

Jonathan MacCarthy *(New Mexico Institute of Mining and Technology),* **Rick Aster** *(New Mexico Institute of Mining and Technology),* **Ken Dueker** *(University of Wyoming),* **Steven Hansen** *(University of Wyoming),* **Karl Karlstrom** *(University of New Mexico)*

Recent crustal thickness and shear wave velocity estimates from the CREST (Colorado Rockies Experiment and Seismic Transects, NSF Continental Dynamics) experiment indicate that the highest elevations of the Colorado Rocky Mountains (> 2.5 km) are not primarily supported in the crust. Mantle buoyancy and dynamics are therefore of fundamental importance. We present results of teleseismic body wave tomography of the upper mantle beneath western Colorado interpreted in consort with ongoing CREST results. Using a network of over 160 CREST and USArray stations with a minimum spacing of ~24 km, we invert approximately 20,000 P arrivals and nearly 10,000 S arrivals for regularized 3-D models of upper mantle Vp and Vs structure. We find Vp perturbations relative to AK135 of >6% and Vs variations of >8%, with structure being largely confined to the upper 300 km of the mantle. The previously noted "Aspen Anomaly" of low mantle velocities in this region is revealed to be fragmented, with the lowest Vp and Vs velocities beneath the San Juan mountains being clearly distinct from low velocities associated with the northern Rio Grande Rift. The San Juan anomaly probably represents thermal and/or chemical heterogeneity in the uppermost mantle related to voluminous Cenozoic magmatism and possible subsequent piecewise lithospheric dripping and/or crustal delamination. CREST thermochronology and Colorado River incision constraints additionally point to significant Neogene uplift and denudation in the southwestern and central Colorado Rockies associated with mantle forcing. A northeast-southeast grain in shallow Vs domains parallel to the Colorado Mineral Belt may be influenced by Proterozoic accretionary lithospheric architecture. We find that the low velocity anomalies beneath southwest Colorado in particular may provide significant support for enigmatic high elevations. These high-resolution tomography results CREST illuminate a remarkably high-degree of spatial heterogeneity in the region of transition between tectonic and stable North America that may reflect vigorous small-scale convection and related processes linking the lithosphere and mantle transition zones, with characteristic length scales of just 10s of km.

Acknowledgements: The CREST project is supported by the National Science Foundation Continental Dynamics Program, award #0607837, with instrument and field support from the IRIS PASSCAL Instrument Center.

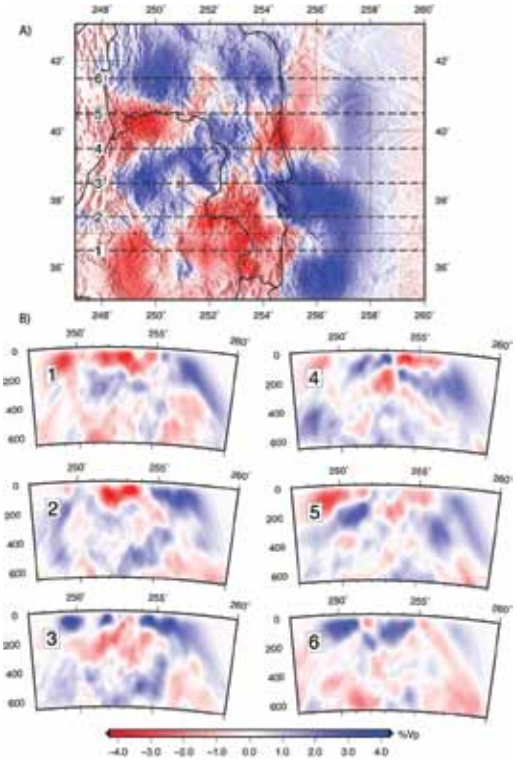

Figure 1 – (A) Depth slices through ΔVp model at 90 km, showing outlines of the Colorado Plateau and southern Rocky Mountains. Cross-section lines 1-6 are shown in (B).

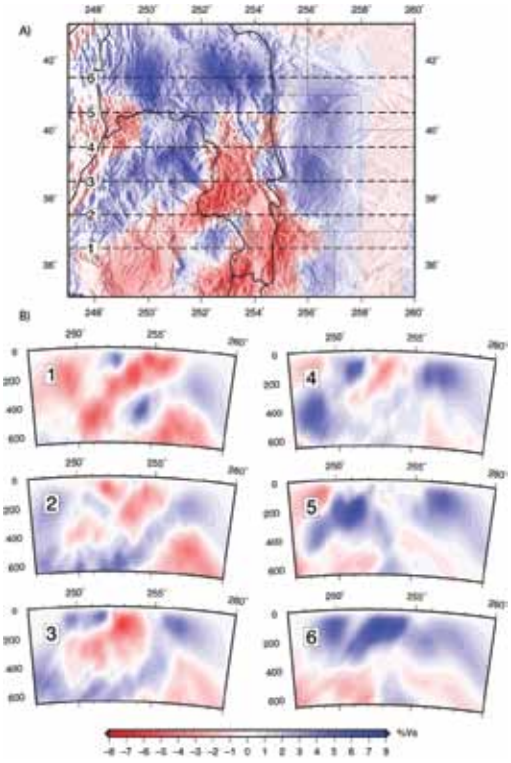

Figure 2 – (A) Depth slices through ΔVs model at 90km, showing outlines of the Colorado Plateau and southern Rocky Mountains. Cross-section lines 1-6 are shown in (B).

The Effect of S-Velocity Heterogeneity in the North American Crust and Mantle on Waveforms of Regional Surface Waves from the February 2008 Nevada Earthquake

Sung-Joon Chang *(Northwestern University),* **Suzan van der Lee** *(Northwestern University)*

We compare observed waveforms recorded at the USArray Transportable Array stations from the 02/21/08 Nevada earthquake (Mw 6.0) with synthetics through three-dimensional (3D) velocity models such as S20RTS [*Ritsema et al., 1999*] and NA04 [*Van der Lee and Frederiksen, 2005*]. A crustal model CRUST2.0 is incorporated into the mantle velocity model S20RTS. We calculate synthetics down to 17 s through: 1) mode summation for a 1D model obtained by averaging velocity variations in the 3D model between the epicenter and the station (path-average method), and 2) the Spectral Element Method [*Komatitsch and Tromp, 1999*]. Because the Nevada earthquake occurred almost at the center of the Transportable Array stations at that time, distances between the epicenter and stations are typically less than 1000 km. In general, the 3D models predict the observed waveforms better than a reference 1D model, but some waveform fits need to be significantly improved by better 3D models of velocity heterogeneity and discontinuity depth. We find the spectral element method and path-averaging method produce similar waveforms for inland, while a little different synthetics are generated with the two methods for ocean-continent boundary.

References

Komatitsch, D. and J. Tromp (1999), Introduction to the spectral-element method for 3-D seismic wave propagation, *Geophys. J. Int., 139,* 806-822.

Ritsema, J., H. J. van Heijst, and J. H. Woodhouse (1999), Complex shear wave velocity structure imaged beneath Africa and Iceland, *Science, 286*, 1925-1928.

Van der Lee, S. and A. Frederiksen (2005), Surface wave tomography applied to the North American upper mantle, in Seismic Earth: Array analysis of broadband seismograms, pp. 67-80, eds. A. Levander and G. Nolet, Geophys. Mono. 157, AGU, Washington, DC.

Acknowledgements: We thank the IRIS DMC for providing waveform data used in this research. This study was supported by NSF EAR-0645752.

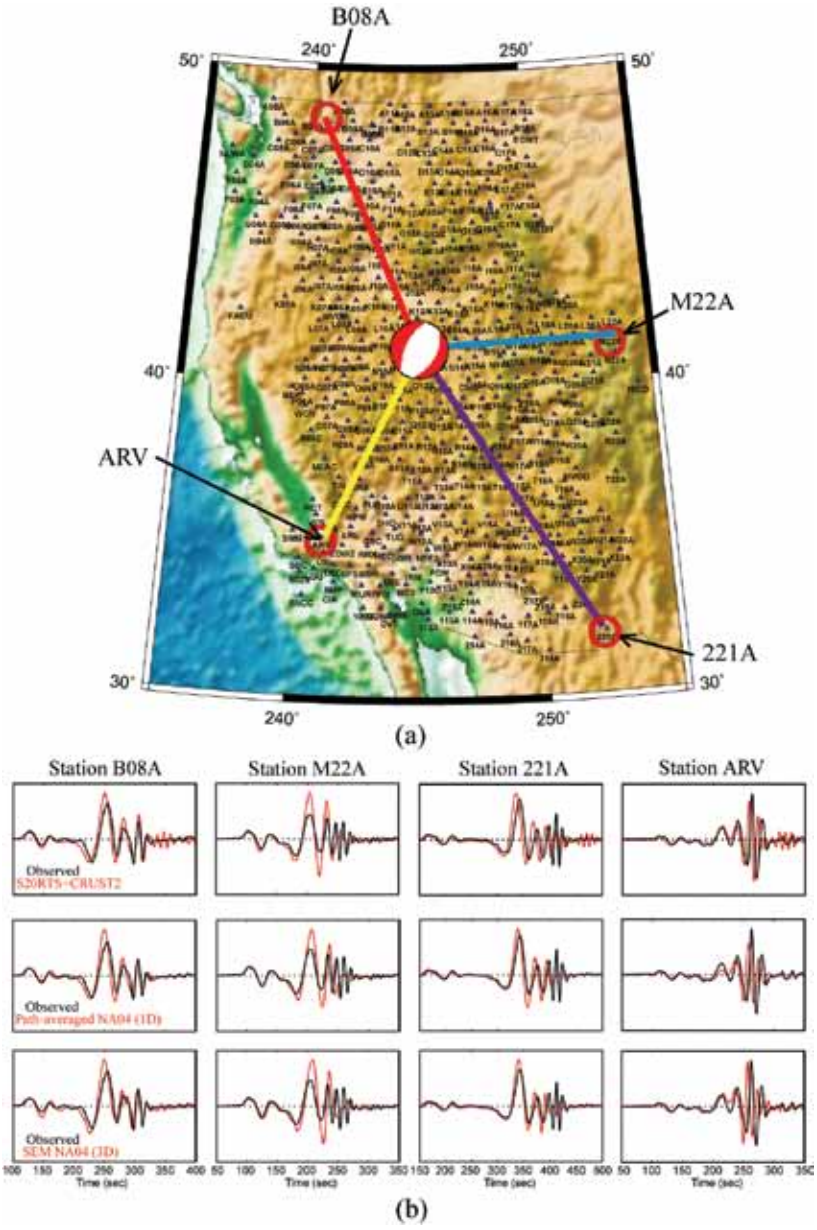

(a) The Nevada Earthquake (Mw 6.0) indicated as a star was recorded at over 400 broadband stations in USArray indicated as triangles. Some stations are surrounded by red circles where observed waveforms are obtained to be compared with synthetics. (b) Comparison between observed waveforms and several synthetics at stations surrounded by red circles in (a).

Mantle Heterogeneity West and East of the Rocky Mountains

Xiaoting Lou *(Northwestern University),* **Suzan van der Lee** *(Northwestern University)*

Separated by the Rocky Mountains, North America is divided into a tectonically active western part and a tectonically stable eastern part. We have measured teleseismic P and S relative delay times using waveforms from IRIS PASSCAL seismic arrays and EarthScopes Transportable Array sampling both western and eastern North America. Relative delay times were corrected for ellipticity, topography, Moho depth and sediments using the Crust 2.0 Model [Bassin et al., 2000]. To investigate the delay time differences between tectonically active and stable North America, seismic stations are divided into two groups: (1) TA stations west of the Rocky Mountains; (2) TA stations east of the Rocky Mountains and stations of MOMA, ABBA, FLED and Abitibi. Delay times within each group of stations are shifted relative to other groups using predicted average delay times by tracing 1D raypath through 3D model NA04 [Van der Lee and Frederiksen, 2005]. The range of relative delay times from seismic stations east of the Rocky Mountains is comparable to that for stations west of the Rocky Mountains, which holds for both station average delay times (Figure 1) and all individual measurements (Figure 2). This suggests that the mantle heterogeneity in the east is comparable to that in the west, despite there being relatively little surface or tectonic expression of this heterogeneity in the east. For both groups of stations, the measured S and P delay times have a significant linear correlation, with S delays at approximately 3 times the P delays, which confirms the dominant effect of mantle temperature on mantle velocity structure.

References

Bassin, C., G. Laske, and G. Masters (2000), The current limits of resolution for surface wave tomography in North America, Eos Trans AGU, 81, F897.

Van der Lee, S., and A. Frederiksen (2005), Surface wave tomography applied to the North American upper mantle, in Seismic Earth: Array Analysis of Broadband Seismograms, Geophys. Monogr. Ser., vol. 157, edited by A. Levander and G. Nolet, pp. 67–80, AGU, Washington, D. C.

Acknowledgements: This study is supported by NSF EAR-0645752 grant to Suzan van der Lee. The authors are grateful to the IRIS DMC for providing seismic waveform data.

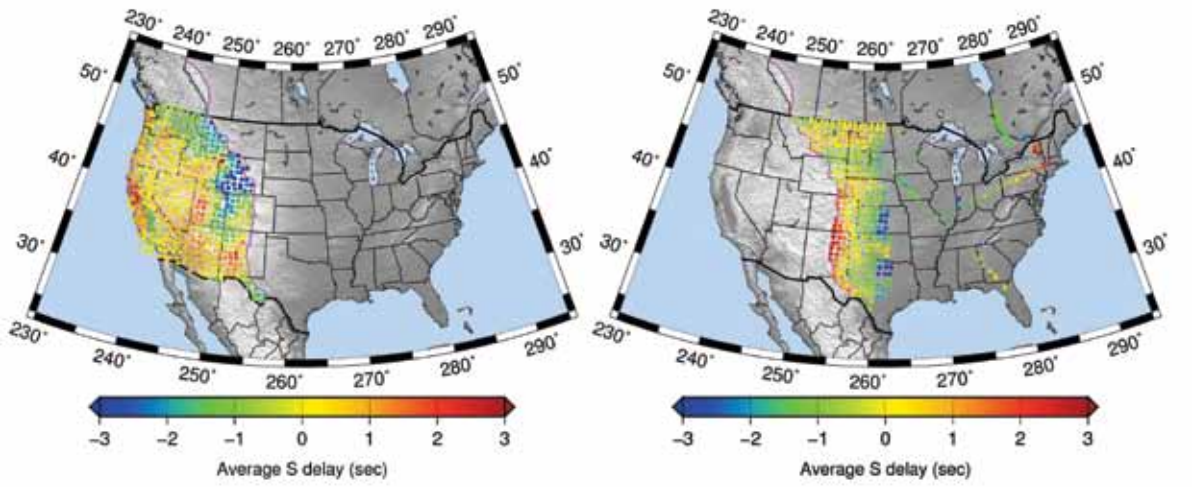

Figure 1: Station average S relative delay times for the two groups of stations west and east of the Rocky Mountains, respectively.

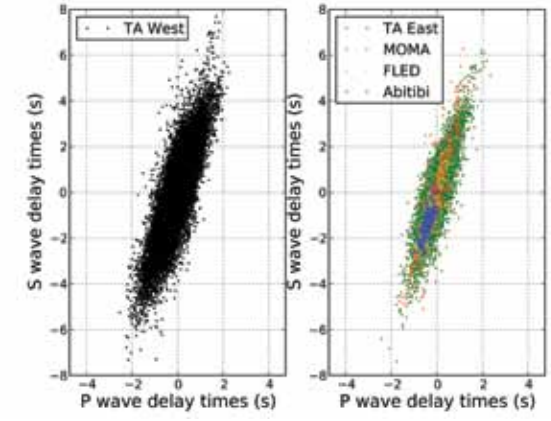

Figure 2: Measured individual relative S delays plotted against P delays for the two groups of stations west and east of the Rocky Mountains, respectively.

Receiver Function Imaging of Upper Mantle Complexity beneath the Pacific Northwest, United States

Kevin C. Eagar *(School of Earth and Space Exploration, Arizona State University),* **Matthew J. Fouch** *(School of Earth and Space Exploration, Arizona State University),* **David E. James** *(Department of Terrestrial Magnetism, Carnegie Institution of Washington)*

Small-scale topographic variations on the upper mantle seismic discontinuities provide important constraints on the thermal influences of upwellings and downwellings in geodynamically complex regions. Subduction of the Juan de Fuca plate and other tectonic processes dominating the Pacific Northwest, United States in the Cenozoic involve massive thermal flux that likely result in an upper mantle that has strong 3-D temperature variations. We address the interaction of such processes in the region using receiver functions to image the upper mantle seismic discontinuities at 410 and 660 km. We utilized over 15,000 high quality receiver functions gathered from 294 teleseismic earthquakes recorded at 277 regional broadband seismic stations, primarily those of the Earthscope/USArray Transportable Array. We find the average depths of the discontinuities to be 412 km and 658 km, respectively, with no obvious 520 km discontinuity detected. The peak-to-peak range is greater on the '410' than the '660', suggesting the possibility of more significant regional dynamic processes at upper mantle depths. Our results are not consistent with a mantle plume below central Oregon in the High Lava Plains region. Our observation of a thinner transition zone beneath the western Snake River Plain region, however, is consistent with a regional increase in mantle temperatures, perhaps due to either asthenospheric flow from beneath and around the southern edge of the Juan de Fuca plate, or to vertical flow in the form of regional mantle upwelling related to the Snake River Plain / Yellowstone hotspot track. Further, our results are not consistent with a simple subducting Juan de Fuca slab morphology, but rather suggest similar levels of significant complexity in slab structure found by recent regional tomographic studies. We find evidence for a thickened and therefore cooler mantle transition zone beneath the Wallowa / Idaho Batholith region, consistent with tomographic models which suggest broad scale increased seismic velocities to transition zone depths. We speculate that this region may be the location of mantle downwelling at larger scales than previously proposed.

References

Eagar, K.C., M.J. Fouch, and D.E. James, Receiver function imaging of upper mantle complexity beneath the Pacific Northwest, United States, in press, *Earth Planet. Sci. Lett., 2010.*

Acknowledgements: This work would not have been possible without high quality seismic data provided through the hard work of the TA and the HLP Seismic Experiment teams (http://www.dtm.ciw.edu/research/HLP), and the services of the IRIS DMC. As always, the IRIS PASSCAL program provided world-class technical field support. A special thanks goes to Jenda Johnson, whose contributions to the project have been innumerable and immeasurable, and Steven Golden for providing field and data support. We would also like to acknowledge the work and productive discussions on the crustal evolution with the other PIs of the HLP project, including Anita Grunder, Bill Hart, Tim Grove, Randy Keller, Steve Harder, and Bob Duncan. This research was supported by National Science Foundation awards EAR-0548288 (MJF EarthScope CAREER grant), EAR-0507248 (MJF Continental Dynamics High Lava Plains grant) and EAR-0506914 (DEJ Continental Dynamics High Lava Plains grant).

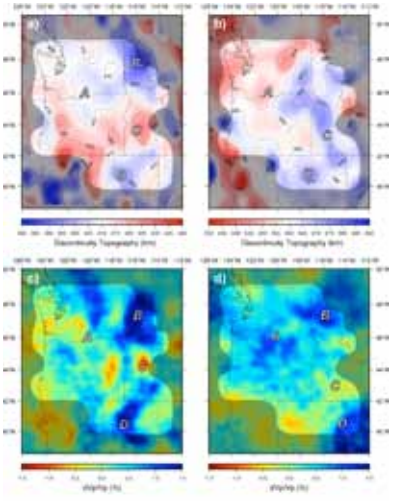

Upper mantle discontinuity topography and regional P wave tomography beneath the Pacific Northwest.

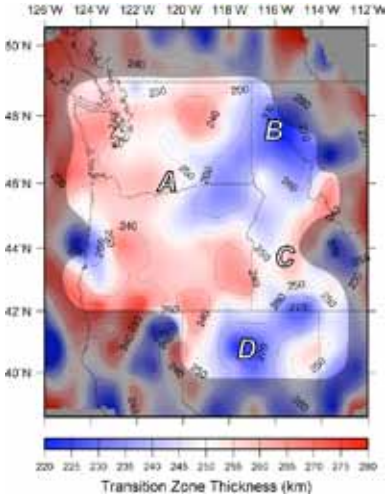

Transition zone thickness beneath the Pacific Northwest.

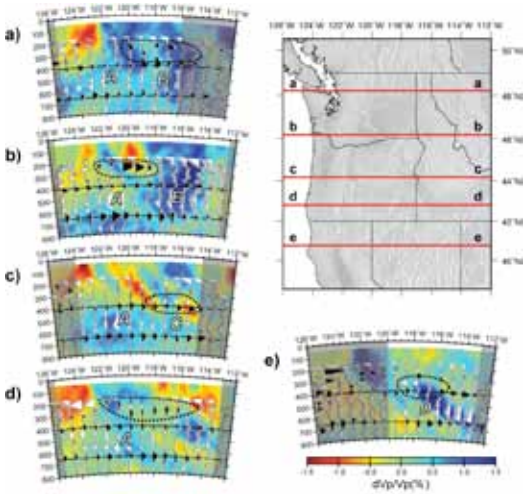

Cross-sections of CCP stacked receiver functions.

New Geophysical Insight into the Origin of the Denali Volcanic Gap

Stéphane Rondenay *(MIT)*, **Laurent Montési** *(University of Maryland)*, **Geoffrey Abers** *(Lamont-Doherty Earth Observatory)*

Volcanic gaps are segments of subduction zones that lack the volcanic activity usually found at these convergent margins. They are regions where the necessary conditions to produce melt may appear favourable, but where volcanoes are surprisingly absent from the surface. In this study, we present a new model that can explain the occurrence of such volcanic gaps. It is based on seismic imaging and geodynamic modelling of the Denali volcanic gap, a ~400 km-wide region at the eastern end of the Alaska-Aleutian subduction zone. Here, the thick crust of the Pacific plate and Yakutat terrane subduct at shallow angle beneath North America. A high-resolution seismic profile across the IRIS-PASSCAL BEAAR array [*Ferris et al., 2003*] clearly images the subducting crust undergoing progressive dehydration between 50-120 km depth, and a negative sub-horizontal velocity contrast at 60 km depth in the overlying mantle wedge. We interpret this 60 km discontinuity as marking the top of a layer of partial melt that pools at the base of the overriding plate. In steady-state subduction models, melt accumulates at the apex of a vaulted mantle wedge, the `pinch zone', from where it may break through the overlying lithosphere to the surface. Beneath the Denali volcanic gap, the pinch zone is absent (or greatly reduced) because shallow subduction of the Yakutat terrane progressively cools the system, and causes the slab to advance and replace the hot core of the mantle wedge. This regime can be seen as the opposite of subduction roll-back. It prevents the formation of a pinch zone, reduces the length of the melting column and causes melt to pool at the base of the overriding plate, thus inhibiting magma generation and extraction.

References

Ferris, A., G.A. Abers, D.H. Christensen, and E. Veenstra, High resolution image of the subducted Pacific (?) plate beneath central Alaska, 50–150 km depth, *Earth Planet. Sci. Lett., 214*, 575–588, 2003.

Rondenay, S., L.G.J. Montési, and G.A. Abers, New geophysical insight into the origin of the Denali volcanic gap, *Geophys. J. Int.*, in press, 2010.

Acknowledgements: This work was supported by National Science Foundation grants EAR-0544996 (SR), EAR-0911151 (LM) and EAR-9996451 (GA).

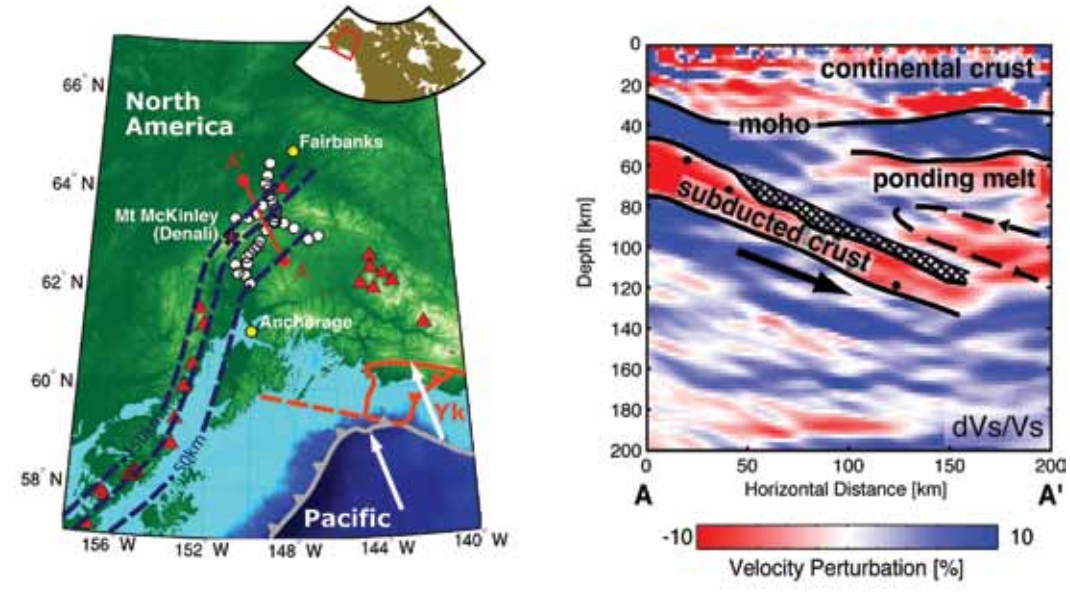

Left panel: Location map. Right panel: Vs perturbation profile across line A-A'. Discontinuities appear as rapid changes in perturbation polarity, where an increase (decrease) in velocity with depth is referred to as a positive (negative) gradient in the text.

Anomalous Seismic Structure beneath the Klyuchevskoy Group, Kamchatka, as Indicated by Receiver Function Analysis

Alex Nikulin *(Rutgers University),* **Vadim Levin** *(Rutgers University),* **Ashley Shuler** *(LDEO, Columbia University),* **Michael West** *(AVO, University of Alaska - Fairbanks)*

The Klyuchevskoy Group (KG) of volcanoes in Kamchatka, Russia is among the largest volcanic features on the planet, yet its position within the Kamchatka subduction zone is hard to explain with a simple tectonic mechanism. Geochemical evidence (Ishikawa et al., 2010) indicates that lavas of the KG are typical products of subduction-induced flux melting, yet the depth to the subducting Pacific plate beneath this volcanic center is much larger than the average depth of subduction associated with arc volcanism (Syracuse and Abers, 2006). We present new seismological constraints on the upper mantle structure beneath the KG, based on receiver function analysis of data collected by the PIRE project (Nikulin et al., 2010). We identify a sharply bounded zone of anomalous velocities in the mantle wedge beneath the KG (Figure 1), which we refer to as the Klyuchevskoy Upper Mantle Anomaly (KUMA). The presence of a sharp velocity deviation in the mantle wedge does not conform to our understanding of the standard subduction model, where a homogeneous velocity profile is expected in the mantle wedge. We contend that the observed anomaly is essential for understanding the location and the exceptional nature of the volcanic activity at the KG. Located at the typical depth of volatile release within the mantle wedge, this feature is a likely source of melts erupting at the KG. Presence of this heterogeneity in the upper mantle beneath the KG may explain the elevated level of volcanic activity of the KG and its position relative to the subducting Pacific Plate.

References

Ishikawa T., F Tera, and T. Nakazawa (2001), Boron Isotope and trace element systematics of the three volcanic zones in the Kamchatka arc. *Geoch. Cosm. A., 65*, 4523-4537

Nikulin, A., V. Levin, A. Shuler, and M. West (2010), Anomalous seismic structure beneath the Klyuchevskoy Group, Kamchatka, *Geophys. Res. Lett.*, in press.

Syracuse, E. M., and. G.A. Abers (2006), Global compilation of variations in slab depth beneath arc volcanoes and implications, *Geochem. Geophys. Geosyst., 7*, Q05017

Acknowledgements: The authors would like to aknowledge the support of the Partnership In Research and Education (PIRE) project, funded by the National Science foundation and the support of the Graduate School of Rutgers University, New Brunswick.

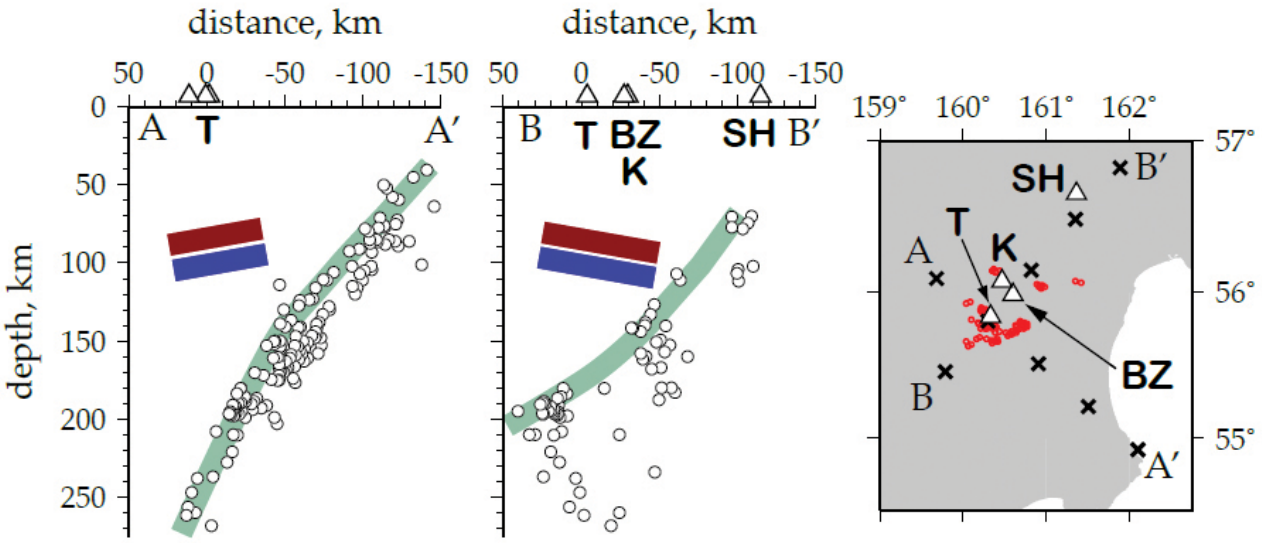

Position of the KUMA (red-blue bar) with respect to the subducting Pacific plate outlined by seismicity and the CKD volcanoes. Vertical cross-sections show earthquakes (circles) located over 10 years (2000-2009) by the Kamchatka Branch of the Geophysical Service of Russian Academy of Sciences. The online catalog (www.emsd.ru) includes events with M=3.5 and larger. Cross-sections are centered on the Tolbachik volcano, aligned along A-A' and normal B-B to the Pacific plate motion direction, and include events within 25 km of the profile. Crosses on the map correspond to 50 km tick marks on the distance axes of cross-sections, red circles denote 100 km depth pierce points of 166 individual rays from earthquakes used to construct RF gather in Figure 2. CKD volcanoes marked by triangles: BZ – Bezymianny, K – Klyuchevskoy, T – Tolbachik, SHShiveluch.

The Plume-slab Interaction beneath Yellowstone Revealed by Multiple-frequency Tomography

Yue Tian *(Princeton University (now at Chevron), USA),* **Ying Zhou** *(Virginia Tech, USA),* **Karin Sigloch** *(Ludwig-Maximilians-Universität, Germany),* **Guust Nolet** *(Université de Nice/Antipolis, France),* **Gabi Laske** *(University of California, San Diego, USA)*

S-velocity structure under the Yellowstone region is obtained from multiple-frequency tomography of a mixed data set of shear waves and Love waves. In this study, we used a total of 211440 data measurements measured from 36344 seismic waveforms, and over 95% of the waveforms are from IRIS. A strong slow anomaly (Y0) with large velocity gradient is observed under the Yellowstone Caldera (Figures 1-2), reaching ~200 km depth. Y0 connects to a slow anomaly (Y1) in the transition zone, which is centered at ~1° north of Y0 (Figure 2AA'). To the southwest, Y0 abuts a belt of strong slow anomalies (SR0) under the eastern Snake River Plain. Down in the lower mantle, a plume-shaped conduit (Y2) is observed with its top directly under Y1. The plume comes from south, tilting ~40° from vertical, reaches as deep as 1500 km, but spreads out at 700–1100 km depth. The spreading of SR2 can be explained either if the 660-km discontinuity acts as a barrier, or if the slab fragment S1 [*Sigloch et al., 2008; Tian et al., 2009*] acts as a barrier for the uprising Y2 (Figure 1b). Y2 might have distorted in two ways in response to the barrier. Part of Y2 might have navigated its path around S1 and found its way up through the slab gap, and the other part of Y2 might have smeared southwestward along the base of S1 and formed SR2. Though much of this explanation is speculative, it is clear that we witness a complex interaction between upwellings and downwellings in this part of the mantle. The very high resolution we obtained under the Yellowstone region would not be possible without the USArray, one of the densest networks in the world. The eastward movement of the USArray will make it possible to image detailed structure under the central and eastern US with similar resolution.

References

Sigloch, K., N. McQuarrie, and G. Nolet (2008), Two-stage subduction history under North America inferred from finite-frequency tomography, *Nature Geoscience, 1*, 458–462.

Tian, Y., K. Sigloch, and G. Nolet (2009), Multiple-frequency SH-wave tomography of the western U.S. upper mantle, *Geophys. J. Int., 178*, 1384–1402.

Acknowledgements: NSF grants EAR-0309298, EAR-0105387, and EAR-0809464.

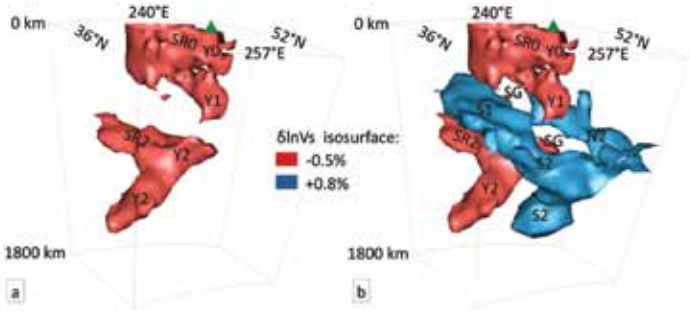

Figure 1. Three-dimensional view of the plume-slab interaction system under the Yellowstone and the eastern Snake River Plain, looking from the southwest. The green triangle represents the location of the Yellowstone Caldera. a: Slow anomalies only. b: Superimposing the fast anomalies on top of the slow anomalies. Labels S1, N1, S2, N2, SG identify the same subduction structure as in Sigloch et al. [2008] and Tian et al. [2009].

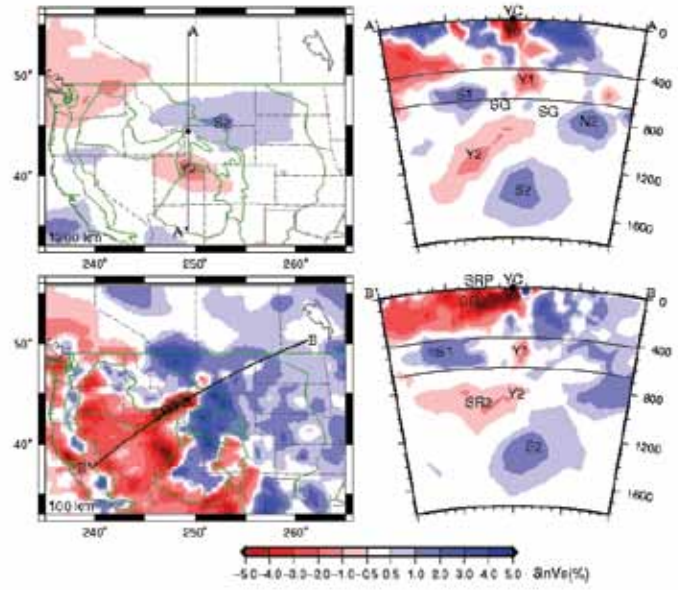

Figure 2. Great-circle cross sections of the velocity structure under the Yellowstone Caldera (YC) and the eastern Snake River Plain (SRP). The black dot and 0° represent the location of the Yellowstone Caldera and the mid-point of the great circle arc. In the cross-section views, each grid along the arc represents 1°. Labels S1, S2, N2, SG identify the same subduction structure as in Sigloch et al. [2008] and Tian et al. [2009].

Yellowstone Hotspot: Insights from Magnetotelluric Data

Anna Kelbert *(College of Oceanic and Atmospheric Sciences, Oregon State University, Corvallis, OR, USA),* **Gary D. Egbert** *(College of Oceanic and Atmospheric Sciences, Oregon State University, Corvallis, OR, USA),* **Catherine deGroot-Hedlin** *(Scripps Institution of Oceanography, University of California, San Diego, La Jolla, CA, USA)*

We have performed a set of three dimensional inversions of magnetotelluric (MT) data in the Snake River Plain and Yellowstone areas. We used a total of 73 sites from USArray MT Transportable Array (Idaho, Montana and Wyoming areas) and a subset of 19 sites from an earlier long-period MT survey in the Snake River Plain (SRP). The images reveal extensive areas of high conductivity in the upper mantle and lower crust beneath Yellowstone and the SRP. A highly conductive (~ 1 S/m) shallow anomaly directly beneath the Yellowstone caldera extends to no more than 20 km depth (Figure 2a), but connects to a deeper (40-100 km) conductive feature in the mantle that extends at least 200 km southwest (Figure 1a) roughly parallel to the direction of North America absolute motion. In several locations beneath the Eastern SRP very high conductivities (a few S/m) are imaged at or near the base of the lower crust (Figures 2b, c).

The lateral spatial extent of the mantle conductive anomalies correlates well with low velocity anomalies in the upper mantle imaged teleseismically [*e.g., Humphreys et al, 2000; Smith et al, 2009*], and with surface wave tomography [*Schutt et al., 2008*]. We see little evidence for a deep narrow plume extending directly beneath Yellowstone, although conductivities remain elevated to depths of at least 200 km over a broad area in the vicinity of the putative hotspot. Plausibly the seismically imaged thermal anomaly is present, but poorly resolved by the MT data, which is much more strongly impacted by partial melt and fluids present at shallower depths. Overall our images are quite consistent with interpretations that emphasize the role of local convection and lithospheric interaction to explain patterns of progressive magmatism along the Yellowstone "hot spot" track [*e.g., Humphreys et al, 2000*]. High conductivites imaged at the base of the crust beneath the Eastern SRP are probably due to a combination of partial melt, and highly saline fluids exsolved during magmatic underplating.

References

Humphreys, E.; Dueker, K.; Schutt, D. & Smith, R. (2000), 'Beneath Yellowstone: evaluating plume and nonplume models using teleseismic images of the upper mantle', *GSA Today, 10*, 1-7.

Smith, R.B.; Jordan, M.; Steinberger, B.; Puskas, C.M.; Farrell, J.; Waite, G.P.; Husen, S.; Chang, W. & O'Connell, R. (2009), 'Geodynamics of the Yellowstone hotspot and mantle plume: Seismic and GPS imaging, kinematics, and mantle flow', *J. Volcanol. Geoth. Res. 188*(1-3), 26 - 56.

Schutt, D.; Dueker, K. & Yuan, H. (2008), 'Crust and upper mantle velocity structure of the Yellowstone hot spot and surroundings', *J. Geophys. Res.* (Solid Earth), 113, 3310-.

Acknowledgements: Support from the US DOE under grant DE-FG02-06ER15819 for development of the 3D inversion code is acknowledged.

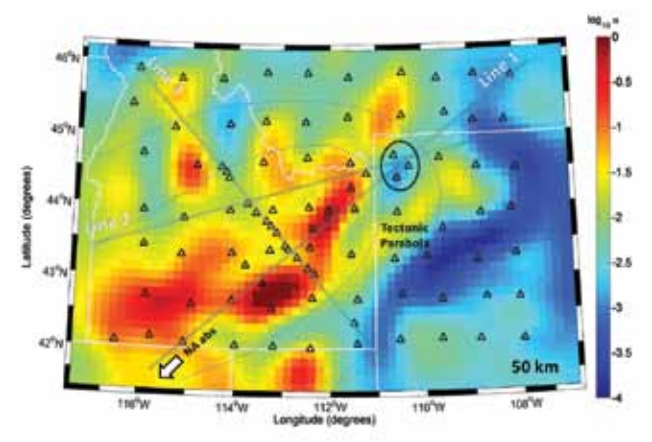

Electrical conductivity model at 50 km depth beneath Snake River Plain. Data locations are indicated by black triangles. The direction of absolute motion of North American plate is marked with a white arrow. Also schematically indicated are the "tectonic parabola" around the Eastern Snake River Plain, and the Yellowstone National Park (black oval). The grey lines are the transects shown in detail in Figure 2.

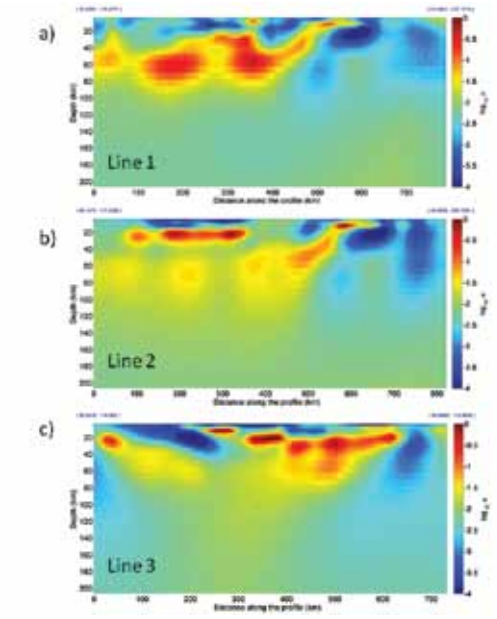

Electrical conductivity transects across the Snake River Plain (see Figure 1).

Imaging the Shear Wave Velocity "Plumbing" beneath the Northwestern United States with Rayleigh Wave Tomography: The High Lava Plains vs Yellowstone

Lara Wagner *(University of North Carolina at Chapel Hill),* **Donald Forsyth** *(Brown University),* **Matthew Fouch** *(Arizona State University),* **David James** *(Carnegie Institution of Washington)*

Since the mid-Miocene, the northwestern United States has experienced extensive flood basalt volcanism, followed by the formation of two time-progressive tracks of silicic volcanism: the Yellowstone/Snake River Plains (YSRP) and the High Lava Plains (HLP). The YSRP track progresses towards the northeast, parallel to North American plate motion, and has therefore often been attributed to a deep mantle plume source. However, the HLP track progresses to the northwest over the same time frame in a direction not consistent with any regional plate motion. The causes of the mid-Miocene flood basalts and the tracks of the YSRP and HLP are a matter of ongoing debate. We performed Rayleigh wave phase velocity inversions and inversions for 3-D shear wave velocity structure of the northwestern United States using data collected from the High Lava Plains Deployment and the EarthScope USArray Transportable Array (TA). The large number of stations used in these inversions allows us to show an unprecedented level of detail in the seismic velocity structures of this tectonically complex area. Our velocity images indicate that low S-wave velocities in the uppermost mantle do not well match the track of HLP volcanism. While at the surface the Newberry caldera appears to anchor the NW end of the HLP hotspot track, the seismic results show that it lies in a separate, north-south trending low velocity band just east of the Cascades that is distinct from the main HLP trace. The eastern edge of this low velocity band also correlates with a change in the magnitude of shear wave splitting delay times, possibly indicating changes in amount of partial melt present [Long et al., 2009]. In contrast, the ultra-low S-wave velocities beneath the YSRP track extend locally to at least 175 km depth and are by far the most prominent seismic anomalies in the region. Along axis, the YSRP hotspot track is characterized by a discrete low velocity channel in the upper mantle that shallows, narrows and intensifies to the northeast, but then deepens rapidly to the north beneath Yellowstone. Because Rayleigh wave tomography loses resolution below ~200 km, we cannot determine whether or not this anomaly is caused by a deep mantle plume source. However, the shallowing of the low velocity anomaly to the northeast is consistent with a moving heat source coming from below 200 km depth.

Geologic map of the northwestern United States with -3% low velocity surface contour shown in 3-D below the map: Shown are the locations of the Blue Mountain Province (BMP), Steens Mountain (SM), and the Owyhee Plateau (OP). Red triangles show Holocene arc volcanism. The black dashed line is the 87Sr/86Sr = 0.706, usually taken to represent the edge of cratonic North America. The boundaries of Basin and Range extension are shown with a purple dashed line. Black contours indicate the age progression for rhyolites in the High Lava Plains and the Snake River Plains. The yellow and blue contours in the HLP track show our <5 Ma and > 7 Ma contours for High Lava Plains rhyolites.

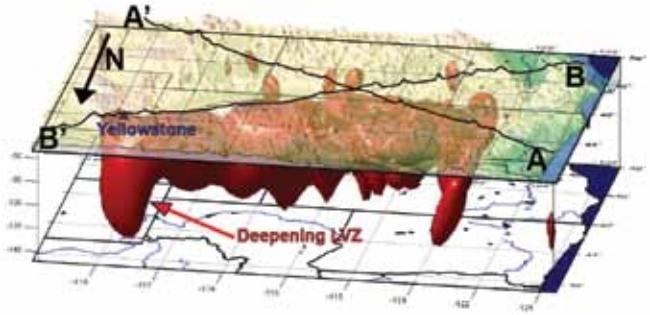

Yellowstone/Snake River Plains low velocity zone: shown is the -3% surface contour in perspective, looking from the north down towards the southeast. Shown is the location of Yellowstone Caldera (blue triangle).

References

Wagner, L., D. Forsyth, M. Fouch, and D. James (2010), Detailed three dimensional shear wave velocity structure of the northwestern United States from Rayleigh wave tomography. *Earth Planet. Sci. Lett.*, in review.

Long, M. D., H. Gao, A. Klaus, L. S. Wagner, M. J. Fouch, D. E. James, and E. Humphreys (2009), Shear wave splitting and the pattern of mantle flow beneath eastern Oregon, *Earth Planet. Sci. Lett., 288*, 359-369.

Acknowledgements: The High Lava Plains deployment was funded through NSF award EAR-0507248 (MJF) and EAR-0506914 (DEJ). LW's participation was supported by NSF award EAR-0809192 and DWF was supported by NSF award EAR-0745972.

Temperature of the Yellowstone Hotspot

Derek L Schutt *(Colorado State University)*, **Ken Dueker** *(University of Wyoming)*

Recent studies show that the Yellowstone hotspot is associated with a plume-like low velocity pipe that ascends from at least the transition zone to the lithosphere-asthenosphere boundary, where the plume is sheared to the southwest by North American plate motion. Rayleigh wave tomography shows this plate-sheared plume layer has an extremely low S wave velocity of 3.8 ± 0.1 km/s at 80 km depth, ~0.15–0.3 km/s lower than the velocity observed beneath normal mid-ocean ridges.

To constrain the temperature of the plume layer, a grid search with respect to grain size and temperature is performed to fit the observed Rayleigh wave phase velocities. Using a variety of velocity-temperature scalings--including testing the effects of grain-size sensitivity--and varying such poorly constrain parameters as activation volume, we find that an excess temperature is needed to explain the upper mantle low velocity trend associated with Yellowstone. At 95% confidence, we find the plume layer is >55–80°C hotter than ambient mantle, strongly implying this is a weak thermal upwelling that nucleated off a deeper thermal boundary layer: i.e. confirming that Yellowstone is a plume.

References

Schutt, D. L. and K. Dueker (2008), Temperature of the plume layer beneath the Yellowstone Hotspot, *Geology, 36*(8), 4.

Acknowledgements: We thank the National Science Foundation (NSF) for support in the form of time to work on the project and for publication costs, as well as for Geophysics/Geochemistry NSF grant EAR-0409538. This work was built on data collected during a 2000 PASSCAL experiment supported by Continental Dynamics Programs Grant EAR-CD-9725431.

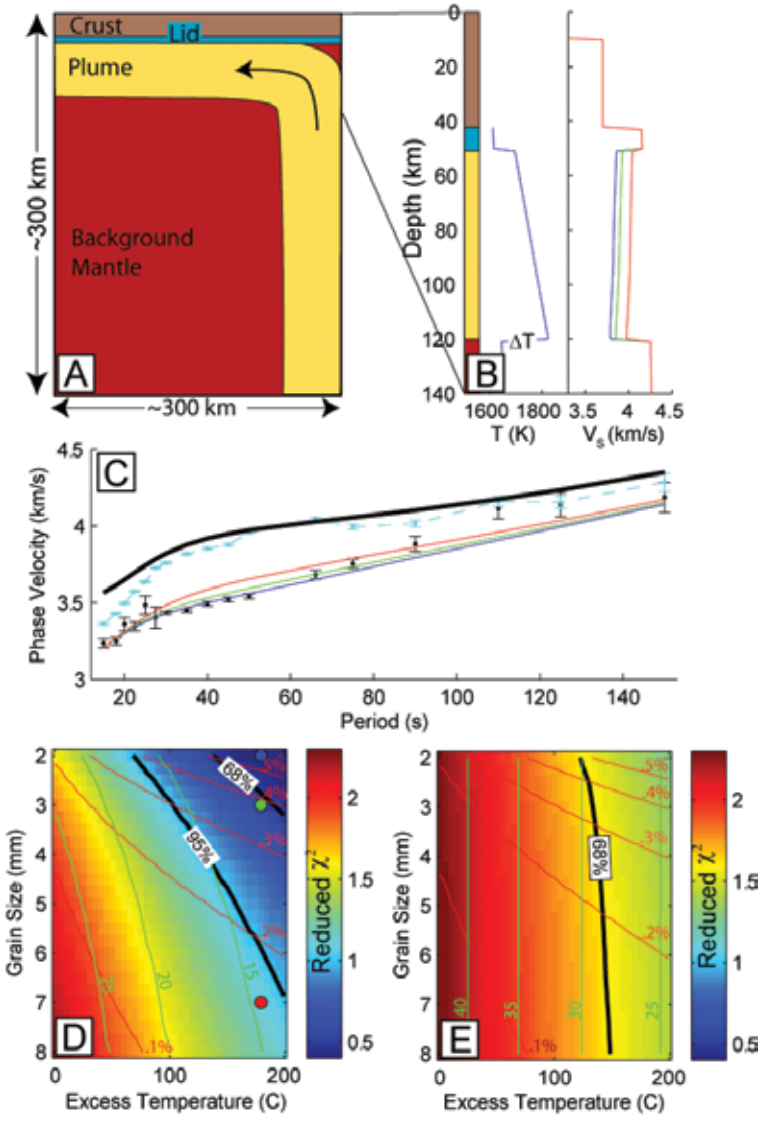

Yellowstone plume layer temperature, melt porosity, and shear wave attenuation. A: Cross section along Yellowstone hotspot track from surface wave tomography. B: Hotspot structure is approximated by four layers: crust, mantle lid, plate-sheared plume layer, and underlying mantle. Example thermal profile is shown for 180°C excess temperature (T). Temperature decreases within plume layer are due to latent heat of melting. Colored lines in plume layer are example VS profiles calculated for this temperature structure using grain-size–sensitive anelastic velocity scaling for grain sizes of 2 mm (blue), 3 mm (green), and 7 mm (red). C: Predicted phase velocities for the three example Vs models shown in B and observations with their one standard error bars. Cyan dashed line and black solid lines are for Wyoming craton and PREM (Dziewonski and Anderson, 1981) velocity models. D&E: Reduced chi-squared error surface for grain-size–sensitive (D) and non-grain-size sensitive anelastic (E) models.

Slab Fragmentation and Edge Flow: Implications for the Origin of the Yellowstone Hotspot Track

D.E. James *(Carnegie Institution/DTM),* **M.J. Fouch** *(School of Earth and Space Exploration, Arizona State University),* **J.B. Roth** *(Exxon/Mobil),* **R.W. Carlson** *(Carnegie Institution/DTM)*

The Snake River Plain/Yellowstone (SRP/Y) volcanic complex is widely considered a classic example of a plume generated continental hotspot (e.g. Smith et al., 2009). By that model, the plume head appeared ca 17 Ma near the Oregon-Idaho-Nevada border with the outpouring of the Steens and Columbia River flood basalts. The SRP/Y hotspot is taken to be the product of plume tail upwelling over the past 12 Ma. Our recent S-wave and P-wave tomographic images, however, instead suggest a subduction-related process by which volcanism along the SRP/Y hotspot track results from slab fragmentation, trench retreat, and mantle upwelling at the leading edge of the descending plate and around its truncated edges (Faccenna et al., 2010; K. Druken and C. Kincaid, pers. comm.). Seismic images of the deeper upper mantle show that the subducted oceanic plate extends locally eastward well into stable North America. The break-up and along-strike fragmentation of the descending plate is related in both time and space to the onset of flood volcanism and the formation of the SRP/Y hotspot. A sub-horizontal branch of subducting oceanic plate, orphaned from the descending plate by the northward migration of the Mendocino triple junction, resides in the mantle transition zone (400-600 km) directly beneath the SRP/Y track (Figure 1a). Its truncated northern edge is parallel to the northwestern margin of the hotspot track itself and marks the southern edge of a slab gap (Figure 1b). Numerical and physical tank modeling show that a rapidly retreating and severely fragmented downgoing plate drives mantle flow around both the tip and the edges of the descending slab. Our seismic results show that the morphology of the subducting slab is appropriate for generating large-scale poloidal flow (flood volcanism) in the upper mantle during the re-initiation phase of slab descent ca 20 Ma and for generating smaller-scale toroidal and poloidal upwellings (hotspot volcanism) around both the leading tip and northern edge of the slab as it descends into the deeper upper mantle. Plate reconstructions are consistent with the timing and position of both flood and hotspot volcanism.

Acknowledgements: This work is part of the High Lava Plains (HLP) Project, supported by Continental Dynamics NSF grants EAR-0507248 (MJF) and EAR-0506914 (DEJ and RWC), as well as EAR-0548288 (MJF EarthScope CAREER grant). We thank the USArray team for a remarkable effort and the superb efforts of the PIC staff and the HLP seismic team in the deployment and operation of the HLP seismic array. Data were provided through the IRIS Data Management Center. We thank ranchers throughout the HLP region who hosted seismic stations. The Eastern Oregon Agricultural Research Center provided critical logistical assistance for the High Lava Plains seismic team during this project.

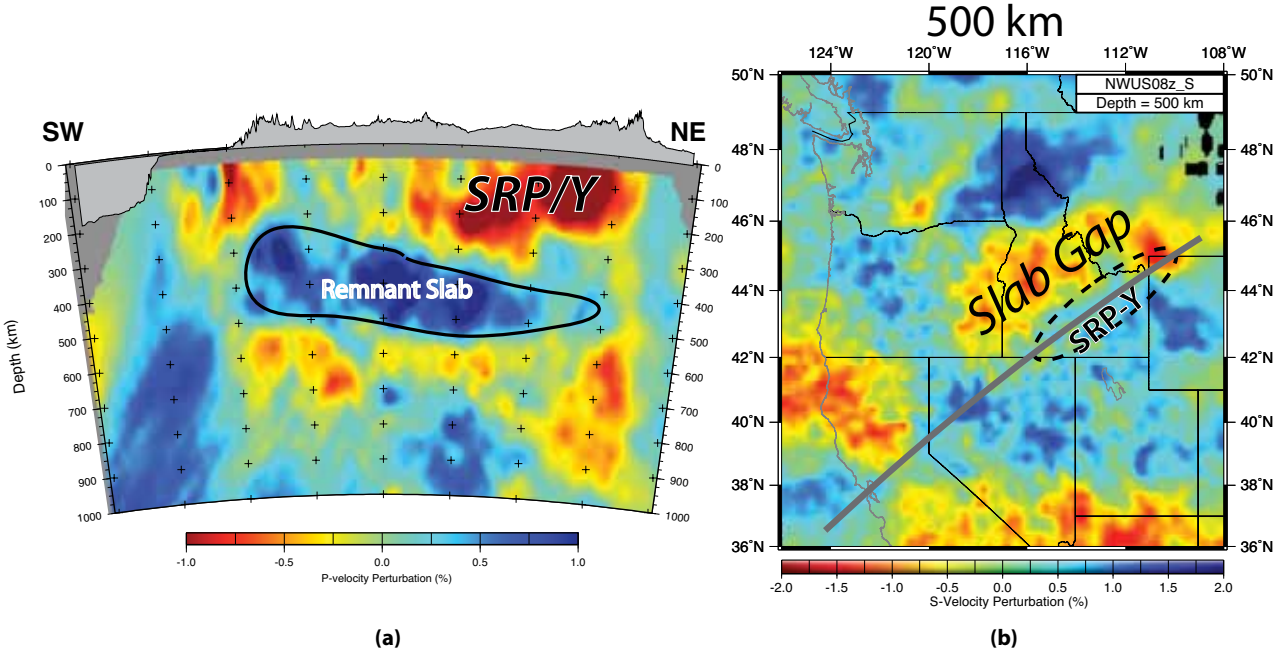

Figure 1. (a) P-velocity vertical cross-section parallel to plate convergence on axis of SRP/Y showing a sub-horizontal remnant of the Farallon slab adrift in the mantle transition zone beneath the SRP/Y hotspot track, its leading edge just beneath Yellowstone; (b) S-velocity perturbations at 500 km depth a "slab gap" just north of and parallel to the SRP/Y track itself. The slab gap extends from north of Yellowstone into eastern Oregon, its southern margin coinciding with the northern boundary of the remnant slab in (a).

Plume-Slab Interaction beneath Western US

Mathias Obrebski *(UC Berkeley),* **Richard Allen** *(UC Berkeley),* **Mei Xue** *(Tongji University),* **Shu-Huei Hung** *(National Taiwan University)*

Using the Earthscope Transportable Array, Flexible Arrays in Cascadia, and regional seismic networks, we have constructed 3D P- and S-velocity models for the mantle structure beneath the western US. The DNA09-P and –S models use teleseismic body-wave traveltime measurements that have been cross-correlated at a range of frequencies for relative arrival times and them inverted for velocity structure using finite-frequency sensitivity kernels. The independent P- and S-velocity models show good agreement in the structures imaged. The figure illustrates some of the more interesting features in the region. Panel (a) maps the structures at 200 km depth and clearly shows the subducting Juan de Fuca slab high velocity anomaly (JdF) and the Yellowstone-Snake River Plain low-velocity anomaly (YS). The three west-to-east cross-sections illustrate the variable nature of the subducting slab. At its southern end (C-C') the slab anomaly is strong, but at the latitude of Oregon it becomes weaker and shallower. Further east a strong low-velocity anomaly is imaged beneath Yellowstone that can be tracked from the Caldera to the base of model resolution at ~1000km depth. This is interpreted as the Yellowstone plume responsible for the hotspot rack at the surface. Panel (e) shows a 3D view of the subducting slab (JdF) and the low-velocity Yellowstone anomaly. The DNA models are available at http://dna.berkeley.edu.

References

Obrebski, M., R.M. Allen, M. Xue, S.-H. Hung, Slab-plume interaction beneath the Pacific Northwest, *Geophys. Res. Lett., 37*, doi:10.1029/2010GL043489, 2010.

Acknowledgements: This work was funded by NSF EAR-0745934 and EAR-0643077. The work was facilitated by the IRIS-PASSCAL program through the loan of seismic equipment, USArray for providing data and the IRIS-DMS for delivering it.

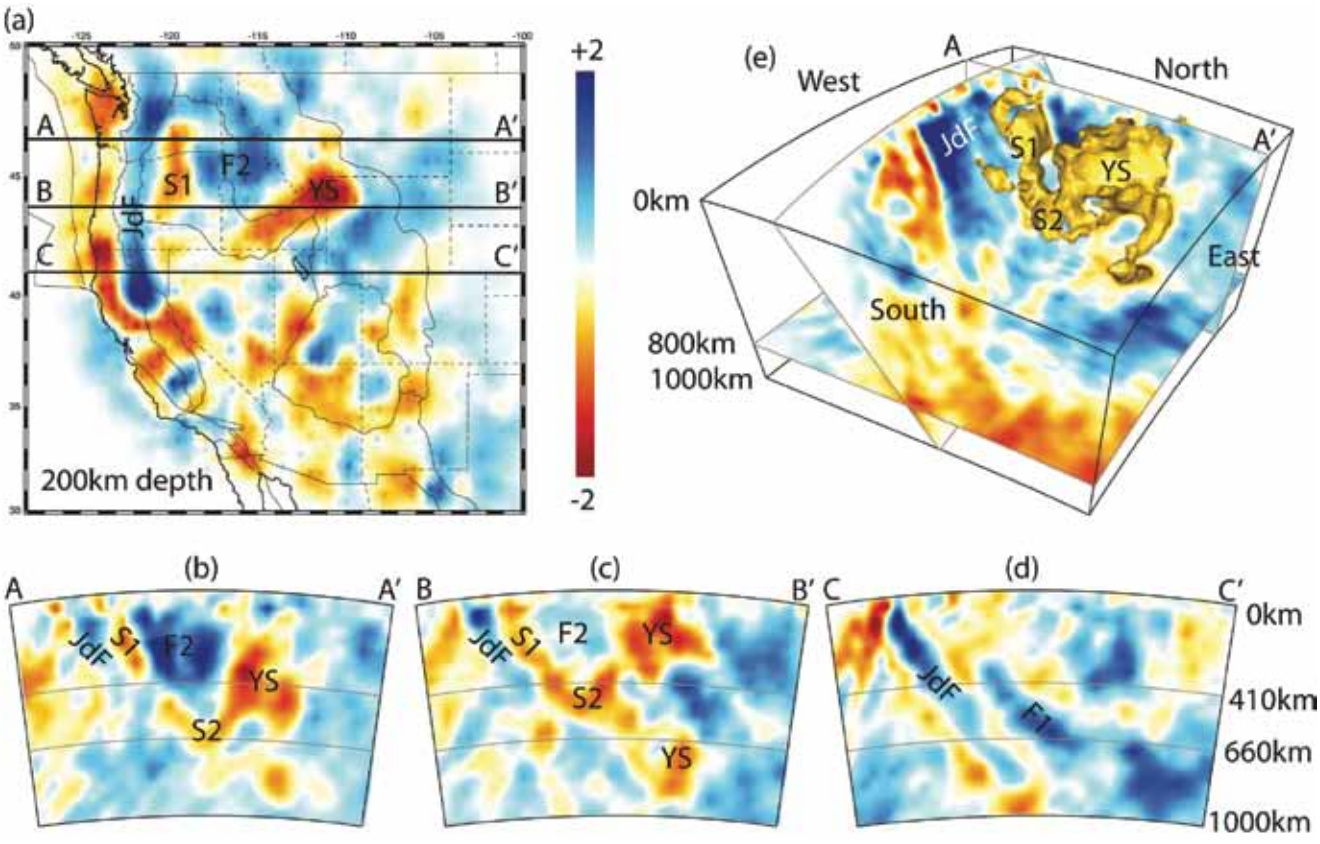

Figure. Slices through the DNA09-P velocity model. See text for description.

Mantle Shear-Wave Velocity Structure beneath the Hawaiian Hotspot

Cecily Wolfe *(University of Hawaii at Manoa),* **Sean Solomon** *(Carnegie Institution of Washington),* **Gavi Laske** *(Scripps Institution of Oceanography),* **Robert S. Detrick** *(Woods Hole Oceanographic Institution),* **John A. Orcutt** *(Scripps Institution of Oceanography),* **David Bercovici** *(Yale University),* **Erik H. Hauri** *(Carnegie Institution of Washington)*

Hawaii is the archetypal hotspot and has been suggested to be the surface expression of a mantle plume, a localized upwelling of hot buoyant material from Earth's deep mantle, although such an origin has been debated. One of the most straightforward indications of whether a hotspot is the result of a plume is the presence of a narrow, vertically continuous zone of low seismic velocities in the underlying mantle, indicative of higher-than-normal temperatures, anomalous mantle composition, or partial melt. Defining the mantle structure that lies beneath hotspots such as Hawaii is thus important for revealing the origin of such features. The Hawaiian Plume-Lithosphere Undersea Melt Experiment (PLUME) was a multidisciplinary program whose centerpiece was a large network of four-component broadband ocean-bottom seismometers and three-component portable broadband land stations [*Laske et al., 2009*]. Data from IRIS Global Seismic Network stations KIP and POHA were used in this study, and all of the collected data were archived at the IRIS Data Management Center.

Three-dimensional images of shear-wave velocity beneath the Hawaiian Islands obtained from the PLUME records show an upper-mantle low-velocity anomaly that is elongated in the direction of the island chain and surrounded by a high-velocity anomaly that is parabola-shaped in map view [*Wolfe et al., 2009*]. Low velocities continue downward to the mantle transition zone between 410 and 660 kilometers depth, a result that is in agreement with prior observations of transition-zone thinning at this location. The inclusion of SKS observations extends the imaging resolution downward to a depth of 1500 kilometers and reveals a several-hundred-kilometer-wide region of low velocities beneath and southeast of Hawaii. These images support the hypothesis that the Hawaiian hotspot is the result of an upwelling high-temperature plume from the lower mantle.

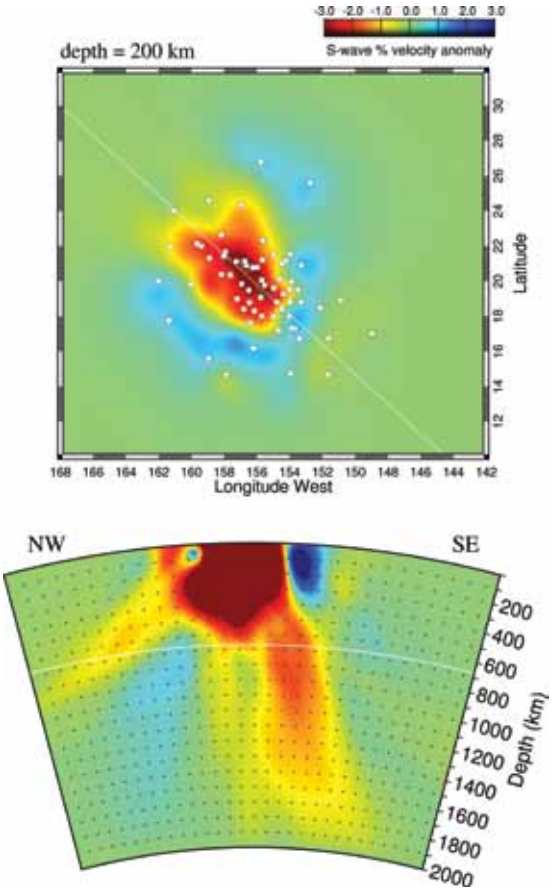

Top plot: Upper mantle shear-wave velocity heterogeneity at 200 km depth. Station locations are indicated by squares. The scale is given at the upper right and ranges ±3%. Bottom plot: Vertical cross section. The scale ranges over ±1%.

References

Laske, G., J. A. Collins, C. J. Wolfe, S. C. Solomon, R. S. Detrick, J. A. Orcutt, D. Bercovici, and E. H. Hauri, Probing the Hawaiian hotspot with new broadband ocean bottom instruments, Eos Trans. AGU, 90, 362-363, 2009.

Wolfe, C. J., S. C. Solomon, G. Laske, J. A. Collins, R. S. Detrick, J. A. Orcutt, D. Bercovici, and E. H. Hauri, Mantle shear-wave velocity structure beneath the Hawaiian hotspot, *Science, 326*, 1388-1390, 2009.

Acknowledgements: This project was supported by the U.S. National Science Foundation. We also acknowledge the crews of the research vessels Melville, Ka'imikai-O-Kanaloa, and Kilo Moana, the Jason remotely operated vehicle team, the Ocean Bottom Seismograph Instrument Pool, the Carnegie Institution's portable seismology laboratory, IRIS, and the hosts of temporary stations on the Hawaiian Islands.

Rayleigh Waves Observed During the Hawaiian Plume Deployment Trace Anomalously Low Shear Velocities in the Lithosphere and Asthenosphere

G. Laske *(UC San Diego),* **J.A. Orcutt** *(UC San Diego),* **J.A. Collins** *(Woods Hole Oceanographic Institution),* **C.J. Wolfe** *(University of Hawaii at Manoa),* **S.C. Solomon** *(Carnegie Institution of Washington),* **R.S. Detrick** *(Woods Hole Oceanographic Institution),* **D. Bercovici** *(Yale University)*

Hawaii has long been viewed as the textbook example of a plume-fed hotspot although other models such as a progressively cracking lithospheric plate have been considered to explain Hawaii's island chain. The plume model has been heavily contested by some as it has been difficult to obtain comprehensive and unambiguous geophysical observational constraints. One major problem that seismology has faced has been its complete reliance on land stations. During two field campaigns from 2005 to 2007, the Plume-Lithosphere-Undersea-Mantle Experiment (PLUME) occupied 83 sites to provide continuous year-long seismic records [*Laske et al., 2009*]. Nearly 70 of these sites were occupied by ocean bottom seismometers (OBSs), most of which featured a broadband seismometer (a Guralp CMG-3T or a Nanometrics Trillium 240). To date, we have compiled two-station Rayleigh wave phase velocity curves for over 600 paths across the 1000-km-wide network, and we have use these curves in inversions for 3-dimensional (3-D) shear velocity structure. Our 3-D images in the lithosphere and asthenosphere reveal a pronounced low velocity anomaly to the west of the island of Hawaii at depths of 80 km and greater. Toward shallower depths, the anomaly appears to diminish in size and magnitude and is centered between the islands of Hawaii and Maui. We interpret this anomaly as the likely source of melt that feeds Hawaii's extensive volcanism.

References

Laske, G., J. A. Collins, C. J. Wolfe, S. C. Solomon, R. S. Detrick, J. A. Orcutt, D. Bercovici, and E.H. Hauri (2009), Probing the Hawaiian hotspot with new broadband ocean bottom instruments, Eos Trans. AGU, 90, 362-363.

Nishimura, C.E. and D.W. Forsyth, (1989), The anisotropic structure of the upper mantle in the Pacfic. *Geophys. J., 96*, 203-229.

Acknowledgements: The waveforms from this experiment are available at the IRIS-DMC. This research was financed by the National Science Foundation under grants OCE-00-02470 and OCE-00-02819.

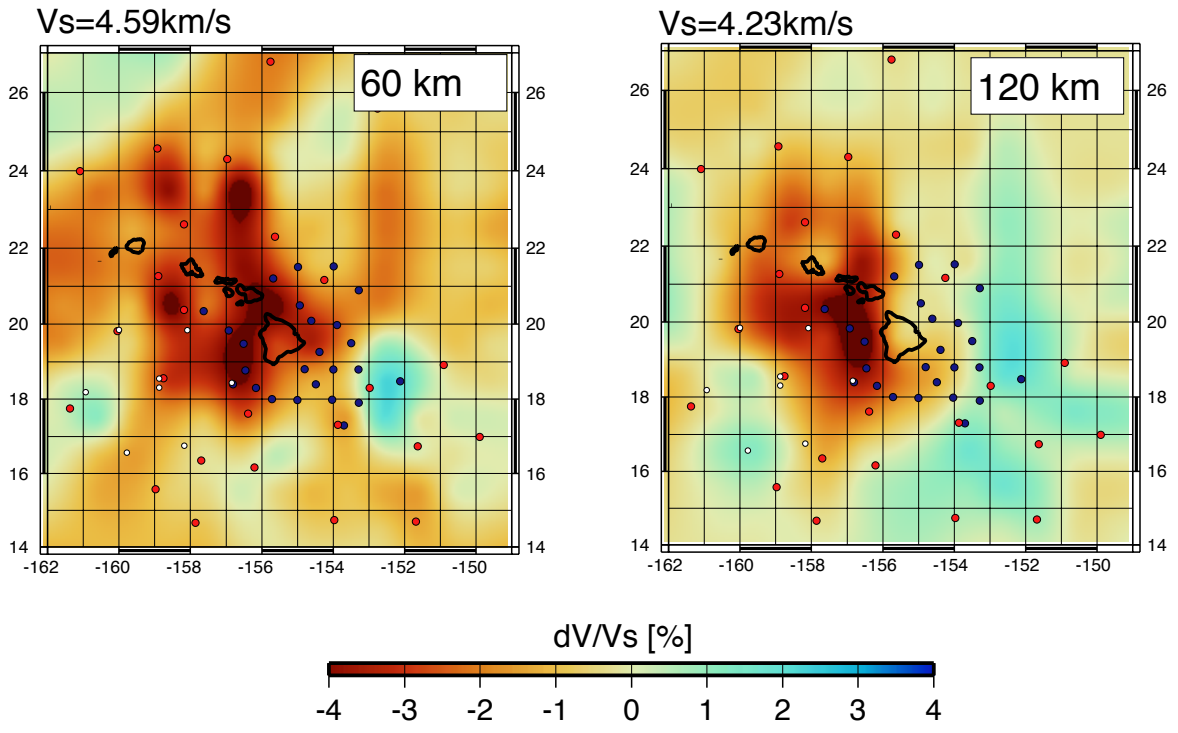

Model of shear velocity anomalies obtained from inverting Rayleigh wave phase velocity curves. The maps show percentage perturbations to reference velocities for 52-100 Ma old oceanic lithosphere (Nishimura and Forsyth, 1989).

Discordant Contrasts of P- and S-Wave Speeds Across the 660-km Discontinuity beneath Tibet: A Case for Hydrous Remnant of Sub-Continental Lithosphere

Tai-Lin Tseng *(University of Illinois, Urbana-Champaign),* **Wang-Ping Chen** *(University of Illinois, Urbana-Champaign)*

Using high-resolution, triplicate shear-waveforms recorded by broadband seismic arrays, we show that a corresponding anomaly of high S-wave speed (VS) is absent where an anomaly of high P-wave speed (VP) was recently recognized in the transition zone of the mantle (TZ) beneath central Tibet. A likely cause of the discrepancy between anomalies in VP and VS is a minor amount of water in nominally anhydrous polymorphs of olivine. Prior to thickening by continent-continent collision, the Tibetan mantle was part of a mantle wedge which has been hydrated during past episodes of subduction. Hydration of the sub-continental lithospheric mantle (SCLM) provides a natural mechanism to facilitate ductile deformation, so rapid thickening of the SCLM, which would have been hindered by advection of cold materials, can take place. Convective instability would then lead to removal and sinking of thickened, cold SCLM, leaving a remnant in the TZ detectable only in VP. This interpretation not only is consistent with previous reconstruction of the SCLM in Tibet based on several types of independent data, but also provides a new pathway for water to enter and be stored in the TZ.

References

Chen, W.-P., and T.-L. Tseng, Small 660-km seismic discontinuity beneath Tibet implies resting ground for detached lithosphere, *J. Geophys. Res.*, ***112***, B05309, doi:10.1029/2006JB004607, 2007.

Tseng, T.-L., and W.-P. Chen, Discordant contrasts of P- and S-wave speeds across the 660-km discontinuity beneath Tibet: A case for hydrous remnant of sub-continental lithosphere, *Earth Planet. Sci. Lett. , 268*, 450-462, 2008.

Chen, W.-P., M. Martin, T.-L. Tseng, R. L. Nowack, S.-H. Hung, and B.-S. Huang, Shear-wave birefringence and current configuration of converging lithosphere under Tibet, *Earth Planet. Sci. Lett., 295*(1-2), 297-304, doi:10.1016/j.epsl.2010.04.017, 2010.

Acknowledgements: Data centers of the IRIS (USA), the Institute of Earth Sciences, Academia Sinica (Taiwan, R. O. C.), and GEOSCOPE (France) kindly provided seismograms to us. We benefited from discussions with C.-T. Lee, P. Kapp, S.-L. Chung, J. Wang, J. Bass, J. Smyth, and S. Jacobsen; and an anonymous reviewer provided insightful comments. This work is supported by the U. S. National Science Foundation Grants EAR9909362 (Project Hi-CLIMB: An Integrated Study of the Himalayan-Tibetan Continental Lithosphere during Mountain Building, contribution I07) and EAR0551995. Any opinions, findings and conclusions or recommendations expressed in this material are those of the authors and do not necessarily reflect those of the NSF.

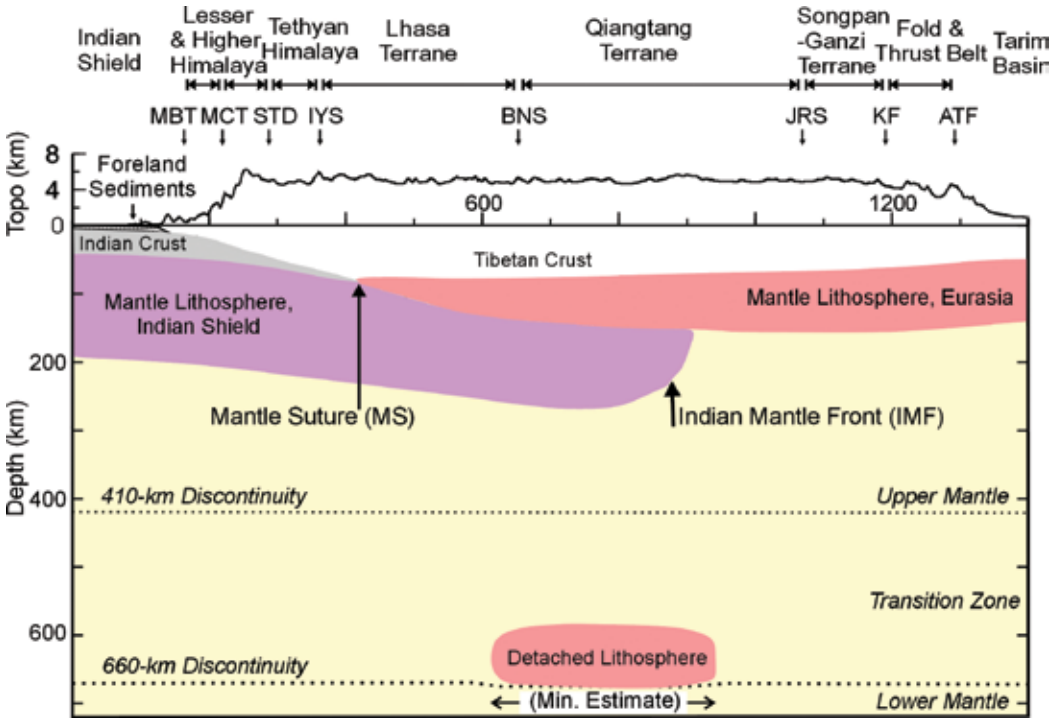

A schematic cross-section (Chen et al., 2010) showing the current configuration of the sub-continental lithospheric mantle, including a large-scale anomaly of high P-wave speed resting on top of the lower mantle and interpreted as the remnant of thickened (and subsequently detached due to Rayleigh-Taylor instability) lithospheric mantle (Chen and Tseng, 2007). This anomaly is invisible to S-waves, indicating the presence of water deep beneath an active zone of continental collision. The dimension of the detached lithosphere shown is a minimal estimate, limited by current coverage of seismic arrays around Tibet. For reference, we also show key geologic units/boundaries and topography at the present (vertically exaggerated by a factor of 13.15).

Deep Mantle Plumes and Convective Upwelling beneath the Pacific Ocean

Nicholas Schmerr *(Carnegie Institution of Washington),* **Edward Garnero** *(Arizona State University),* **Allen McNamara** *(Arizona State University)*

The 410 and 660 km discontinuities arise from solid-to-solid phase changes in the mineral olivine, and lateral variations in temperature and composition incurred by dynamical processes in the mantle produce topography on each boundary. To query discontinuity structure in the presence of mantle downwellings and upwellings, we use underside reflections of shear waves, a technique that requires the stacking of hundreds to thousands of seismograms. This method has flourished from the deployment of global and regional seismic arrays, whose data are freely available from the IRIS DMC. We collected a dataset of over 130,000 broadband seismograms that sample beneath the Pacific Ocean. In our study, we resolve the discontinuities to be relatively flat beneath most of the Pacific, except under subduction zones and volcanic hotspots. We find the phase boundaries are closer together beneath the Hawaiian hotspot, and also in a larger region of the south Pacific that is flanked by a number of volcanic hotspots. This region overlies the southern part of the large-scale low shear velocity province in the lowermost mantle, indicative of a large plume head or cluster of several plumes originating in the lowermost mantle and impinging upon the south Pacific 660 km discontinuity. This feature may be related to large volume volcanic eruptions, such as the Cretaceous Ontong Java Plateau flood basalts, which have been proposed to originate in the south Pacific.

References

Schmerr, N., et al. (2010), Deep mantle plumes and convective upwelling beneath the Pacific Ocean, *Earth Planet. Sci. Lett., 294*, 143-151.

Acknowledgements: NSF Grants EAR-0711401, EAR-0453944, EAR-0510383, EAR-0456356

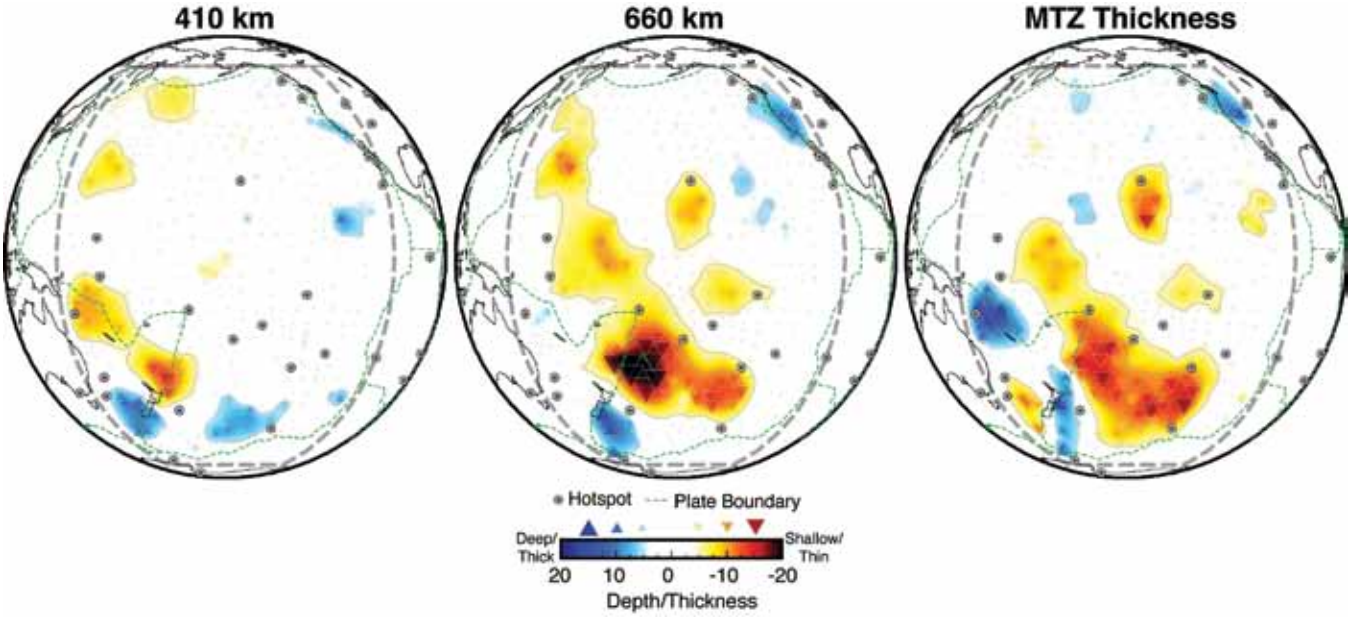

Topography maps for discontinuity depths and transition zone thickness in our Pacific study region. The depths are plotted relative to average values of 418 km, 656 km, and an average transiton zone thickness of 242 km.

Upper Mantle Discontinuity Topography from Thermal and Chemical Heterogeneity

Nicholas Schmerr *(Carnegie Institution of Washington),* **Edward Garnero** *(Arizona State University)*

Utilizing high resolution stacks of precursors to the seismic phase SS, we investigated seismic discontinuities associated with mineralogical phase changes at approximately 410 and 660 kilometers deep within the Earth beneath South America and the surrounding oceans. We utilized a dataset of over 17,000 broadband seismograms collected from the IRIS DMC and EarthScope. Our maps of phase boundary topography revealed deep 410- and 660-km discontinuities in the down-dip direction of subduction, inconsistent with cold material at 410-km depth. We explored several mechanisms invoking chemical heterogeneity within the mantle transition zone to explain this feature. In some regions, we detected multiple reflections from the discontinuities, consistent with partial melt near 410-km depth and/or additional phase changes near 660-km depth. Thus, the origin of upper mantle heterogeneity has both chemical and thermal contributions, and is associated with deeply rooted tectonic processes.

References

Schmerr, N., and E. Garnero (2007), Upper mantle discontinuity topography from thermal and chemical heterogeneity, *Science, 318*(5850), 623-626.

Acknowledgements: NSF Awards EAR-0453944 and EAR-0711401

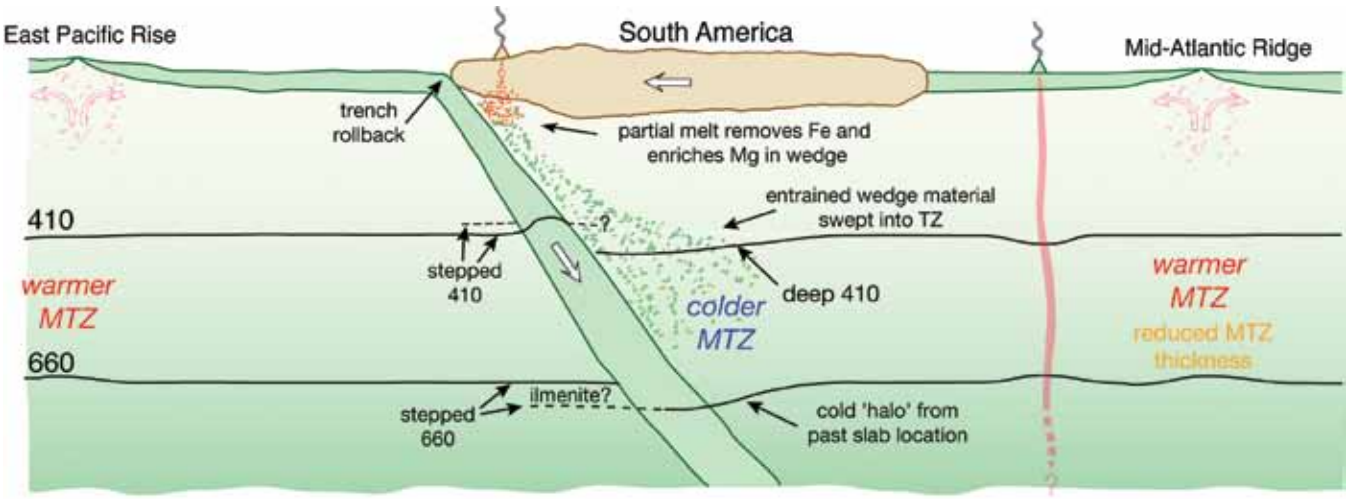

A cross section explaining our results, whereby iron is removed by melting in the mantle wedge and the Mg-enriched residue is swept into the transition zone along with the subducting lithosphere. This increases the pressure at which olivine transforms into wadsleyite, deepening the 410 km boundary.

Mantle Dynamics beneath North Central Anatolia

C. Berk Biryol *(University of Arizona),* **George Zandt** *(University of Arizona),* **Susan L. Beck** *(University of Arizona),* **A. Arda Ozacar** *(Middle East Technical University),* **Hande E. Adiyaman** *(University of Arizona),* **Christine R. Gans** *(University of Arizona)*

The North Anatolian Fault Zone (NAFZ) is a transform structure that constitutes the boundary between the Anatolian Plate to the south and the Eurasia Plate to the north. In this study we used shear-wave splitting analysis to study the upper mantle dynamics beneath Anatolia region and the the northward convex part of the NAFZ. The seismic data for our analysis comes from 39 broadband seismometers of the North Anatolian Fault passive seismic experiment (NAF) deployed at the central north Anatolia between 2005 and 2008 (Figure 1). The instruments for this experiment are provided by the IRIS-PASSCAL consortium. Our results reveal fairly uniform NE-SW trending anisotropy directions with decreasing delay times from west to east (Figure 1). The existence of significant and uniform anisotropy across major tectonic boundaries and plate margins in the study area argues for an asthenospheric source for the anisotropy rather than a lithospheric source. Our analysis also show that the lag times of the measured anisotropy varies with short spatial wavelengths beneath central Anatolia and the eastern section of the region is associated with lower lag times. We suggest the slab roll-back taking place along the Aegean trench and the different amounts of trench retreat for the Aegean and Cyprean trenches contributes significantly to the upper mantle dynamics of the region and induces a SW-directed astheonospheric flow with differential strengths from east to west (Figure 1). The similar patterns of variation for both crustal strain filed and observed fast polarization directions also support the idea of SW asthenospheric flow under the effects of Aegean and Cyprean slab roll-back processes.

References

Hatzfeld, D., Karagianni, E., Kassaras, I., Kiratzi, A., Louvari, E., Lyon-Caen, H., Makropoulos, K., Papadimitriou, P., Bock, G., & Priestley, K., 2001. Shear wave anisotropy in the upper-mantle beneath the Aegean related to internal deformation, *J. Geophys. Res., 106*, 737-753.

McClusky, S., Reilinger, R., Mahmoud, S., Ben Sari, D. & Tealeb, A., 2003. GPS constraints on Africa (Nubia) and Arabia plate motions, *Geophys. J. Int., 155*, 126–138.

Sandvol, E., Turkelli, N., Zor, E., Gok, R., Bekler, T., Gurbuz, C., Seber, D. & Barazangi, M., 2003. Shear wave splitting in a young continent-continent collision: An example from Eastern Turkey, *Geophys. Res. Lett.,30*(24), 8041.

Acknowledgements: This research was supported by NSF grant EAR0309838.

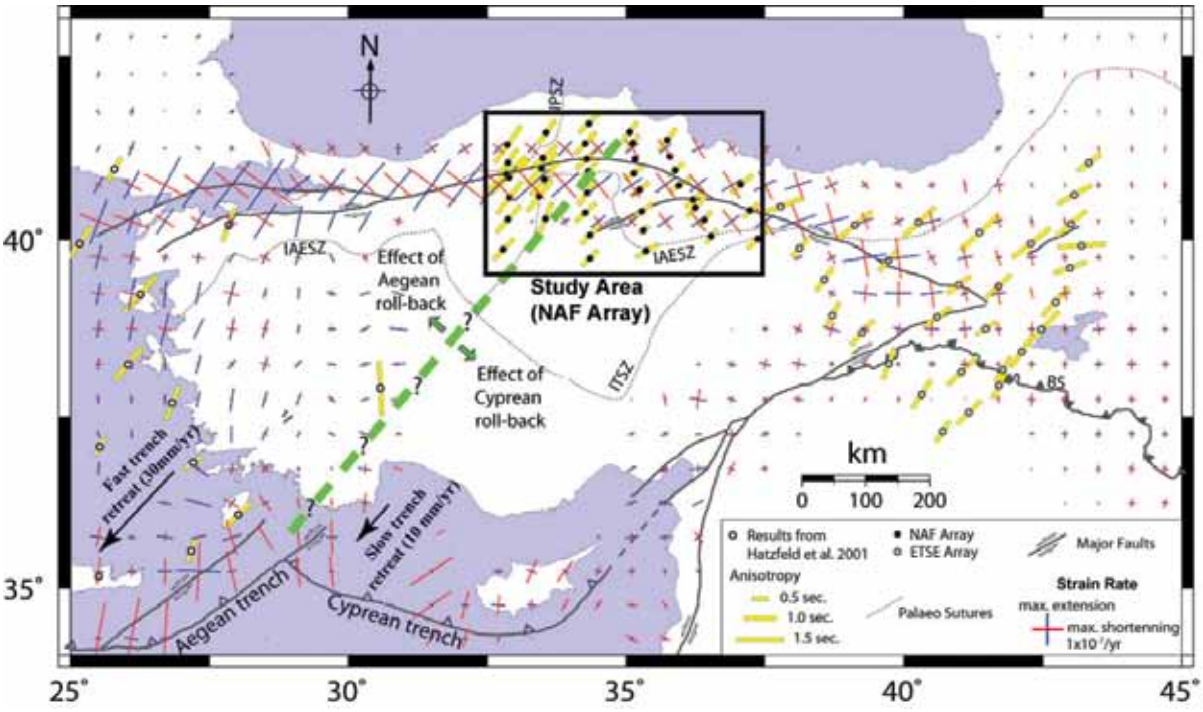

Results of splitting analysis from ETSE (Sandvol et al., 2003), NAF and Hatzfeld et al. (2001). BS: Bitlis Suture, IASZ: Izmir-Ankara-Erzincan Suture Zone, ITSZ: Inner Tauride Suture Zone, IPSZ: Inner Pontide Suture Zone.The trench retreat rates (black arrows) are from McClusky et al. (2003).

Edge-Driven Convection beneath the Rio Grande Rift

Jay Pulliam *(Baylor University),* **Stephen P. Grand** *(University of Texas at Austin),* **Tia Barrington** *(Baylor University),* **Yu Xia** *(University of Texas at Austin),* **Carrie Rockett** *(Baylor University)*

The Rio Grande Rift is a series of north-south trending faulted basins extending for more than 1000 km from Colorado to Chihuahua, Mexico and the Big Bend region of Texas. The rift is a Cenozoic feature with a mid-Oligocene (~30 Ma) early rifting stage, possibly related to foundering of the flat-subducting Farallon plate, and a recent late Miocene (~10 Ma) phase, which continues today.

There is no clear cause for the resurgence in magmatism and extension. However, the rift location at the edge of the stable, thick lithosphere Great Plains suggests that edge-driven convection along the eastern border of the Southern Rockies may play an important role in the current tectonics of the Rio Grande Rift. In particular, edge-driven convection may erode the lithosphere beneath the Rift and Great Plains, cause the lower crust to flow, and produce magma.

In 2008, a group of university scientists and high school teachers deployed 71 broadband seismographs interspersed between the EarthScope Transportable Array stations (Figure 1). The dense SIEDCAR (Seismic Investigation of Edge Driven Convection Associated with the Rio Grande Rift) network increases resolution of tomographic and receiver function images and shear wave splitting measurements, and allows construction of a detailed 3-D model of the eastern edge of the Rio Grande Rift structure.

Initial results of SKS splitting measurements to constrain patterns of mantle anisotropy (Figure 1), receiver functions to show crustal thickness (Figure 2), and body-wave and surface-wave tomography to determine P and S wave velocities show patterns consistent with edge-driven convection. Tomographic images indicate that the fast upper mantle anomaly beneath the eastern flank of the Rio Grande Rift is clearly separated from the Great Plains craton and that it extends southward to at least the Big Bend region of Texas. SKS splitting measurements show a marked decrease in splitting times above the fast "downwelling" anomaly in the mantle and generally larger splits on the rift flank proper. Receiver function images suggest a thickening of the crust to the east, which might indicate lower crustal flow induced by the edge convection or even delamination of lithosphere

Edge-driven convection may explain why, after a long period of quiescence, the Rio Grande Rift again became active. The SIEDCAR project seeks to understand how this process continues to modify the sub-continental lithosphere long after the formation of the rift.

Acknowledgements: The SIEDCAR project is supported by NSF grant #0746321 (EAR Division, EarthScope Program).

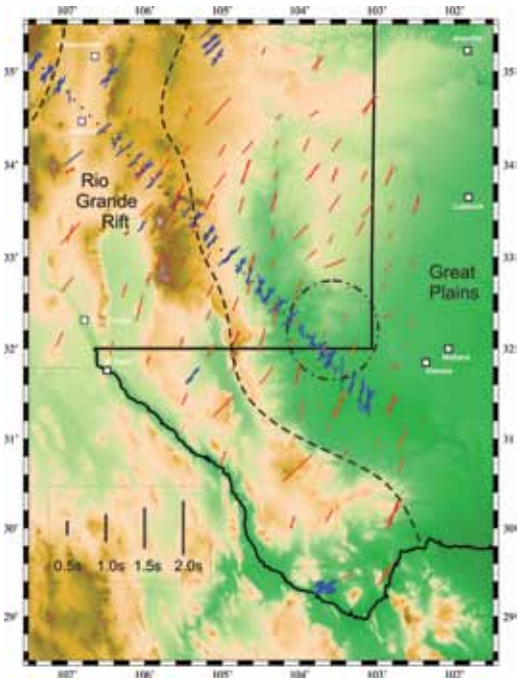

SKS splitting parameters for SIEDCAR (red) and TA (green) stations deployed 2008-2010 in the study area. Previous splitting measurements (La Ristra linear array and others) are shown in blue. Dash-dot circle indicates area where the SKS delay-times decrease; this area coincides with the "downwelling" fast anomaly in the mantle. The NW-SE-oriented La Ristra line is indicated by a dotted line.

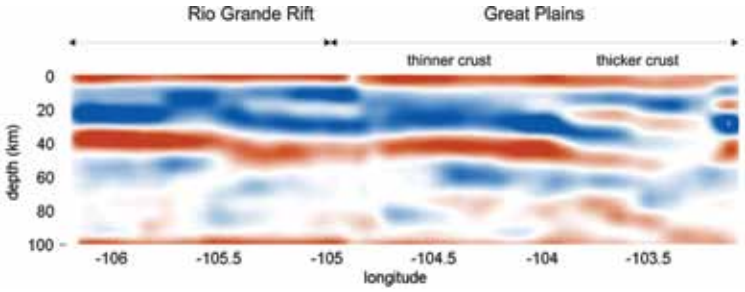

Receiver function image of crust and uppermost mantle beneath the eastern flank of the Rio Grande Rift from SIEDCAR and TA data for the NW-SE oriented La Ristra transect (dotted line in Figure 1). Thickened crust beneath the Great Plains extends both to the north and to the south, but, south of this cross-section, the transition from thick to thin crust moves to the southwest.

The Mantle Flow Field beneath Western North America

Matthew J. Fouch *(School of Earth and Space Exploration, Arizona State University),* **John D. West** *(School of Earth and Space Exploration, Arizona State University)*

The goal of this study is to image the mantle flow field beneath western North America. We utilize broadband data from regional and portable seismic arrays, with an emphasis on stations from EarthScope's USArray Transportable Array, to image seismic anisotropy and constrain deformation in the lithosphere and asthenosphere across the region.

Regional shear wave splitting parameters show clear variations with geologic terrane. In the Pacific NW, splitting times are large and fast directions are ~E-W with limited variability. Away from the Pacific-North American plate boundary, and sandwiched between broad regions of simple and strong splitting, stations within the Great Basin (GB) exhibit significant complexity. Fast directions show a clear rotation from E-W in the northern GB, to N-S in the eastern GB, to NE-SW in the southeastern GB. Splitting times reduce dramatically, approaching zero within the central GB.

While lithospheric fabric likely contributes to the shear wave splitting signal at many of the stations in this study, the broad-scale trends in both fast directions and delay times argue for a substantial asthenospheric source to the anisotropy. The regional mantle flow field therefore appears to be strongly controlled by significant and recent changes in plate boundary geometry. Assuming a North American plate reference frame, mantle flow appears to be controlled by absolute plate motion away from tectonic North America; conversely, rapid westward slab rollback of the Juan de Fuca plate dominates the Pacific NW U.S. flow field. To fill this gap in asthenospheric material, mantle flows strongly eastward S of the Juan de Fuca plate. Beneath the Great Basin, the paucity of shear wave splitting, combined with tomographic images and a range of geochemical and geologic evidence, supports a model of downward mantle flow due to a lithospheric drip.

Acknowledgements: This work would not have been possible without high quality seismic data provided through the hard work of the USArray Transportable Array team, the USArray Array Network Facility, and the IRIS Data Management Center. This research was supported by National Science Foundation awards EAR-0548288 (MJF EarthScope CAREER grant) and EAR-0507248 (MJF Continental Dynamics High Lava Plains grant).

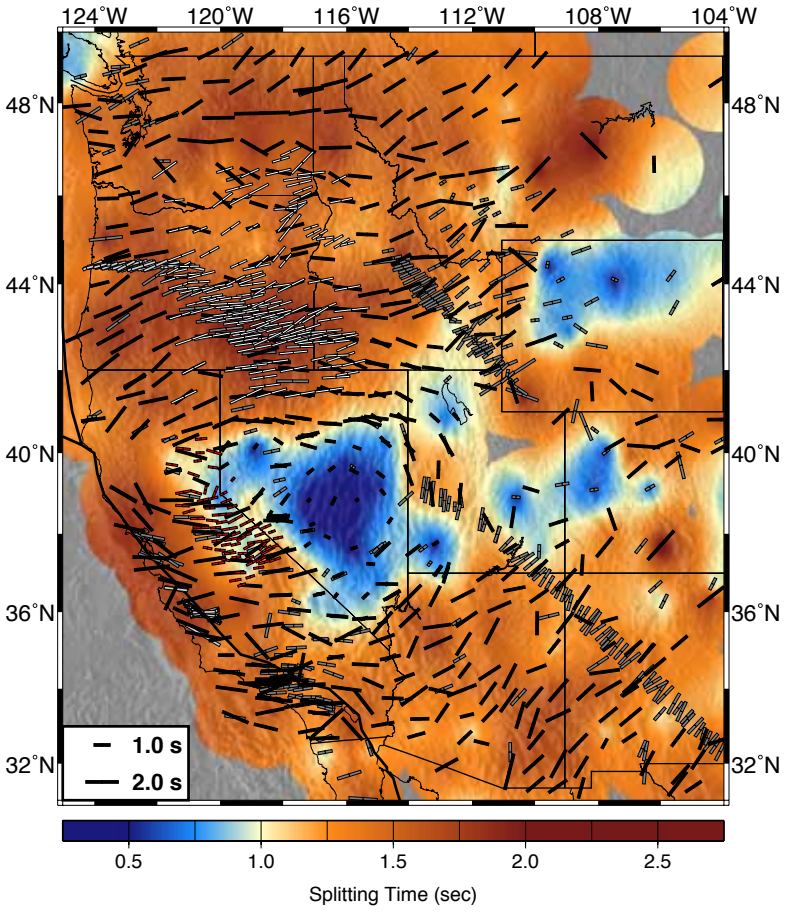

Station-averaged shear wave splitting beneath the western United States. Fast polarization directions denoted by azimuth of bar; splitting times denoted by length of bar. Background is smoothed, contoured splitting time magnitude. Black symbols represent new measurements from this study; red symbols represent splitting measurements from the SNEP experiment (courtesy Ian Bastow); white symbols represent measurements from Long et al. [2009]; gray symbols from other previous published studies. Clear, broad-scale regional similarities exist over hundreds of km, with significant complexity over shorter spatial scales in some regions. Large splitting times dominate most of region with the exception of very small splitting times beneath Great Basin.

Imaging Attenuation in the Upper Mantle with the GSN

Colleen A. Dalton *(Boston University),* **Goran Ekstrom** *(LDEO, Columbia University),* **Adam M. Dziewonski** *(Harvard University)*

Seismic-wave attenuation (1/Q) is thought to be highly sensitive to variations in temperature, and joint interpretation of attenuation and velocity models should aid in distinguishing between thermal and chemical heterogeneity in the mantle. However, imaging attenuation remains a challenging problem, because factors other than attenuation influence wave amplitude. Principally, amplitudes are affected by focusing due to lateral velocity variations, but uncertainties in the calculation of source excitation as well as inaccuracies associated with the instrument response can also obscure the attenuation signal in the data. We have developed a method to remove these extraneous effects and isolate the signal due to attenuation. We invert a large data set of fundamental-mode Rayleigh wave amplitudes, measured from waveforms recorded by the IRIS GSN and other global networks, in the period range 50--250 seconds simultaneously for a 3-D model of upper-mantle shear attenuation, maps of phase velocity, and amplitude correction factors for each source and receiver in the data set. The new three-dimensional attenuation model (QRFSI12) contains large lateral variations in upper-mantle attenuation, 60% to 100%, and exhibits strong agreement with surface tectonic features at depths shallower than 200 km. At greater depth,QRFSI12 is dominated by high attenuation in the southeastern Pacific and eastern Africa and low attenuation along many subduction zones in the western Pacific. QRFSI12 is found to be strongly anti-correlated with global velocity models throughout the upper mantle, and individual tectonic regions are each characterized by a distinct range of attenuation and velocity values in the shallow upper mantle. By comparing with laboratory experiments, we have found that lateral temperature variations can explain much of the observed variability in velocity and attenuation, although oceanic and cratonic regions appear to be characterized by different major-element composition or volatile content for depths < 225 km.

References

Dalton, C.A., G. Ekstrom, and A.M. Dziewonski. The global attenuation structure of the upper mantle, *J. Geophys. Res., 113*, doi:10.1029/2007JB005429, 2008.

Kustowski, B., G. Ekstrom, and A.M. Dziewonski. Anisotropic shear-wave velocity structure of the Earth's mantle: A global model, *J. Geophys. Res., 113*, doi:10.1029/2007JB005169, 2008.

Faul, U.H., and I. Jackson. The seismological signature of temperature and grain size variations in the upper mantle, *Earth Planet. Sci. Lett., 234*, 119-134, 2005.

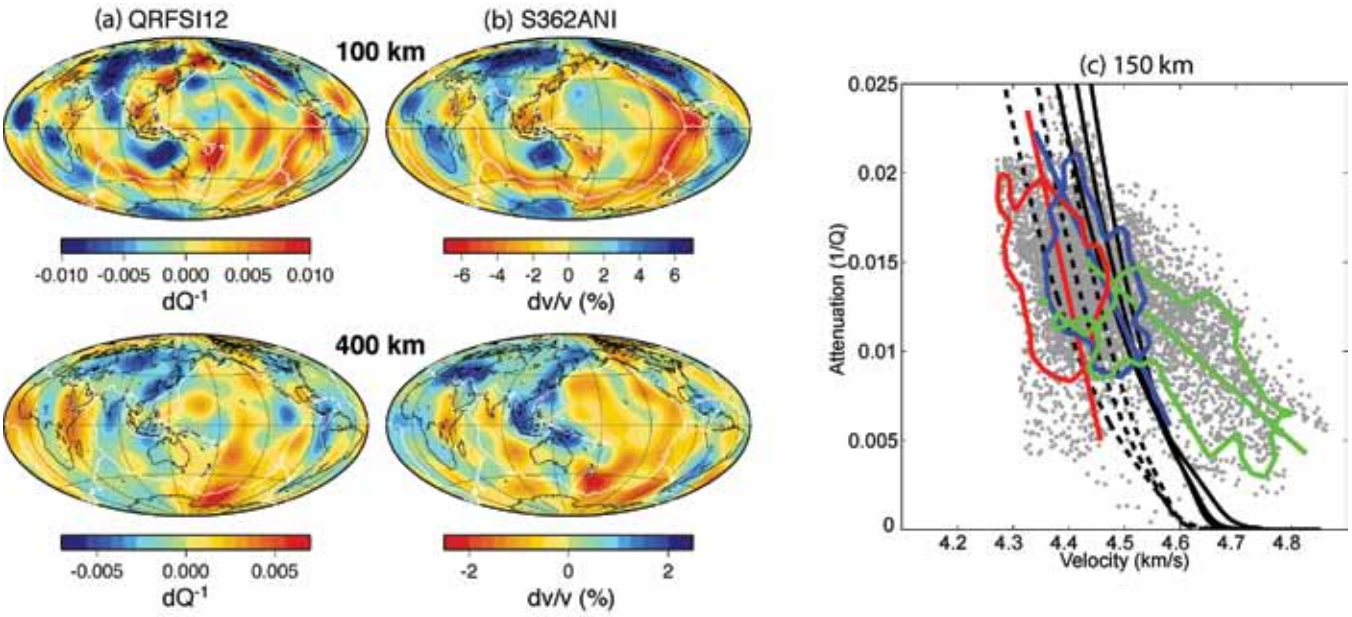

Comparison of global shear-attenuation (a) and shear-velocity (b) models at 100-km and 400-km depth. The attenuation model is from Dalton et al. (2008) and the velocity model is from Kustowski et al. (2008). (c) Grey points show seismologically observed shear velocity (S362ANI) and attenuation (QRFSI12) models sampled at 5762 points at 150-km depth. Colored contours enclose 75% of points from oceanic regions of age < 70 Myr (red) and > 70 Myr (blue) and from old-continental regions (green). Black lines show the predicted relationship between shear velocity and attenuation using the experiment-derived model of Faul and Jackson (2005).

S-Wave Velocity Structure beneath the High Lava Plains, Oregon, from Rayleigh-Wave Dispersion Inversion

Linda M. Warren *(Saint Louis University),* **J. Arthur Snoke** *(Virginia Tech),* **David E. James** *(Carnegie Institution of Washington)*

The High Lava Plains (HLP) "hotspot" track is a prominent volcanic lineament that extends from the southeast corner of Oregon in the northern Great Basin to Newberry volcano in the eastern Cascades. With the age of silicic volcanism decreasing along track to the northwest, the HLP and Newberry volcano are a rough mirror image to the Eastern Snake River Plain and Yellowstone but, in the case of the HLP, at an orientation strongly oblique to North American plate motion. Since this orientation is incompatible with plate motion over a fixed hotspot, other proposed origins for the HLP, such as asthenospheric inflow around a steepening slab, residual effects of a Columbia River/Steens plume, backarc spreading, and Basin and Range extension, relate it to various tectonic features of the Pacific Northwest. To begin distinguishing between these hypotheses, we image upper-mantle structure beneath the HLP and adjacent tectonic provinces with fundamental-mode Rayleigh-waves recorded by stations of the USArray Transportable Array, the recently-initiated HLP seismic experiment, the United States National Seismograph Network, and the Berkeley seismic network [*Warren et al., 2008*]. We estimate phase velocities along nearly 300 two-station propagation paths that lie within and adjacent to the HLP and cross the region along two azimuths, parallel to and perpendicular to the HLP track. The dispersion curves, which typically give robust results over the period range 16-171 seconds, are grouped by tectonic region, and the composite curves are inverted for S-wave velocity as a function of depth. The resulting variations in upper-mantle structure correlate with variations in surface volcanism and tectonics. The lowest velocities (~4.1 km/s) occur at ~50 km depth in the SE corner of Oregon, where there has been extensive basaltic volcanism in the past 2-5 Kyr, and suggest uppermost mantle temperatures sufficient to produce basaltic partial melting. While the seismic velocities of the uppermost mantle beneath the volcanic High Lava Plains are low relative to the standard Tectonic North America (TNA) model [*Grand and Helmberger, 1984*], they are only slightly lower than those found for the adjacent northern Great Basin and they appear to be significantly higher than upper mantle velocities beneath the Eastern Snake River Plain. Our results provide no evidence for a residual plume signature beneath the HLP region, leaving open questions as to the origin of the HLP volcanic track itself.

References

Warren, L.M., J.A. Snoke, and D.E. James, S-wave velocity structure beneath the High Lava Plains, Oregon, from Rayleigh-wave dispersion inversion, *Earth Planet. Sci. Lett., 274*, 121-131, 2008.

Grand, S.P., and D.V. Helmberger, Upper mantle shear structure of North America, *Geophys. J. R. Astron. Soc., 76*, 399-438, 1984.

Acknowledgements: This work was supported by the National Science Foundation through grant EAR-0506914 and by the Carnegie Institution of Washington.

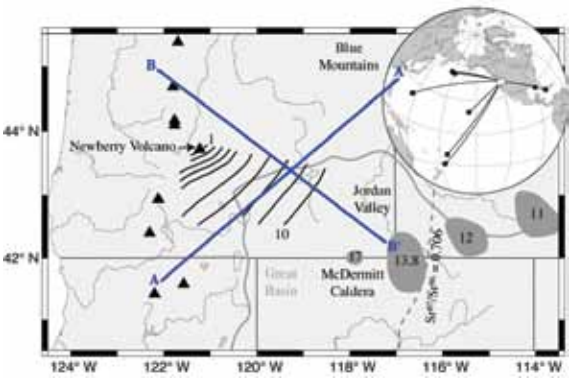

The tectonic setting of the High Lava Plains. Black triangles mark locations of Cascade volcanoes. Black lines beginning at Newberry Volcano and extending to southeast show increasing age of rhyolitic volcanism [Jordan et al., 2004]. McDermitt Caldera indicates onset of volcanism 16.1 Ma. Colored gray regions show rhyolite calderas along the Snake River Plain [Priest and Morgan, 1992]. Gray line outlines the Great Basin [Wernicke, 1992]. The dashed Sr87/Sr86 = 0.706 line approximates the western boundary of Proterozoic North America [Ernst, 1988]. Lower Sr87/Sr86 values lie to the west. The blue lines labeled A-A' and B-B' indicate the locations of the cross-sections in Figure 2. The inset shows the geographic setting of the study area and the great circle paths to that area from the nine analyzed earthquakes (black circles).

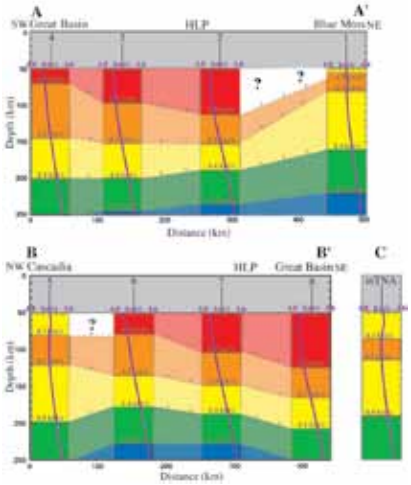

Cross-Sections interpreting S-wave velocity with depth along lines A-A' and B-B' of Figure 1. Velocity profiles for the eight regionalized paths are plotted at the center of the appropriate region and dashed lines with question marks interpolate structure between the regions. The large question marks in two of the transition regions indicate possible discontinuities in structure for which we have no constraints. S-wave velocity structure shallower than 50 km is not interpreted because it trades off with crustal thickness. (c) The velocity-depth profile for the modified TNA model is shown for comparison.

Three-Dimensional Electrical Conductivity Structure of the Pacific Northwest

Gary D. Egbert *(Oregon State University),* **Prasanta K. Patro** *(NGRI, Hyderabad, India)*

In conjunction with the USArray component of EarthScope, long period magnetotelluric (MT) data are being acquired in a series of arrays across the continental US. Initial deployments in 2006 and 2007 acquired data at 110 sites covering the US Pacific Northwest. The MT sites, distributed with the same nominal spacing as the USArray seismic transportable array (~70 km), produced data in the period range 10-10,000s of very good (2007) to excellent (2006) quality. Three-dimensional inversion of this dataset (Patro and Egbert, 2008) reveals extensive areas of high conductivity in the lower crust beneath the Northwest Basin and Range (C1), and beneath the Cascade Mountains (C2-C3), contrasting with very resistive crust in Siletzia (R1), the accreted thick ocean crust which forms the basement rocks in the Cascadia forearc and the Columbia Embayment). The conductive lower crust beneath the southeastern part of the array is inferred to result from fluids (including possibly partial melt at depth) associated with magmatic underplating. Beneath the Cascades high conductivities probably result from fluids released by the subducting Juan de Fuca slab. Resistive Siletzia represents a stronger crustal block, accommodating deformation in the surrounding crust by rigid rotation. Significant variations in upper mantle conductivity are also revealed by the inversions, with the most conductive mantle beneath the Northeastern part of the array, and the most resistive corresponding to subducting oceanic mantle beneath the Pacific plate (R2).

References

Patro P. K., G. D. Egbert, 2008. Regional conductivity structure of Cascadia: Preliminary results from 3D inversion of USArray transportable array magnetotelluric data, *Geophys. Res. Lett., 35*, L20311.

Acknowledgements: This work was partially supported by grants from the National Science Foundation (NSF-EAR0345438) and the U.S. Department of Energy 212 (DE-FG02-06ER15819).

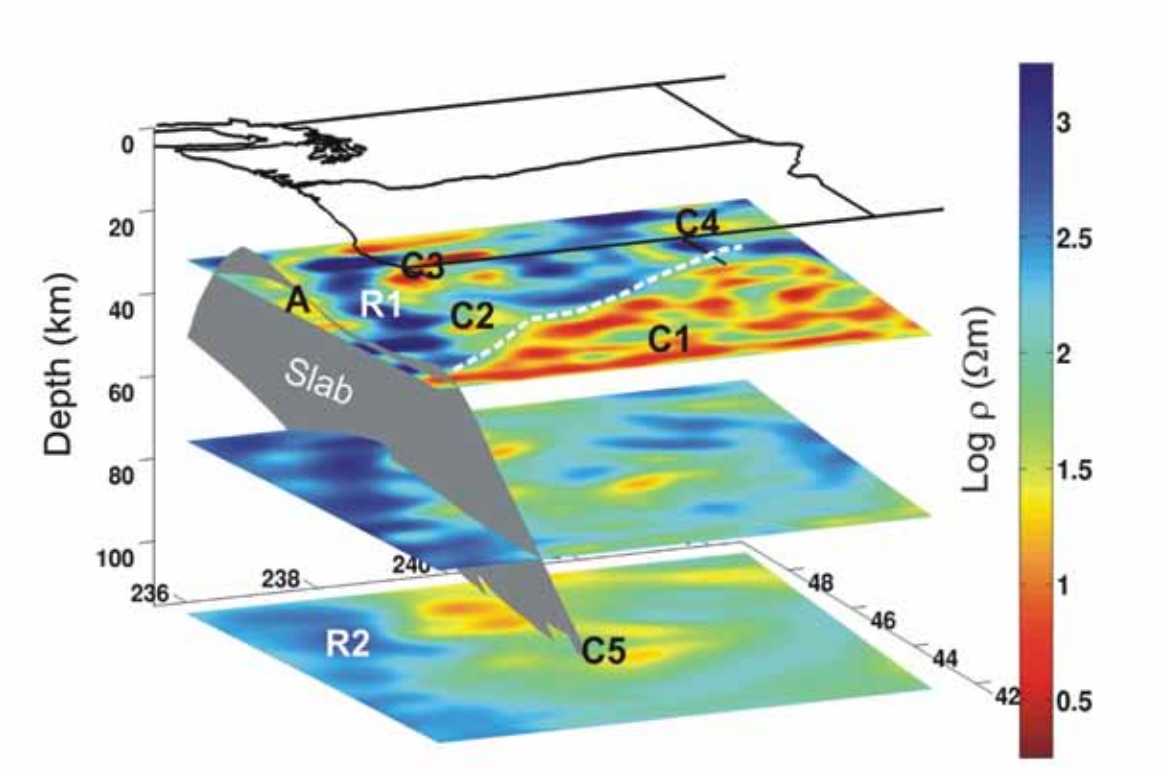

3D resistivity image of Pacific Northwest derived from the 3D inversion A: conductive zones in the forearc; C1: conductive lower crust in the Basin and Range, High lave plains and Blue Mountains; C2-C3: conductive features beneath the Cascades; R1: resistive Siletz terrane; R2: resistive oceanic mantle. Dashed white line marks contact interpreted as the southern boundary of Siletzia.